1989

Thermal hydraulic aspects of an unconventional liquid metal reactor

Cemal Niyazi Sökmen
Iowa State University

INFORMATION TO USERS

The most advanced technology has been used to photograph and reproduce this manuscript from the microfilm master. UMI films the text directly from the original or copy submitted. Thus, some thesis and dissertation copies are in typewriter face, while others may be from any type of computer printer.

The quality of this reproduction is dependent upon the quality of the copy submitted. Broken or indistinct print, colored or poor quality illustrations and photographs, print bleedthrough, substandard margins, and improper alignment can adversely affect reproduction.

In the unlikely event that the author did not send UMI a complete manuscript and there are missing pages, these will be noted. Also, if unauthorized copyright material had to be removed, a note will indicate the deletion.

Oversize materials (e.g., maps, drawings, charts) are reproduced by sectioning the original, beginning at the upper left-hand corner and continuing from left to right in equal sections with small overlaps. Each original is also photographed in one exposure and is included in reduced form at the back of the book. These are also available as one exposure on a standard 35mm slide or as a 17" x 23" black and white photographic print for an additional charge.

Photographs included in the original manuscript have been reproduced xerographically in this copy. Higher quality 6" x 9" black and white photographic prints are available for any photographs or illustrations appearing in this copy for an additional charge. Contact UMI directly to order.

U·M·I

University Microfilms International
A Bell & Howell Information Company
300 North Zeeb Road, Ann Arbor, MI 48106-1346 USA
313/761-4700 800/521-0600

Order Number 8920186

Thermal hydraulic aspects of an unconventional liquid metal reactor

Sökmen, Cemal Niyazi, Ph.D.

Iowa State University, 1989

U·M·I
300 N. Zeeb Rd.
Ann Arbor, MI 48106

Thermal hydraulic aspects of an unconventional liquid metal reactor

by

Cemal Niyazi Sökmen

A Dissertation Submitted to the
Graduate Faculty in Partial Fulfillment of the
Requirements for the Degree of
DOCTOR OF PHILOSOPHY

Major: Nuclear Engineering

Approved:

Signature was redacted for privacy.

In Charge of Major Work

Signature was redacted for privacy.

For the Major Department

Signature was redacted for privacy.

For the Graduate College

Iowa State University
Ames, Iowa
1989

TABLE OF CONTENTS

LIST OF TABLES

LIST OF FIGURES

ACKNOWLEDGEMENTS

I would like to express my thanks to my major professors Dr. B. I. Spinrad and Dr. M. M. Razzaque for their guidance and help during the course of this study. I also would like to thank Dr. R. A. Danofsky, Dr. G. H. Junkhan and Dr. M. B. Pate for their valuable suggestions as committee members.

The work reported in this study is part of a project on which several persons have worked for three years. As a late comer to the project, I would like to acknowledge all the previous work done by the members of the project group. In particular, work performed by Mr. Joe Lofshult's on the thermal hydraulics and DSNP is greatly appreciated. I am also indebted to Dr. J. T. Sankoorikal for providing the neutronics parameters and many suggestions.

My special thanks goes to Dr. B. I. Spinrad who originated the Trench Reactor concept and introduced me to the subject. His enthusiasm for exploring new concepts and his insightful ability were the major motivating factors of this study.

I want to extent my appreciation to my friends and fellow graduate students Zekeriya Altaç, Serhat Alten, Üner Çolak and Ramin Mikaili for their help, invaluable suggestions and friendship during my stay at the I.S.U. Serhat provided Figure 1.1. Chapter 2 was written with help of Üner. Ramin provided his personal computer during the initial stages of this study.

1 INTRODUCTION

Nuclear power plants constitute a major source of electricity worldwide. There were 417 nuclear power plants being operated worldwide in 1988 [1]. The amount of electricity generated by nuclear power plants was 308 GWe. In the U.S.A. 108 operating nuclear power plants generated 95 GWe during 1988. During the same year only 6 new units began operation in the U.S.A. [1]. Yet, among other things, increasing and unpredictable costs and time to construct and operate nuclear power plants as well as concerns about safety have slowed the growth of the share of nuclear energy despite its apparent advantages and immense potential as a future energy source. In response to this situation the nuclear community is responding by proposing safer, smaller and more economical reactor designs. This study is part of such an effort.

The concept is a liquid sodium cooled fast breeder reactor concept. It is called the Trench Reactor (TR). In particular, this study deals with the thermal-hydraulic behavior of the main components and preliminary safety assessment of the reactor concept. The purpose is to assess an alternative reactor concept with regards to its thermal hydraulic behavior and safety. The core physics, economic assessment and fuel management aspects of the TR can be found in references [2,3,4]. Previous work on the thermal hydraulic behavior and safety of the TR can be found in [5].

1.1 Concept

The concept can be summarized as a simple and an inherently safe fast power reactor for a wide range of operating conditions. The requirement that the reactor should be simple implies simplicity in construction and operation. One of the most direct ways to achieve simplicity in construction and operation is designing for units producing relatively small amounts of power with relaxed requirements on the components in a simple geometry. The requirement for inherently safe behavior means that the reactor should be able to compensate for any major disturbance in the balance of the plant in the absence of any action from the plant control and protection system. This requirement can be met by isolating the reactor core from the rest of the plant as much as possible and providing passive responses to malfunctioning components. The economic competitiveness of this concept is expected to be a result of these two characteristics.

The major disadvantage of a nuclear power plant with small electric output is its high specific cost [6] and high operation and maintenance costs [7]. However, the small absolute power of the reactor offers several advantages in terms of both economic competitiveness and safety. Table 1.1 clearly indicates the effect of smaller electric output on the availability of the nuclear plants operating in the US. The same trend is also observed in the world; 14 of the best performing 20 nuclear reactors were rated below 600MWe and only one had a rating greater than 800 MWe [8].

Besides ease of operability, the smaller rated power plants allow more of the components to be manufactured in factories rather than on the site of the nuclear plant. This allows for quality assurance to be performed easily resulting in shorter

Table 1.1: Nuclear power plant performance during 1971-1980 [8,page:108]

Size Category (MW)	Number of Units	Cumulative Capacity(%)	Equivalent Availability (%)	Equivalent F.O.R[a]
400-599	11	72.3	79.6	8.0
600-799	8	68.1	71.0	11.5
800-999	30	56.1	63.1	22.4
1000 and over	13	56.2	64.9	23.3

[a]The forced outage rate represents the total time the unit was unavailable due to the unanticipated equipment failure.

construction times. It is also easier to standardize smaller reactors which will make the licensing process faster. In order to obtain higher electrical power ratings several small reactor modules can be grouped together to achieve the desired power rating. The passive mechanisms of safety, which are not as important in large power plant as they are in small power plants, offer a large potential for reductions in the costs associated with the safety related systems of the power plant by eliminating or at least reducing the necessity for fast acting systems.

Although the concept described in this study is not proposed to be used in the near future, the results of a survey indicate that, if new nuclear power plants are ordered in the US by the electric utilities in the near future, their electrical power will be in the small to medium power range [7]. This has also been expected for developing countries who are planing to introduce or expand nuclear power plants [9].

Designing components for tasks less than it is possible to achieve allows for longer operating times due to low demands on the components and there is considerable margin to complete failure in an abnormal operating condition. The penalty paid for not utilizing the full potential of the materials may be compensated by

increasing the overall lifetime of the components. In terms of plant protection, this implies that there are fewer events that can lead to the complete failure of a component, hence, the requirements on the plant protection system are relaxed.

The safety of a nuclear power plant is one of the most important aspects of its design and operation. Most nuclear reactors have been designed with a defense in depth approach; first to avoid the accidents from occurring, and if this step fails, to prevent accidents from causing plant failure. A third level of protection is included to avoid damage to the public should an accident in which the first two levels of defense have failed occur. The first level of defense includes designing stable reactors for all operating ranges, assuring the quality of components and operating and maintenance practices. The second level of defense includes redundant protection and reactor shutdown systems and decay heat removal systems. The third level of defense includes all the measures taken to avoid radioactive release to the environment, most importantly the containment buildings.

Nuclear power plants are composed of thousands of components and any one or a group of these components may fail completely or malfunction resulting in an accident. Also, as with both the Three Mile Island [10] and Chernobyl [11] accidents operator error can cause accidents. Environmental effects such as earthquakes and tornadoes may also act as accident initiators. Designing a safety system that can assure public safety under foreseeable possible and credible circumstances results in extremely complex systems.

Another approach to reactor safety is to design a reactor that can protect itself from a wide variety of accident initiators without the action of safety systems. Such a reactor is inherently safe for a wide range of operating conditions. Basically, one

can then neglect the role of the plant control and protection systems in the second level of safety. This has several advantages. Since plant control and protection systems are not required for a wide range of accidents they do not need to be as complex as they usually are. Less complex systems will increase the understanding of the how the system works and the reliability of the system.

The results of a survey in which the management, operating and maintenance employees of the utilities operating nuclear power plants in the US were asked to state their concerns related to the safety and operability of nuclear power plants, indicate how this safety approach can be achieved [8]. Some of the major concerns of the persons interviewed were: that additions of safety related equipment required by NRC reduces operability, maintainability and availability; that present plants respond too rapidly to transients; and that nuclear plants should be less sensitive to events in secondary systems. A reactor design that decouples the primary system from the rest of the plant, that does not require rapid responses from the operating system, and that assures adequate heat removal from the reactor core and the primary system under all conditions can satisfy these criteria.

An example of this safety approach is the Experimental Breeder Reactor-II (EBR-II). EBR-II is a liquid sodium cooled fast reactor using uranium metal based fuel elements. Loss of flow and loss of heat sink tests were conducted from full power without scramming the reactor [12]. The reactor was able to shut itself down safely without the use of control systems. These two events, which are two of the most severe reactor accidents that can lead to core damage, were shown to be of minor significance in EBR-II. The response of the rector was due to a large thermal inertia in the form of the sodium pool, to the characteristics of the metal fuel used

and to the availability of natural circulation cooling after pumping power was lost. The TR concept as well as the other current US fast reactor concepts follow the example of EBR-II.

Although the liquid metal cooled fast reactors (LMFR) have only recently begun to be used as commercial power plants in Europe, there is a vast amount of experience gained through several experimental facilities worldwide [13]. It is generally agreed that the risks from the fast breeder reactors to the public are considerably less than the risks from the light water reactors [14,15]. Besides their advantage in terms of safety, the LMFRs, by producing new fissile material by breeding, offer a large potential for supplying future electricity demands [14].

The use of sodium as the coolant and the pool configuration are the current design tendencies for LMFRs with the exception of the MONJU reactor which is a loop type reactor designed in Japan [16]. The concepts developed in the US advocate using metal fuel as the reactor fuel whereas the European and Japanese designs employ oxide fuels.

The current reactor designs give more emphasis to passive systems as a means of assuring plant safety than previous reactor designs. In order to achieve this, plants are designed for small electrical outputs. The US concepts such as Power Reactor Inherently Safe Module (PRISM) [17] and Sodium Advanced Fast Reactor (SAFR) [18] are modular reactors with small electrical power outputs of 135MWe and 330MWe per module, respectively. Emphasis is put on shop fabrication of components and minimization of the construction work on site. There is a major effort to limit the nuclear safety grade components to the primary system and employ conventional construction practices for the rest of the plant. These reactor

concepts can withstand a wide range of accidents including loss of flow, reactivity insertion and loss of heat sink accidents without control system action [17,18].

In summary, several features of the TR concept, simplicity and inherent safety, also characterize the current LMFR design practices. Yet, the TR concept is quite different from the current reactor design concepts.

1.2 Description of the Trench Reactor

The TR is a liquid sodium cooled fast power reactor. Basic design data are given in Table 1.2. Figure 1.1 shows the basic configuration of the reactor. The reactor core is fueled with U-Pu-Zr metal fuel and generates 800MW of thermal power. The core is located in a sodium pool which is contained in a rectangular vessel. Control rods are located above and to the side of the core. Also located in the pool are the two intermediate heat exchangers and the two primary pumps. The liquid sodium exits the core at 485^oC and is pumped through the intermediate heat exchangers where it is cooled to 343^oC and enters the core through an inlet plenum. The reactor building atmosphere is nitrogen which circulates through the guard tank and reactor vessel. The secondary sodium enters the intermediate heat exchangers at 294^oC and exits at 465^oC. It is then used to generate superheated steam at 425^oC and 15MPa in the steam generators. The electric power output of the plant is 300MWe.

The geometry of the primary system of the reactor, a slab reactor core located in a thin rectangular prism, reduces the problems associated with the design of the primary system components and operational difficulties that would arise in other geometries. The shape of the reactor also makes the control of the reactor

easier by allowing control rods in the reflector rather than inside the core. The low power density of the reactor system resulting in lower operating temperatures allows considerable margin to failure during transients and normal operation. The large sodium pool, with its high thermal capacity, serves as a heat sink in case of an accident that results in a loss of heat removal capacity from the intermediate heat exchangers. The low thermal capacity of the inlet plenum due to the elimination of the cold pool from the reactor inlet, causes the reactor inlet temperature to respond to changes or disturbances more rapidly than the currently practiced design concepts. The pool temperature, by limiting the increase in the core inlet temperature, avoids any undesirable increase in the core temperatures. The large surface area of the reactor vessel enables the cooling of the reactor vessel by natural circulation of the building atmosphere. The primary pumps with their coastdown characteristics supply the necessary coolant flow through the reactor core in case of a loss of electrical power accident. The difference between the elevations of thermal centers of the intermediate heat exchangers and the reactor core helps natural circulation which can remove the decay heat generated in the core.

The properties of the metal fuel material are essential to the inherently safe behavior of the reactor. The basic characteristics of the metal fuel are high thermal conductivity, small heat capacity, high expansion coefficients, and low strength at high temperatures. The high thermal conductivity and the small amount of heat stored in the fuel elements cause the fuel temperature to follow the coolant temperature closely resulting in an increase in the negative feedback mechanisms associated with the fuel. The expansion characteristics of the metal fuel from an increase in temperature on short time scales are augmented by fission gas pressure buildup to

Table 1.2: Basic design parameters of the Trench Reactor

Thermal Power (MW)	800
Electrical Power (MW)	300
Power Density (MW/m^3)	155.2
Core Inlet Temperature (^oC)	343
Core Exit Temperature (^oC)	485
Core Flow Rate (kg/s)	4400
Core Pressure Drop (kPa)	836
Number of Secondary Loops	2
IHX Inlet Temperature (^{o}C)	293
IHX Outlet Temperature (^{o}C)	465
Secondary Flow Rate (kg/s)	1800
Steam Temperature (^{o}C)	425
Steam Pressure (MPa)	15
Feedwater Temperature (^{o}C)	237
Feedwater Flowrate (kg/s)	172
Fuel Material Composition	U-10Pu-10Zr
Cladding Material	HT-9
Fuel Pin Radius (mm)	6.0
Pitch (mm)	13.0
Number of Fuel Pins	23450
Fuel Reactivity Coefficient (10^{-2}\$/^{o}C)	-0.281
Coolant Reactivity Coefficient (10^{-2}\$/^{o}C)	-0.129
Power Reactivity Coefficient (10^{-2}\$/^{o}C)	-40.5

introduce more negative feedback reactivity during transients. The decrease in the strength of the fuel material with increasing temperature reduces the mechanical stresses on the cladding material thereby reducing the chance of a cladding failure. In terms of normal operation of the plant, less reactivity is required to change the reactor power which results in a reactor which is more easily controlled than would be possible otherwise.

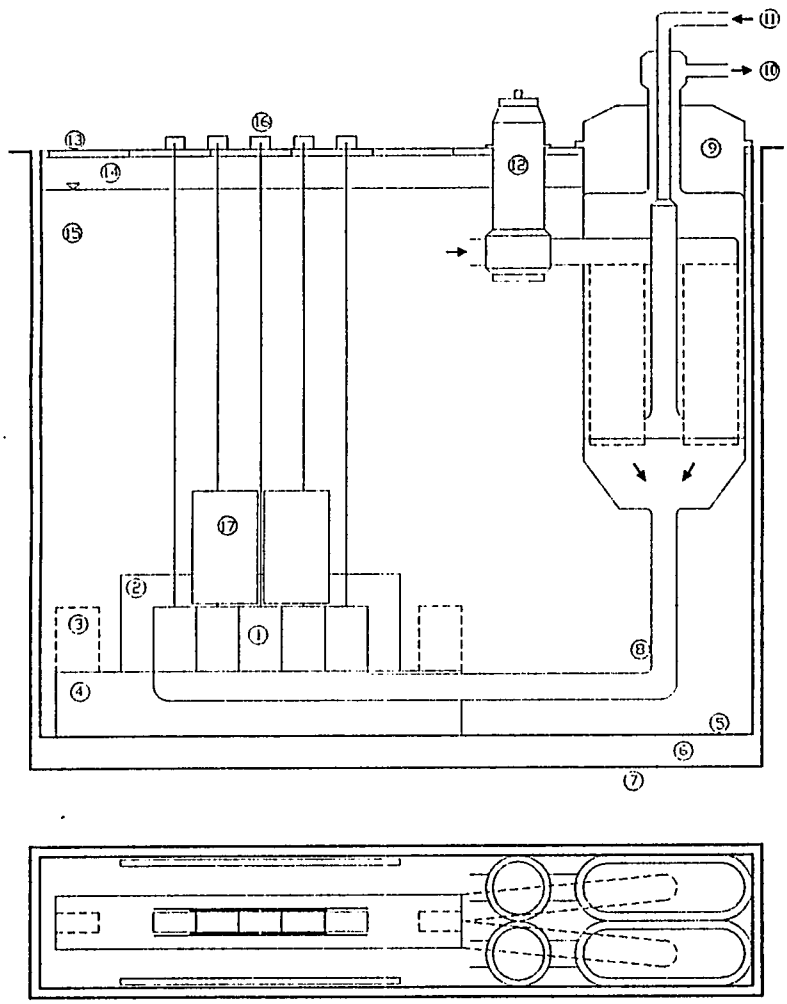

1	Core boxes	7	Guard vessel	13	Top shield
2	Core shield	8	Primary inlet	14	Cover gas plenum
3	Fuel storage	9	IHX	15	Sodium pool
4	Core table	10	Secondary outlet	16	Control blade drive mechanism
5	Reactor vessel	11	Secondary inlet		
6	Nitrogen	12	Pump	17	Shut down blades

Figure 1.1: Cross section view of the TRENCH reactor

1.3 Scope and Limitations

As mentioned earlier the main purpose of this study is to assess the the thermal-hydraulic behavior and safety of the TR concept. Only the main components of the reactor system will be considered. The main components of the reactor system that will be considered are the reactor core, intermediate heat exchangers, pumps and steam generators. The detailed engineering design of any one of these components is an enormous task; this study does not attempt to reach such a final design.

The main limitation of this study results from the level of detail employed in the calculations. Most of the calculations were done with simple one dimensional models. This required an attempt to be on the conservative side when making certain predictions rather than to attempt to model the physical phenomenon in more detail with possibly more accuracy.

The safety of the TR concept is assessed based on its response to unprotected accidents. These unprotected accidents are expected to cover the upper bound of all the credible possible transient operating modes. The modeling used in this evaluation was based on lumped parameter models for most of the components. The level of complexity employed in these calculations was, in part, determined by the length of the computation time.

In Chapter 2, the important safety considerations will be summarized. This includes the behavior of metal fuel, a short summary of the difficulties arising due to use of sodium as the coolant and a discussion of the anticipated transients and their implications on the reactor configuration. The basic design of the main components are described in Chapter 3. In Chapter 4, the response of the TR to unprotected accidents will be discussed. Some the control and protection system concepts that

are applicable to the TR are described in Chapter 5. The conclusions and the suggestions for future work are given in Chapter 6 and Chapter 7, respectively. In order to help the reproducibility of the numerical results that will be presented, a list of the various correlations and material properties used in the calculations and a listing of the input of the DSNP program are included in the Appendix.

2 SAFETY CONSIDERATIONS

2.1 Materials Considerations

The properties of the materials used in building the various components in the primary and secondary heat transport systems of a liquid sodium cooled fast reactor determine the steady state and transient operating limits. The components of the primary system are affected by irradiation. They have to work at high temperatures for long periods of time and they have to withstand the undesirable effects of varying temperatures and of contact with flowing sodium. The components of the secondary system have to be able to mitigate the consequences of a possible sodium-water reaction in the steam generator. Therefore, a knowledge of the behavior of materials used in the design is important in deciding on the conditions which may cause a failure in any particular component.

In the following discussion the behavior of the metal fuel and its interactions with the cladding materials will be reviewed, based on EBR-II and IFR experimental results. The effects of sodium and high operating temperatures will be summarized.

2.1.1 Fuel Element Behavior

One of the most important components of the reactor is the reactor core comprised of the fuel pins and the core boxes which contain these pins. A viable fuel

element must be able to [19]

- perform to high burnup with this performance not being very sensitive to fuel element fabrication,
- be able to be fabricated by simple manufacturing processes,
- be able to be reprocessed in a simple and safe manner,
- respond to transients in an inherently safe manner.

For a fuel element to have a high burnup potential, the cladding material has to stand not only the pressure due the fission gas buildup and fuel element swelling but the thermal stresses as well. The effects of irradiation and high operating temperatures on the cladding mechanical properties are important. The wastage of the inner cladding surface by chemical interactions with the fuel material and the wastage of the outer surface of the cladding by sodium reduce the level of the stresses the cladding can stand. Another consideration is the differential thermal expansion between the fuel material and the cladding. The behavior and strength of the fuel material with increasing burnup determines the loads on the cladding. Failure, that is the breach of the cladding of one or a group of fuel pins, may have a major impact on the safety of the reactor.

The fuel material used in the TR is a ternary metallic alloy composed of U-9Pu-10Zr where the numbers denote the approximate weight fractions of the components they precede. The material used for the cladding and for other structural components of the reactor core is a type of ferritic steel denoted as HT9. The compositions of HT9 and some other cladding materials that will be referred to in this chapter

Table 2.1: Compositions of commonly used cladding materials

	Weight Percent								
Alloy	Cr	Ni	Mo	Ti	W	V	Si	Mn	C
HT9	12.0	0.5	1.0	-	0.5	0.3	0.3	0.2	0.20
D9	13.5	15.5	1.5	0.2	-	-	0.6	2.0	0.04
T91	9.2	0.2	1.0	0.2	0.01	0.21	0.3	0.5	0.10
316 SS	18.0	11.2	2.1	-	-	-	0.6	1.8	0.04

are given in Table 2.1. Metallic fuels with stainless steel cladding had been used in early fast reactor designs such as EBR-II and DFR [20]. After a shift to oxide and carbide fuels, metallic fuels are now being used in fast reactor design concepts such as PRISM, and IFR [19,20]. Most of the data available on the behavior of metallic fuels come from the experience gained through the operation of EBR-II. EBR-II uses a U-Fs fuel element. The cladding materials used were 304 and 316 stainless steels. Fs, which is an abbreviation for fissium, is an equilibrium concentration of non-gaseous and non-volatile fission products [21]. Although the fuel materials are different most of the information obtained on the behavior of metallic fuel elements is applicable to the U-Pu-Zr fuel because in both fuel element types the continuous phase is uranium. Recent data from irradiation experiments from the IFR project using U-Pu-Zr fuel elements with HT9 cladding support this conclusion.

2.1.1.1 Normal Operation One of the reasons for a shift to fuel types other than metallic fuels was the low burnup potential of the metallic fuel element. The reason for this was the fast rate of expansion of the fuel element due primarily to fission gas induced swelling. The Mark-I fuel element of the EBR-II was capable of achieving 1.2 at.% burnup whereas the Mark-II fuel element achieved burnups in excess of 10 at.% [20]. The differences between the Mark-II design and Mark-I

design are a lower smear density, a larger fission gas plenum and a thicker cladding which are attempts to strengthen the cladding or reduce the stresses on the cladding by reducing the pressure buildup and swelling due to the fission products [20].

It has been experimentally observed that if large amounts of fission gas can be released to the plenum before fuel and cladding contact occurs then the contact pressure on the cladding will be reduced greatly. However, in this case the plenum volume must be large enough to eliminate high pressure buildup. The gaseous fission products, which are basically Xe and Kr, tend to accumulate in the pores or form bubbles in the solid fuel matrix [20]. The reason for this can be related to the fact that both of these gases are noble gases eliminating the possibility for their chemical interaction with other elements present. The formed bubbles occupy more space than the more dense elements hence causing an increase in the fuel volume. If there were no mechanism for releasing these gases the cladding would have to accommodate for the increasing volume of the fuel and eventually would have to breach. However, as the fuel swells the gaseous fission products tend to combine and be released to the gas plenum associated with the fuel pin. The pressure of the gas collected in the bubbles and the pores is higher than the pressure in the plenum which forces the fission gas in the fuel to the fission gas plenum.

Although fuel swelling is a widely varying function of the fuel burnup and operating temperature history, the fission gas release for metal fuels is a function of fuel swelling and does not depend on the metal fuel type significantly. It has experimentally been observed that after a 25% increase in the fuel volume the fission gas release increases rapidly [19]. The fuel swelling is not isotropic; the fuel swells in the radial direction more than it does in the axial direction until fuel and

cladding contact occurs [22]. Fission gas is generated approximately at a rate of 3.5 STP cc gas per cc fuel per a/o burnup and this gas is retained in the fuel up to 2% burnup [23]. At low operating temperatures the retained fraction of the fission gas is almost independent of the burnup level of the fuel [24,25]. However, at operating temperatures higher than $\approx 450^{o}$C the retained fission gas fraction is relatively independent of the burnup level. This would indicate that in the lower regions of the fuel pin where operating temperatures are lower more gas will be retained than the upper regions of the fuel. The fission gas plenum pressure was observed to increase linearly with burnup [22,26].

The fission products that are not in gaseous form also contribute to the fuel swelling. It has been observed that the liquid fission products, basically cesium, are distributed between the fuel and the bond sodium. The solid fission products remain in the solid fuel matrix either in solid solution or as intermetallic compound precipitates. Their contribution to fuel swelling ($\approx$ 2vol% per atomic burnup) is important only in high smear density fuels [20]. However, if one considers the EBR-II fuel element, which is an alloy of solid fission products with uranium, it may be concluded that under certain conditions the solid fission products may reduce fuel swelling [19,27].

During irradiation the U-Pu-Zr fuel shows a three layered structure [19,28,29]. The zirconium in the fuel element migrates towards the center and the cladding resulting in higher zirconium fractions in these regions. Uranium migrates to the middle zone and fission products migrate to the center and outer zones. This results in higher solidus temperatures in the zirconium rich regions. Also the heat generation rate in each region changes according to the concentration of uranium

Table 2.2: Radial fuel composition of U-8Pu-10Zr at 1.9% burnup [28]

Zone	Radial position[a] r/r_{clad}	Alloy Composition
Inner	0.00 to 0.25	78.27U-7.66Pu-14.07Zr
Middle	0.25 to 0.70	83.29U-7.65Pu- 9.06Zr
Outer	0.70 to 0.86	81.59U-7.39Pu-11.02Zr

[a]Clad inner radius r_{clad}=0.584 cm.

and plutonium in each region. It is believed that this restructuring of the fuel takes places shortly after irradiation and does not affect the fuel behavior in a negative way [30,19]. Table 2.2 shows the concentrations of uranium, plutonium and zirconium after irradiation [28,29]. This restructuring is also believed to be the cause of the cracks that appear on the outer surface of the fuel [30].

The postirradiation examination of metallic fuels with different Pu concentrations (0, 8, 19 % weight fraction) after 1.9% and 3.0% burnup shows that fuel cracking is not very important in low plutonium content fuel elements [28,29]. Since fuel element cracking also reduces the amount of fission gas retained in the fuel, the U-8Pu-10Zr element had more fission gas retained than the U-19Pu-10Zr element [28,29].

The mechanical interaction between the swelling fuel element and the cladding was not found to be very important [26,27]. The strength of the fuel material as a function of temperature and porosity fraction decreases rapidly with increasing temperature and porosity fraction [31]. The cladding material has a high strength at elevated temperatures [32]; therefore, the differential thermal expansion between the fuel material and the cladding material is not a significant source of stress on

the inner cladding surface after the fuel and the cladding touch each other.

Radiation caused creep and swelling were the major sources of cladding deformation for the regions of cladding in contact with the fuel in EBR-II [26,27]. The swelling of cladding was not uniform but showed ovalities due to the effect of the wire wraps used. However, ferritic steels like HT9 have much lower swelling rates from void formation than do austenitic steels [29,33]. At irradiation temperatures between 400 and 650^{o}C HT9 did not exhibit swelling at a fluence of 1.4 x 10^{23}n/cm^{2} for neutron energies greater than 0.1MeV [33]. Examination of HT9 cladding with uranium based metal fuels after 2.9% burnup showed that the measured cladding diameter changes did not exceed the manufacturing tolerances of $\pm$0.2% [29].

Chemical interaction between the fuel and cladding materials is also an important consideration. Two basic interaction mechanisms are diffusion of materials from the cladding at normal operating temperatures and, at higher temperatures formation of low melting point alloys, or eutectics, between the cladding and fuel. Both of these mechanisms contribute to the wastage of the cladding and, therefore, can lead to early breach of the cladding.

In EBR-II with 316 SS cladding nickel diffusion from the cladding to the fuel was observed [27]; however, the HT9 cladding contains very small amounts of nickel (0.5% weight) which should limit this problem. Nickel transport is important because it accelerates the formation of $U_6Ni - U_7Ni_9$ eutectics [19]. Also another important component of the cladding is the carbon. Loss of carbon results in reduced strength properties at high temperatures. Loss of carbon from the HT9 cladding was investigated and it was found that below 700^{o}C carbon transfer was minimal [34].

The eutectic formation temperature is the lowest temperature limit in terms of metal fuel element steady state operation. If the reactor is operated above the eutectic formation temperature for long periods of time, then the cladding will breach due to eutectic penetration into the cladding. The EBR-II experiments indicate the basic characteristics and effects of eutectic formation on fuel element lifetime.

The U-Fs alloy has a eutectic temperature of 715^{o}C and the eutectic composition is U-34wt%Fe. In order to determine how long the EBR-II fuel elements can endure temperatures higher than the eutectic temperature before they fail, experiments were done on unirradiated fuel elements in a furnace [19]. Therefore, the fuel element failure mechanism is due to eutectic formation. It was observed that the eutectic penetration was very slow for temperatures slightly higher than the eutectic temperature and for temperatures higher than 900^{o}C the failure times was very short.

The experiments performed with EBR-II Mark-II core were in agreement with the above observations. In these experiments, it has been observed that the two most important failure mechanisms were stress rupture of the cladding for high burnup elements and eutectic wastage of the cladding for low burnup elements. It is argued that the fuel cladding mechanical interaction is not important. The failure mechanisms are explained as [35]:

> "When the cladding temperature is above the eutectic temperature, the stress rupture breach will occur sooner then the measured eutectic penetration rates would predict. Element breach will ultimately be the result of thinning of the cladding by eutectic penetration to the point where stress rupture can occur. Consequently, the stress rupture mechanism will control element lifetime of medium or high-burnup elements while eutectic penetration will control the lifetime of low-burnup elements."

When the operating temperature is high enough to cause eutectic formation in a low-burnup element the eutectic liquid is able to flow downward and solidify since the fuel and cladding are not in contact. However, in a high-burnup element the eutectic liquid causes the fission gas bubbles to coalesce and avoids further eutectic formation by absorbing some of the eutectic liquid in the pores. The observed eutectic penetration distances were 33% of the cladding for fresh fuel operating at 54^{o}C above the eutectic temperature. For a high-burnup fuel element (7.69%) the penetration was 4.2% for an operating temperature of 78^{o}C above the eutectic temperature. Also two fuel assemblies were operated slightly above the eutectic temperature for 12 hours without failure [35]. For EBR-II fuel elements, the time to cladding breach due to eutectic formation only was correlated as [35]

$$t_{cb} = 5.4 \times 10^{-15} exp\left(\frac{44574}{T}\right) \tag{2.1}$$

where t_{cb} is the breach time in seconds for the penetration of the cladding whose thickness is 0.305mm and T is the operation temperature in K. These results were obtained by measuring the penetration rates in an eutectic bath. Since there are several mechanisms that inhibit eutectic penetration in fuel elements the above equation was found to be conservative [35].

The eutectic temperature of ternary fuels is not known as precisely as the eutectic temperature of the EBR-II fuel element. Earlier references [19,21,36] list the eutectic temperature for ternary fuels as 825^{o}C and attribute this increase to the addition of zirconium whereas a recent reference [37] gives 720^{o}C for the eutectic temperature. There are not enough studies done with ferritic cladding materials to precisely define the eutectic temperature. Table 2.3 lists the recent experimental data for U-Pu-Zr fuels with various types of cladding [38].

Table 2.3: Eutectic temperatures of U-Pu-Zr fuel with several cladding materials [38]

Fuel	Cladding	Temperature (°C)	Time (h)	Condition
U-8Pu-10Zr	HT9	731	300	NEF[a]
U-8Pu-10Zr	HT9	757	300	NEF
U-8Pu-10Zr	T91[b]	706	300	NEF
U-8Pu-10Zr	T91	731	300	EF[c]
U-8Pu-10Zr	T91	757	300	EF
U-8Pu-10Zr	304 SS	758	700	NEF
U-8Pu-10Zr	316 SS	777	150	NEF
U-8Pu-10Zr	316 SS	802	150	EF
U-8Pu-10Zr	D9[d]	758	700	EF
U-8Pu-10Zr	D9	777	150	EF
U-8Pu-10Zr	D9	802	150	EF
U-19Pu-10Zr	HT9	731	300	EF
U-19Pu-10Zr	HT9	757	300	EF
U-19Pu-10Zr	T91	731	300	EF
U-19Pu-10Zr	D9	758	300	EF
U-15Pu-11Zr	HT9	656	724	NEF
U-15Pu-11Zr	T91	757	300	NEF
U-15Pu-11Zr	D9	802	150	NEF
U-15Pu-11Zr	316 SS	802	150	NEF
U-15Pu-11Zr	304 SS	802	150	NEF

[a]NEF: No eutectic formation.
[b]T91: 9Cr-1Mo ferritic stainless steel.
[c]EF: Eutectic formation.
[d]D9: 14Cr -15Ni-1Mo austenitic stainless steel.

Based on the temperatures listed in Table 2.3, a higher zirconium concentration of the fuel element results in a remarkably high eutectic temperature for all the cladding alloys. The high plutonium content elements have consistently lower eutectic temperatures. Also a comparison of the eutectic temperatures for U-8Pu-10Zr fuel with HT9 and T91 cladding alloys shows that the chromium content of the cladding alloy is another important consideration. Since the fuel configuration of the TR is very similar to the U-8Pu-10Zr fuel with HT9 cladding, 750^{o}C will be used for the eutectic formation temperature. This is a rather conservative temperature since the restructuring of the fuel element will produce high zirconium concentrations near the cladding resulting in a higher eutectic formation temperature.

2.1.1.2 Failure Mechanisms and Prediction The failure mechanisms of the fuel elements during transient conditions can be due to eutectic penetration, fission gas pressure, high pressure caused by vaporization of the bond sodium or differential thermal expansion of fuel and cladding. The mechanism that causes the failure can be any one or any combination of these mechanisms depending on the transient and the previous operating conditions. The severity of the transient in terms of the maximum temperatures and the duration of the elevated temperature or the rate of increase in the power are also important. Typically the eutectic temperature may be considered to be the lowest temperature limit in terms of transient operation, and it depends on the alloy in consideration. However, in order to predict whether a cladding breach will occur during a particular transient one has to be able to predict the thinning of the cladding due to eutectic penetration

throughout the transient. The evaporation temperature of the bond sodium is approximately 1150^oC which also corresponds to the melting temperature of the fuel. The cladding melting point is even higher ($\approx 1400^oC$).

During normal operation the basic mechanism of failure for the Mark-II core in EBR-II was cracks that occurred outside the cladding surface. It is argued that the increase in the plenum pressure coupled with radiation induced swelling and creep caused the crack to penetrate into the inside surface of the cladding. Most of the cladding breaches occurred at a location where a stress concentration was high. It is stated that [35]

> "Continued operation after a breach of this type is not a safety issue and, in EBR-II, breached driver fuel elements are allowed to remain in the reactor until the next scheduled shutdown."

Another important result is that, although negligible below 10% burnup, cladding breach events increased rapidly thereafter [26].

Transients such as loss of flow or overpower accidents result in higher operating temperatures. Higher operating temperatures will result in an increase in the fission gas pressure in the fission gas plenum and in the fuel. If the transient temperatures are higher than the eutectic formation temperature the eutectic compound will cause thinning of the cladding. If the eutectic penetration rate is high enough to cause cladding breach, depending on the location of the breach either fuel and sodium or fission gases and sodium will come into contact. In the first case the compatibility of fuel and sodium and in the second case the sodium voiding effect caused by the fission gases are important parameters that influence the outcome of the accident.

Both steady state and transient operation failure predictions will be based on the cumulative damage fraction (CDF) approach. In this approach the cladding is

assumed to fail if the cumulative damage fraction which is defined as [39]

$$CDF = \int_0^{t_f} \frac{dt}{t_r(\sigma_\theta, T)} \tag{2.2}$$

is equal to unity. In Eq. (2.2) t_r is the time to rupture which is a function of cladding midwall hoop stress (σ_θ) and cladding temperature (T), and t_f is the final time in consideration. Cladding hoop stress contains contributions from fission gas pressure and thermal stresses.

In order to predict the rate of eutectic penetration into the cladding Eq. (2.1) will be used. It is realized that this equation is for the U-Fs and 316 SS combination. However, due to lack of better information on the eutectic penetration rates in U-Pu-Zr fuels and HT9 cladding and the similarity between the fuel types this seems to be the best choice. Rearranging Eq. (2.1) so that it gives the penetration rate into the cladding for temperatures greater than the eutectic temperature

$$\dot{x} = 5.55 \times 10^{10} exp\left(-\frac{44574}{T}\right) \tag{2.3}$$

where $\dot{x}$ is the penetration rate into the cladding in m/s and T is the cladding inner surface temperature in K.

The amount of fission gas in the plenum and fuel depend on the burnup level of the core. The maximum pressure can be obtained for a high burnup fuel due to increased amount of released fission gas and also decreased plenum volume due to axial fuel swelling. If the fission gas in the plenum is assumed to be an ideal gas then the pressure in the fission gas plenum can be calculated by using ideal gas relationships. The prediction of fission gas pressure in the fission gas plenum at a given burnup level and operating temperature will be made based on the approximate model described in reference [23] and mentioned in Section 2.1.1.1.

Until 2% atomic burnup the plenum is assumed to be at atmospheric pressure. For burnups greater than 2% the fission gas pressure in units of MPa is computed by

$$P_{fg} = 0.1013 \frac{T}{298.15} 3.5 \frac{V_f}{V_p} BU \tag{2.4}$$

where T is the fission gas plenum temperature in K, V_f and V_p are the fuel and fission gas volumes and BU is the atomic burnup in percent. Since the main source of loading on the cladding is fission gas pressure, in Eq. (2.4) all the fission gas is assumed to be released to the plenum resulting in a conservative prediction for the plenum pressure.

An interesting property of the metal fuels is to exhibit rapid, large-scale swelling when subject to overheating because of the reduction in the strength of the fuel material at high temperatures [23]. As mentioned earlier, the retained fission gas fraction is relatively independent of the burnup level at high operating temperatures. For burnup levels higher than 2% the fission gas retained would be seven times the fuel volume if this gas were expanded to standard temperature and pressure [20,23]. The retained gas volume will increase in volume due to overheating and will try to expand. Since the fuel strength diminishes with increasing temperature, the fission gas can expend freely. This expansion has important effects in terms of introducing negative reactivity feedback at high temperatures. The reactivity feedback associated with this rapid expansion was estimated to be an order of magnitude larger, a few cents per ^{o}C [23] than the other reactivity feedback mechanisms which are typically a few tenths of a cent per ^{o}C. In reference [40], it is argued that this expansion is not significant if the fuel and cladding are assumed to be locked to each other. However, for temperatures higher than the eutectic formation temperature the eutectic fluid between the fuel and cladding interface will allow relative

motion of fuel with respect to cladding. The analysis of reference [25] shows that the measured axial elongation of the fuel in overheating cases is twice the amount that will be computed if the fuel and clad are assumed to be locked to each other at temperatures above the eutectic temperature. For rapid increases in temperature, the main mechanism of this swelling is attributed to the growth of bubbles on the existing grain boundaries by diffusion [25,41]. The time scales associated with the expansion precludes other expansion mechanisms from being important.

When a cladding breach occurs, depending on the location of the breach either the fission gas or the fuel will come into contact with the flowing sodium. For a high burnup fuel element the difference between the fission gas pressure and the sodium pressure will cause the fission gas to expand and void the channel in which the fuel element is located. If the breach occurs at the top of the fuel column where the fission gas plenum is located, the positive reactivity effect due to the resulting void in the sodium will be small. Also EBR-II experience indicates that this kind of breach will not affect the surrounding fuel pins. If the breach occurs at a location below the fission gas plenum, then the fuel will come into contact with the sodium. Since the sodium and fuel material is compatible no dangerous reactions will occur.

2.1.2 Effects of Sodium

Sodium is the most commonly used fast reactor coolant. Low fast neutron absorption cross section, high thermal conductivity, low pumping power, compatibility with fuel materials, low cost and high boiling point at atmospheric pressure are among the advantages of sodium as a fast reactor coolant. The high boiling point of sodium allows the primary system to be at atmospheric pressure.

The main disadvantage of sodium is its high chemical activity. Materials exposed to operating in a sodium environment at high operating temperatures may be subject to several forms of corrosion. The basic corrosion mechanism is by mass transfer [42,43]. There is a net movement of material from one part of the loop to another due to composition and temperature differences. In a reactor environment, the materials transported from the hot parts will be deposited in the cold parts.

A form of this mass transfer occurs as carbon transfer from high carbon content components to low carbon content components. Carbon transfer should be of minor importance in the TR, because the core structural and cladding material, HT9, forms stable carbides, hence reducing the carbon transfer potential [34]. The solubility of oxygen in sodium is high at the operating temperatures around 500^oC [44]. Sodium and oxygen react to form sodium oxide which is not very soluble in sodium. This compound is then deposited in the cold parts of the sodium circuit which may result in plugging of narrow passages. Sodium oxide can react with chromium to form a sodium-chromium dioxide which will contribute to the cladding wastage. Since the fuel element configuration in TR uses a tight lattice with pitch to diameter ratio around 1.13, the oxygen concentration in the primary circuit must be kept below 5 ppm [42]. Typically this is done by using cold traps [42] in the cold parts of the circuit. The thinning of cladding surface due to operating in the sodium environment at steady state is be correlated by [39]

$$d = 2.20 \times 10^6 exp\left(-\frac{18127}{T}\right) t_y + \frac{B+C}{1000}\sqrt{t_y} \qquad (2.5)$$

where t_y is the exposure time in years and T is the operating temperature in K. In

Eq. (2.5), B and C are given by

$$B = \begin{cases} 0 & T \leq 844K \\ 0.17T - 143.41 & T > 844K \end{cases} \tag{2.6}$$

$$C = \begin{cases} 0 & T \leq 873K \\ 0.22T - 192.06 & T > 873K \end{cases} \tag{2.7}$$

Sodium ignites in air around 200^{o}C. In order to avoid a sodium fire the containment building must be sealed to avoid air leakage. The reaction of sodium with water releases hydrogen which in the case of a fire will burn. Therefore, contact of sodium with air, and water and hydrogen must be avoided. In the TR concept this is accomplished by using argon as the cover gas on the pool and nitrogen as the containment atmosphere. The sodium water reaction is of major concern in steam generator design.

Sodium upon absorbing a neutron becomes highly radioactive. The resulting nucleus, ^{24}Na, decays by emitting gammas and has a half life of 14.8 hours. This requires gamma shielding around the primary system.

The experience obtained with operating fast reactors using sodium as a coolant shows that sodium technology is well developed and the the above operational problems can be avoided or limited.

The major safety safety concern due to the using sodium as coolant is due to the positive feedback of sodium boiling. If sodium boiling occurs during a transient a large amount of positive feedback, several dollars, will be inserted due to the voiding of the core which may result on a complete failure of the core. The time it takes to void the whole core after boiling starts depends on the core inlet temperature,

the pressure drop characteristics of the channels, and the temperature difference between the surrounding channels; and may be as short as a second. The resulting reactivity insertion in such a short time will result in a very rapid increase in the power generated and dryout of the cladding. Therefore, sodium boiling must be avoided during normal operation and transients.

2.2 Anticipated Transients

Nuclear power plants might conceivably be subject to a large number of accidents during their lifetime. The severity of these accidents ranges from minor operational faults with minor consequences to catastrophic events posing a threat to public. The main safety goal is to reduce the probability of large consequence event occurrence as much as possible and avoid permanent damage to the reactor components during more frequently occurring accidents. The accidents are very commonly a result of imbalances in the production and removal of the power and result from malfunctioning components or from external sources. The first category includes accidents resulting from positive reactivity insertion, decrease in heat removal due to loss of flow or loss of heat sink. The plant control and protection system is normally expected to terminate the accidents in a safe manner, which typically will result in reactor scram should the accident be severe enough. After a reactor scram, adequate cooling must be available to remove the decay heat generated. The accident sequences during which the plant control and protection systems fail to respond might have more severe consequences.

Positive reactivity insertion may be due to a withdrawal of the control element, overcooling of the primary system, sodium voiding resulting from either whole core

sodium boiling or release of entrained gases in the sodium. Decrease of heat removal may be due to loss of power to the pumps, pump mechanical failure, blockage of the associated coolant channel of a fuel pin, loss of secondary sodium flow, intermediate heat exchanger failure, or loss of feedwater supply to the steam generator. The second category of accidents may be caused by external sources, for example earthquakes, tornadoes, missiles, etc., or may occur during normal plant maintenance such as refueling or repairing.

Some of these accidents may occur every year whereas some may not occur during the lifetime of the reactor. For example, for light water reactors, events such as control rod withdrawal, feedwater flow rate increase, and feedwater temperature decrease are expected to occur every calendar year [45]. Primary pump mechanical failure and loss of forced flow in the primary circuit are among the accidents that are expected to occur once during the plant lifetime. In general, an accident during which the plant protection system functions, or a protected accident, will result in a reactor scram and is expected not to cause a reduction in plant lifetime. However, an unprotected accident may result in a complete loss of the plant and release of radioactive materials to the atmosphere. Such accidents are referred to as core disruptive accidents (CDA) and have received a lot of attention [46]. Until recently CDAs were considered as the design basis accidents (DBA) [47,48] and thus as the limiting fault conditions. The reactor must be designed so that for frequent events permanent damage is to be avoided and for limiting fault conditions a coolable geometry should be maintained so that potential danger to the public is avoided.

Since there are a number of accident initiators resulting from failure or malfunction of various components, the design and construction of the plant protection

and control system is subject to stringent requirements in terms of quality assurance and control. It is desirable to have the smallest number of safety related components without comprising the safety of the reactor. A reduction in the components which, if malfunctions occur, would lead to a major accident will help to reduce the number of safety related components.

The configuration and the selection of the basic design characteristics of the TR concept reflect such a concern. Although a probabilistic failure analysis has not been performed to quantify the reduction in failure rates compared to other reactor concepts, basic characteristics of the TR concept indicate such a reduction. These are reduction of the magnitude and frequency of uncontrolled positive reactivity insertions, provisions for natural circulation cooling and passive decay heat removal from the primary system. Only the last two items will described in the following chapters; a short summary of the first item will be given here. More detailed discussion of these can be found in the references cited.

The most common mode of positive reactivity insertion is from control rod withdrawal. The small power produced and the narrow, thin configuration of the reactor core makes it possible to locate the control elements outside the core boxes [2]. This eliminates the use of separate control assemblies in the reactor core. The adopted fuel managment scheme in which refueling is done every ten years reduces the probability of an accident occurring during refueling periods [4]. Also a metal fueled core, by not causing a large reactivity swing, reduces the amount of control rod reactivity required in the core. The reactor vessel is suspended on cables in order to reduce the possibility of reactivity insertion due to seismic events [3].

Apart from a reduction in the accident initiators, a reactor that can survive

a wide range of accidents without relying on the plant control system or operator action would permit major savings, both by limiting the consequences of accidents and by direct economy. The major parameters that influence such behavior are the initial margins to failure, the feedback reactivity coefficients and the thermal hydraulic behavior of primary system components. The reason that only the primary system components are included in this list is due to the decoupling of the primary and secondary systems that results from the large heat capacity of the pool. The unprotected accidents are described in Chapter 4.

The use of sodium as the primary coolant enables using self actuating shutdown devices [18,49]. Such devices are based on the principle that certain materials lose their magnetic properties at high temperatures. Such a plant protection system will be described in Chapter 5.

3 DESCRIPTION OF MAIN COMPONENTS

3.1 Core

The thermal-hydraulic behavior of the core of the TR is important from both the safety and operational points of view. In general it is desirable to have a reactor core that can be fabricated and controlled easily. In order to achieve inherent safety, the configuration of the core must produce reactivity feedbacks that mitigate the consequences of an upset in the operating conditions. Since sodium voiding is the only way to initiate a CDA this requires reduction of the sodium volume fraction in the core which can for example, be achieved by using a smaller pitch between the pins in the reactor core [50]. In order to have large margins to sodium boiling and eutectic formation the core outlet temperature should be reduced which implies a larger sodium flowrate through the reactor core. In order to assure the adequate cooling of the reactor when the pumping power is lost requires a low pressure drop in the core to help natural circulation. Therefore, there are several competing arguments with regard to the layout of the reactor core and the final layout is a compromise between these competing effects.

The core of the TR is composed of five rectangular boxes containing the fuel and blanket pins. The fuel material is U-Pu-Zr metallic alloy. The pins are separated from each other by the use of helically wrapped wires along their length. The core

boxes are located on a table on the inlet plenum. The control element guides are located at the sides of the core boxes. The important geometrical dimensions of the core are given in Table 3.1. The major differences of the layout of the TR core from the currently employed core concepts are;

- The prismatic shape of the core enabling reactor control by the control rods outside the reactor core,
- The elimination of subassemblies resulting in a simple structure and a more uniform core exit temperature due to mixing,
- Closely packed large diameter fuel pins which can be manufactured easily and enables the amount of sodium in the core to be reduced,
- A large fission gas plenum reducing the fission gas induced stresses on the cladding.

The first and the third point in the above list are direct consequences of the small power and power density of the reactor. The main disadvantage of the configuration of the reactor is the high pressure drop due the small pitch between the fuel pins. However, the increase in the pressure drop in the core can be compensated by changes through the other parts of the primary circuit or by decreasing the length of the fission gas plenum. In Section 4.9, it will be shown that with the current dimensions of the fission gas plenum cladding failure due to fission gas pressure does not occur even during unprotected accidents.

Figure 3.1 shows the axial variations of the coolant, cladding inner surface and fuel centerline temperatures for the average core conditions. The margin to

Table 3.1: Trench Reactor core design parameters

Parameter	Value
Number of Boxes	5
Box width (m)	0.52
Box Length (m)	1.30
Core Area (m^2)	3.432
Core Volume (m^3)	5.148
Number of fuel pins per box	4690
Clad outer diameter (cm)	1.20
Clad inner thickness (cm)	0.057
Fuel Diameter (cm)	0.968
Wire wrap diameter (cm)	0.05
Wire wrap pitch (cm)	50.0
Fuel pin pitch (cm)	1.30
Active fuel length (m)	1.50
Lower axial blanket length (m)	0.10
Upper axial blanket length (m)	0.10
Fission gas plenum length (m)	2.00
Average Reynolds Number	70516
Average Peclet Number	316
Average Sodium Velocity (m/s)	6.84
Core exit temperature (°C)	485
Core inlet temperature (°C)	343
Core flow rate (kg/s)	4400
Core pressure drop (kPa)	876
Max. fuel temperature (°C)	590
Max. clad inner temperature (°C)	493
Fuel time constant (s)	0.35
Coolant transit time (s)	0.22
Transport time lag of coolant (s)	2.06

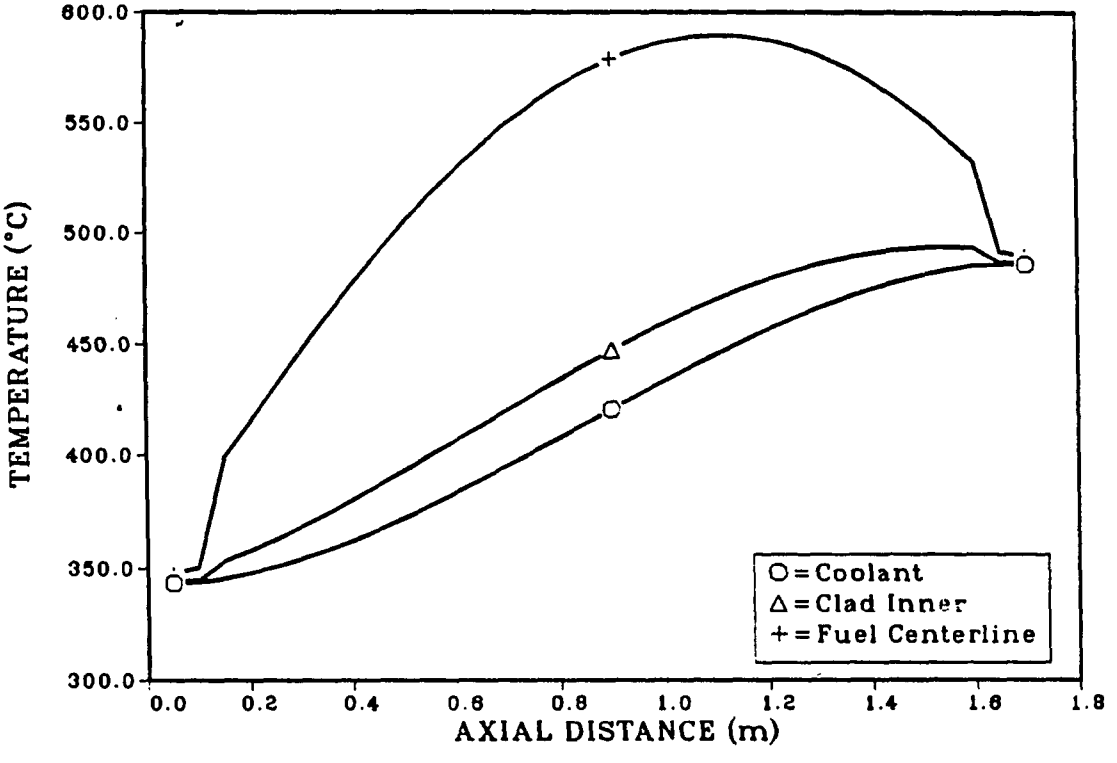

Figure 3.1: Axial temperature variation for fuel, clad and coolant

sodium boiling is approximately 400^oC and the margin to eutectic formation is 250^oC. The core pressure drop is 876kPa. Figure 3.2 shows the radial variation of the temperature at selected axial locations for an average fuel pin. The effect of the high thermal conductivity of the fuel and the cladding as well as the high heat transfer coefficients that can be achieved by using a metallic coolant can be seen from the low temperature drop between the fuel centerline and the coolant bulk temperatures.

It should be noted that almost all the correlations developed for rod bundles are based on data obtained from sodium experiments conducted on hexagonal assemblies containing at most 217 pins; these show a more pronounced effect of the

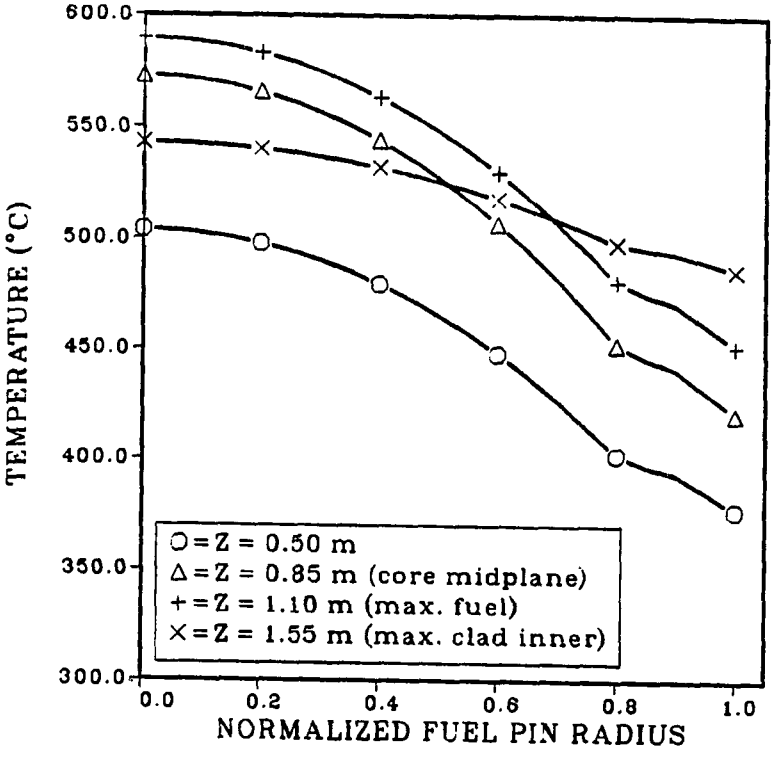

Figure 3.2: Radial temperature distribution in and average fuel pin (fuel pin radius 6mm.)

corner and wall subchannel hydraulic characteristics than should be applicable to the TR concept.

The variation of the cladding and the fuel temperatures with the burnup is also an important consideration. It was mentioned that the fuel element will swell and touch the cladding at approximately 2% atomic burnup. This will result in a change in the effective thermal conductivity between the fuel and the cladding. Also the restructuring of the fuel element due to irradiation will result in different regions with different heat generation rates and different thermal properties due to different porosity and material distribution along the radius of the fuel pin. At steady state,

such structural changes in the fuel element will not influence the coolant sodium axial temperature variation.

Two cases were calculated to see the effects of irradiation on the fuel element thermal behavior. In the first case, it was assumed that the fuel element had swollen and touched the cladding but the effect of restructuring was neglected. The second case accounted for the effects of the restructuring as well as the change in the fuel radius. The radial variation of the temperature across the fuel pin is given in Figure 3.3. The decrease in thermal conductivity results in a higher temperature gradient across the fuel pin; however there is still considerable margin left to the failure limits. Since it is indicated that the restructuring may take place shortly after the irradiation starts [30], this case was also investigated by using the original dimensions of the fuel pin; however, temperature gradients across the fuel pin showed only small variations of the order of few degrees. Since the power density will decrease with increasing burnup, as the fuel column gets longer, the above conditions should set an upper bound on the fuel and cladding operating temperatures for the average core conditions.

In order to estimate the maximum cladding and coolant temperatures due to uncertainties and power peaking factors, the uncertainty factors listed in Table 3.2 were used [39]. Originally, these factors were computed in detail for CRBR cores [51,52] and have been modified for metal fueled cores in an *"overly conservative fashion"* [39]. The overall hot spot factor for the channel in consideration is obtained by a combination of the direct factors and statistical factors. The statistical hot spot factors arise from the fact that the contributing mechanism to the increase in the temperature from the nominal conditions has a normal distribution [51,52].

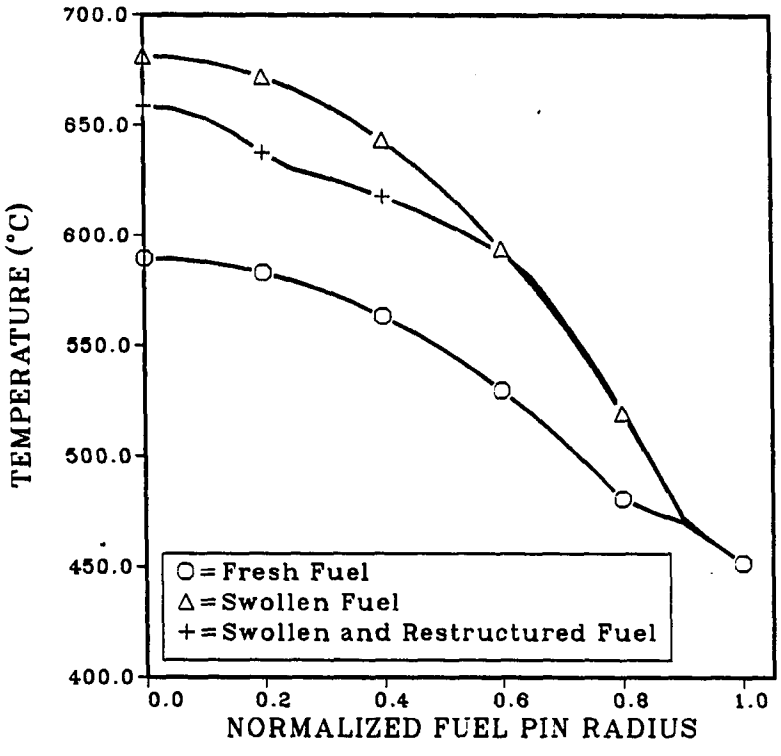

Figure 3.3: Radial temperature distribution in a fuel pin at 2% burnup (axial location: 1.1m, fuel pin radius: 6mm)

An example will be the variation of geometrical parameters due to manufacturing tolerances. The statistical hot spot factors show the magnitude of the deviation from the normal value which is found by applying the direct hot spot factors to the corresponding temperature drop. The details of these procedures are well-documented in references [51,52].

These hot spot factors were applied to the fuel element with the highest peaking factor. The numerical results obtained for the coolant exit, cladding inner surface and fuel centerline are given in Table 3.3. Although the margins to failure are reduced especially for the the swollen fuel elements, there is still considerable margin

Table 3.2: Hot spot factors used in the calculation of peak temperatures [39]

Direct subfactors	Coolant	Film	Clad	Bond	Fuel
Inlet flow maldistribution	1.050	1.012			
Flow modelling	1.140	1.035			
Wire wrap peaking		2.000			
Fuel pin eccentricity		1.010	1.010	1.010	1.010
Physics modelling	1.020	1.100	1.100	1.100	1.100
Control rod banking	1.020	1.020	1.020	1.020	1.020
Combination of direct subfactors	1.245	2.374	1.133	1.133	1.133
3σ subfactors					
Reactor ΔT and inlet temp.	1.143				
Inlet flow maldistribution	1.059	1.016			
Loop temperature imbalance	1.010				
Subchannel flow area	1.011				
Heat transfer coefficient		1.266			
Fuel pin eccentricity		1.010	1.010	1.010	1.010
Clad thickness and conductivity			1.120	1.017	1.100
Coolant properties	1.017				
Flow distribution	1.058	1.005			
Power distribution	1.060	1.065	1.065	1.065	1.065
Power level	1.079	1.079	1.079	1.079	1.079
Fuel maldistribution	1.075	1.075	1.075	1.075	1.075
Combination of 3σ subfactors	1.208	1.295	1.175	1.128	1.162

both for the eutectic and fuel element melting temperatures. These temperatures should be regarded as the upper bounds for all the fuel elements. No credit was taken for the flow mixing due to the wire wrap and large cross sectional area of the core box. The hot spot factor for the cladding circumferential temperature variation due to the wrap was also included in the fuel element centerline calculation. Due to the high thermal conductivity of the fuel this effect should be mitigated around the fuel surface resulting in lower fuel centerline temperatures [39].

Table 3.3: Nominal and peak coolant, clad inner surface and fuel temperatures

	Nominal			3σ		
	Fuel	Clad Inner	Coolant	Fuel	Clad Inner	Coolant
Fresh fuel	590	494	485	802	643	557
Swollen fuel[a]	683	494	485	901	643	557
Restructured[b]	660	494	485	878	643	557

[a]Fuel and cladding are touching and 25% uniformly distributed porosity.
[b]Fuel and cladding are touching and three region fuel. Region properties are; region boundaries r_i/r_{ci}=0.25,0.7,1.0, zirconium weight percent=14,9,11 and porosity percent =0.50,0.02,0.23.

3.2 Intermediate Heat Exchangers

The fundamental function of the intermediate heat exchangers (IHX) is to remove heat from the primary sodium to the secondary sodium. Since the IHX is the boundary between the radioactive primary system and the non-radioactive secondary system, it must be designed to avoid leakage of the primary sodium to the secondary sodium. This can achieved by having the secondary sodium at a higher pressure than the primary pressure. On the other hand, the IHX must be strong enough to endure the pressure pulses resulting from a possible sodium-water reaction in the steam generator should the systems in the secondary system fail to mitigate the consequences of such a reaction. In order to help the natural circulation cooling of the primary system, the pressure drop on the primary side of the IHX should be low.

IHX are typically counterflow shell and tube type heat exchangers. There are two basic IHX design concepts depending on the flow arrangement. In the first one the primary sodium flows in the shell side whereas in the second one the primary

sodium flows in the tube side. The first concept offers advantages in terms of having the higher pressure secondary sodium in the tubes thereby reducing the stresses in the shell; the tubes can be designed to be thick enough to endure the pressure pulses from the sodium water reaction in the steam generator. However, primary in the shell concept is disadvantageous when one considers the higher pressure drops associated with the shell side. The second concept, primary sodium in the tube side, has the main advantage of a low pressure drop on the primary side but needs a thicker shell since the secondary sodium is contained in the shell. The thermal conductivity of the sodium is higher than that of stainless steels which implies that most of the resistance to heat transfer will be across the tube wall. Since the primary sodium in the tubes concept allows a thinner tube wall thickness than the primary sodium in the shell concept, the overall heat transfer coefficient will be larger resulting in a smaller IHX; however, the shell of the IHX needs to be thicker.

The IHX concept selected for the TR is based on a CE design concept [53] with the primary sodium in the tube side. The tube bundle is straight. The reactor vessel head is the main support for the IHX. The basic parameters of the IHX are given in Table 3.4. Figure 3.4 gives the axial temperature distribution in the IHX for the primary sodium, tube wall and the secondary sodium at design conditions.

In this design, the primary sodium enters from the top of the IHX and flows through the tubes downward where it is collected in an exit header and discharged into the lower plenum. The secondary sodium also enters the IHX from the top and then is directed to the bottom of the IHX from where it is distributed into the shell side. After reaching the top of the IHX, the secondary sodium is send to the secondary cooling circuits by the outlet piping. Use of straight tubes contributes

Table 3.4: Basic parameters of intermediate heat exchangers

Parameter	Value
Thermal Rating (MW)	395
Primary inlet temperature (°C)	485
Primary exit temperature (°C)	343
Secondary inlet temperature (°C)	293
Secondary exit temperature (°C)	464
Logarithmic temperature difference (°C)	33.4
Primary flow rate (kg/s)	2200
Secondary flow rate (kg/s)	1800
Number of tubes	3500
Tube outer diameter (cm)	1.27
Tube inner diameter (cm)	1.17
Pitch (cm)	1.78
Active tube length (m)	7.5
Total length (m)	14

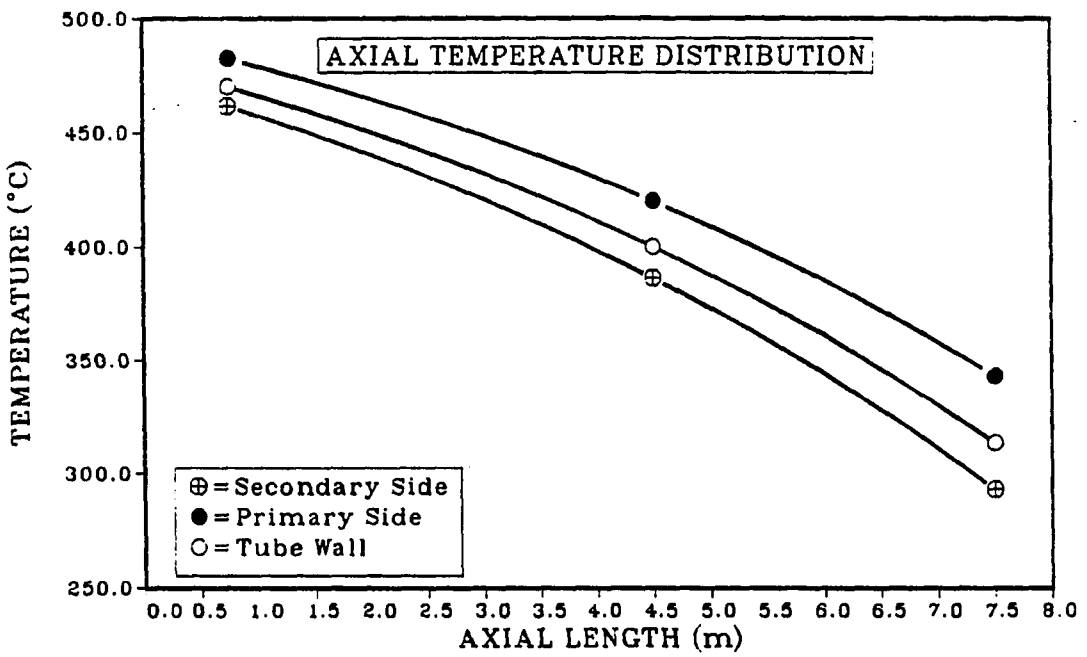

Figure 3.4: Primary, tube and secondary temperatures for the IHX

to the the low pressure drop on the primary side. Also, the construction and maintenance of the straight tube concept is easier than for other tube configurations such as bent tubes.

Since the IHXs are the only heat transfer mechanisms between the primary and the secondary systems, their performance during steady-state and transient operation are important to the safety of the reactor. The influence of the secondary conditions on the primary system is felt through the change in the IHX exit temperature on the primary side for all the transients and, in addition to this, the development of the natural convection head during transients which involve loss of forced flow in the primary system.

3.3 Primary Pumps

The primary pumps are used to circulate the primary sodium through the IHXs and the core. With the exception of the PRISM [54] concept, the primary pumps used in LMRs are vertically mounted centrifugal pumps. This is the type of pump selected for the TR. Table 3.5 summarizes the main parameters of the primary pumps for TR.

The important parameters that influence the safety of the plant are the margin to cavitation and the coastdown characteristics. Cavitation may reduce the lifetime of the pump and the noise generated by the cavitation may interfere with the measurements done by the plant control system. The coastdown characteristics of the primary pumps are important during transients involving a loss of electric power to the pump motors and reactor scrams. A longer pump coastdown is desirable in the first case because it reduces the rate at which the flow decreases and reduces the

Table 3.5: Basic parameters of the primary pumps

Parameter	Value
Rated Head (m)	142
Rated flow (m^3/s)	2.6
Angular speed (rpm)	890
Operating temperature (^oC)	485
Net positive suction head (m)	12.5
Impeller diameter (m)	1.09

peak temperatures obtained during such a transient. A shorter pump coastdown time is desirable in order to avoid a rapid overcooling of the core after a rapid reactor scram. Also, since a large coastdown time implies a large inertia of the pump, the pump speed control can be achieved more rapidly with a short coastdown time since the pump will respond to the changes in the motor torque more rapidly due to its lower inertia. However, since the transient response of the reactor during an unprotected accident involving loss of power to the primary pumps is more limiting, a longer pump coastdown time, and hence, a large inertia of the primary pumps is better in terms of achieving inherent safety.

Basically there are two pumping concepts employed in LMRs. A schematic of these concepts along with the concept employed in TR is given in Figure 3.5. The most common pumping concept is to have the pump suction in a cold sodium plenum where the primary sodium exiting from the IHX enters and the pump discharge is connected to the core inlet. This concept eliminates a need for the connection between the primary pumping and the IHXs but usually requires two separate pools, one containing the hot sodium that exits from the core and the other containing the cold sodium that exits from the IHXs. An example of this concept is the SAFR

plant [55]. The concept employed in EBR-II is a variation of this concept in which the sodium that exits the core is connected to the IHX thereby eliminating the need for a hot pool.

The concept employed in the TR is to have the pump suction in the hot pool and the pump discharge into the IHX. This requires connections between the pumps and the IHX inlet and the IHX exit and the core inlet. This arrangement is very similar to the the arrangement of a loop type plant. This concept can be considered as a loop type plant flow configuration while keeping all the main advantages of a pool type plant such as high margin to cavitation, containment of all radioactive components in the primary system, elimination of the consequences of a pipe break accident, assurance of natural circulation and large heat sink. Besides these advantages the concept employed in the TR helps the core inlet feedback reactivity to be felt early in the transients. The location of the pumps in the hot pool above the core eliminates the need for long shafts. The high operating temperature that the pumps must endure during their lifetime seems to be the only disadvantage. However, the tests conducted on the CRBR pumps show that the high operating temperature does not pose any unsolvable problems [56].

3.4 Steam Generators

The steam generators (SG) are used to transfer the heat from the secondary sodium to the feedwater to produce steam. The use of sodium and water in the same heat exchanger forces most of the design considerations towards eliminating a sodium water reaction. The effect of the SG on the reactor primary system is felt through its effect on the inlet temperature of the IHX at the secondary side

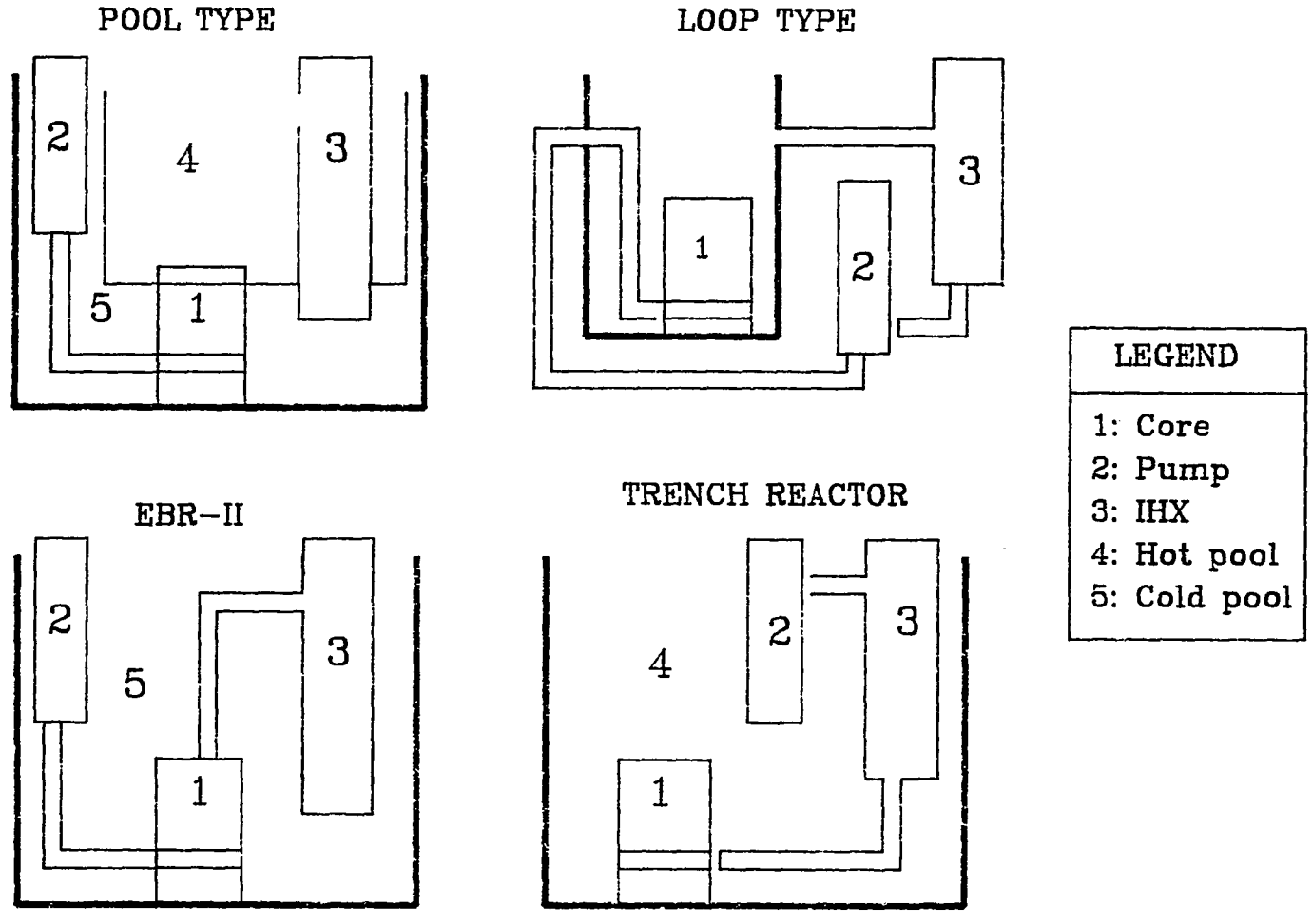

Figure 3.5: Pumping concepts employed in LMRs

and possible transportation of reaction products or pressure pulses to the shell side of the IHX. The second effect should be a minor effect due the ease of limiting the results of a sodium-water reaction in the secondary loop. Therefore, the SG units do not have significant effects on the safety of the primary system. They are conventional heat exchanger units having the necessary precautions taken to avoid a sodium-water reaction.

There are currently several SG concepts employed in LMRs. Table 3.6 gives a summary of these concepts along with some examples. For higher thermal efficiency superheated steam conditions are desirable. The superheat conditions can be obtained by using either once-through (OT) or recirculating evaporation modes. The first has the disadvantage of having certain parts of the SG unit working in the boiling heat transfer region related to departure from the nucleate boiling, whereas, the second has the disadvantage of having a large amount of water inventory which may be dangerous during a large sodium water reaction. The current tendency in the US is towards OT operation mode [37,57] or recirculation operation mode with small recirculation ratios [58]. In order to avoid the sodium water reaction, the tubes in which the water flows are covered with another tube. This concept is employed in EBR-II and has been observed to avoid the sodium-water reaction resulting in a high availability of the SG units. However, using double-walled tubes requires approximately twice the amount of tubes that will be necessary in a single tube SG unit [57] and increases the cost of the SG units considerably. Another design option is to have an integral unit, or to have the evaporators and superheaters as separate modules. Integral units have the advantage of simplicity whereas modular SG can be more efficient.

Table 3.6: Currently employed steam generator concepts [58,59,60,61]

Parameter	Concept	Examples
Evaporation type	Once-through evaporation	Phenix, Fermi
	Recirculating evaporation	CRBR, CDFR
Steam conditions	Superheated steam	EBR-II, Phenix
	Saturated steam	CRBR
Reheat Type	Sodium Reheat	Phenix, PFR
	Steam Reheat	SuperPhenix, SNR 300
	No Reheat	CRBR
Tube type	Straight tubes	SAFR ,EBR-II
	Helically coiled tubes	Phenix
	Hockey-stick configuration	CRBR
Tube wall type	Single wall	Phenix
	Double wall	EBR-II
Module type	Integral module	SuperPhenix
	Separate evaporator and superheater	EBR-II, CRBR
Number of units	One SG per IHX	SuperPhenix
	Several SG per IHX	Phenix(12 modules)
		CRBR (2 modules)

Table 3.7: Basic design parameters of the steam generator units

Parameter	Value
Sodium superheater inlet temperature (°C)	465
Sodium superheater exit temperature (°C)	425
Sodium evaporator exit temperature (°C)	293
Feedwater inlet temperature (°C)	237
Feedwater inlet pressure (MPa)	16
Steam evaporator exit temperature (°C)	342
Steam superheater exit temperature (°C)	425
Steam superheater exit pressure (MPa)	15
Sodium flow rate per evaporator (kg/s)	900
Feedwater flow rate per evaporator (kg/s)	87
Evaporator thermal power (MW)	72
Superheater thermal power (MW)	80
Number of evaporators per IHX	2
Number of superheaters per IHX	1
Number of steam generator units per IHX	1

The basic design parameters for the SG concept employed in the TR is given in Table 3.7. The evaporation mode is OT. The amount of superheat required is approximately half of the amount of heat required for evaporation. This makes the use of two evaporator modules working in parallel and a superheater module possible. With this arrangement the superheaters and the evaporators can be identical units resulting in manufacturing and operational ease.

4 INHERENT SAFETY OF THE TRENCH REACTOR CONCEPT

4.1 Introduction

This chapter will examine the concept of an *inherently safe* reactor as applied to the Trench Reactor (TR). The TR is a metal fueled, pool type, low power density, liquid sodium cooled fast reactor. These three features of the TR which, with the exception of low power density, characterize the recent tendencies in Liquid Metal cooled fast Reactor (LMR) designs, are essential to the inherently safe behavior. The term inherently safe implies that the reactor is able to reach a stable, safe condition after a major change in the balance between the heat production in the reactor core and removal of the produced heat through various mechanisms; and in doing so in the absence of any action from plant control and protective systems the temperatures of various components are not high enough to cause sodium boiling or unacceptable damage to the reactor primary system components. The major disturbances in plant balance can be due to a loss of or increase in heat removal through the intermediate heat exchangers (IHX), or due to a reduction in the coolant flow rate through the reactor core and IHX, or due to an increase in the power production resulting from a positive reactivity insertion. For the rest of this report the acronyms LOHS and LOF will be used for the loss of heat sink and the reduction in coolant flow rate, respectively. The case of positive reactivity insertion which

would most probably result from accidental removal of control elements from the reactor core will be abbreviated as TOP standing for transient overpower accidents. The accidents that result in chilling of the core due to increased heat removal from the IHX will be denoted as overcooling (OCL) accidents.

The severity of these accidents ranges from mild to severe with consequences ranging from a reduced component lifetime to a complete loss of the primary system. The expected rates at which these accidents occur range from frequent to infrequent. Also, although very small, there exists a probability that a combination of these accidents may occur simultaneously. The frequency of LOHS and LOF accidents were estimated to be approximately 0.2/reactor-year and for TOP resulting from a single control rod withdrawal to be 0.01/reactor-year [62]. These accidents will normally trigger the plant protection system and will result in a reactor scram. Based on light water reactor data the failure to scram upon demand was estimated to be $3x10^{-5}$ per demand [62]. Then, the probability of the unprotected accidents occurring is at the order of 10^{-6}. The probability that a combination of these accidents will occur simultaneously will be even smaller. These combined accidents are thus characterized as "*it appears that the likelihoods of these combination scenarios are so remote that their contribution to risk is negligible...*" [62].

There are two different time scales for the unprotected transients; one characterizes the rapidly developing initial phase of the transient the other characterizes the quasi-steady termination phase of the transient. The acceptable temperature levels and damage levels are different for each of these phases. The limiting temperatures are selected so that the core and vessel integrity is not challenged. The nominal temperatures obtained from the simulation program and the temperatures

with 3σ hot spot factors applied will be considered. Table 4.1 lists the limiting temperatures for accidents. For the rapidly developing initial phase of the transient, which is typically less than half an hour, the sodium boiling temperature becomes the limiting temperature. Although the eutectic formation temperature is lower than the sodium boiling temperature, cladding failure due to eutectic formation requires a considerably longer time at operating temperatures slightly above eutectic temperature. The thinning of the cladding due to eutectic formation is rapid for temperatures close to and higher than the sodium boiling temperature. The cumulative damage fraction method of Section 2.1.1.2 will be used to estimate the damage fraction accumulated by the cladding during the accident. A cumulative damage fraction of 1.0 will indicate that the cladding has failed. During the termination phase of the transient, which can be as long as days, the eutectic formation temperature and the creep rupture of the structural components of the primary system become the important limiting temperatures. Therefore, the core exit temperature limit is in the short term the sodium boiling temperature and in the long term the eutectic formation temperature. The pool temperature is limited by the temperature at which the creeps of the structural components are accelerated. Other than the upper temperature limits on various components, due to the rapidly changing temperatures thermal shock may be a problem in the initial stages of the transient [37].

The consequences of a coupled accident such as a combined TOP-LOF accident will be greater than the above accidents. Although it is possible to modify the basic plant parameters so that a combined unprotected accident will not result in severe damage to the primary system components, the small probability that these events

Table 4.1: Limiting temperatures in unprotected accidents

Limit	Temperature (°C)
Fuel Melting	1200
Sodium Boiling	902
Eutectic formation	750
Vessel Integrity	676

will occur makes such modification unlikely to be economical or reasonable. Instead it will be required that the consequences of the accident be contained in the primary system and that release of radioactive materials to the atmosphere should not occur.

4.2 Nuclear Kinetics Parameters

Important kinetics parameters are the delayed neutron spectra and the reactivity feedback coefficients. The delayed neutron yield, prompt neutron lifetime and reactivity coefficients were evaluated by Mr. R. Schmidt [2] and Dr. J. Sankoorikal [50]. The 6 group delayed neutron yields are given in Table 4.2. The decay constants for each delayed neutron group were taken from the corresponding ^{239}Pu data [63]. Total delayed neutron yield is β=0.00311. Prompt neutron lifetime is 0.1004 10^{-6} seconds.

Reactivity feedback mechanisms considered were Doppler, fuel axial expansion, sodium density change, and structure expansion [2,50]. Doppler and fuel axial expansion coefficients are associated with fuel temperature changes whereas sodium density and structure expansion effects are associated with average sodium temperature changes in the core. A change in fuel temperature will result in a longer fuel pin hence a reduced number density. The radial expansion of the fuel pin will

Table 4.2: Delayed neutron fractions and decay constants

Group No i	Delayed Neutron Fraction β_i	Decay Constant λ_i (s)
1	0.000118	0.0129
2	0.000870	0.0311
3	0.000671	0.1340
4	0.001019	0.3310
5	0.000320	1.2600
6	0.000109	3.2100

force the gap sodium out and therefore will reduce the sodium number density. The doppler effect is due the effect of temperature on the capture and fission cross sections in the resonance region. The effect of an increase in the temperature of the sodium will reduce the number density of the sodium hence increasing the number of neutrons at higher energies and neutron leakage. Also the structural components of the reactor core, such as upper and lower grid plates, cladding and core boxes will expand. This will result in a larger core so that the fuel pins will be separated from each other hence introducing a negative reactivity. In reality an increase in the sodium temperature at core inlet will effect the lower grid plate whereas an increase in the core exit temperature will affect the upper grid plate. The cladding and core box expansion will be related to the average sodium temperature in the core. Also a time delay will exist depending on the heat capacity of the structural component. However, as a first approximation the different time scales and temperatures of the components were neglected and the average sodium temperature in the core was used to determine the effects of the structural expansion effects [2,50]. The reactivity feedback coefficients used are given in Table 4.3.

The coefficients in Table 4.3 relate the changes in the fuel temperature and

Table 4.3: Reactivity feedback coefficients

Mechanism	Reactivity Coefficient $10^{-2}\$/°C^a$
Doppler[b]	-0.165
Fuel axial expansion	-0.116
Sodium expansion	+0.206
Structure expansion	-0.335

[a]Based on β=0.00311. See Table 4.2.
[b]Average assuming $\frac{dk}{dT} = -\frac{0.004089}{T}$ for temperature in the range of 450-600°C.

average sodium temperature to feedback reactivity as

$$\rho_{fd} = (\alpha_d + \alpha_e)\delta T_f + (\alpha_{Na} + \alpha_s)\delta T_{Na} \tag{4.1}$$

where ρ_{fd} is the feedback reactivity α_d, α_e, α_{Na}, α_s are the Doppler, fuel expansion, sodium density and structure expansion reactivity coefficients, respectively. δT_f and δT_{Na} represent the changes in average fuel and sodium temperatures.

This equation does not provide any information about the effects of changes in core inlet temperature, power produced and core flow rate. In order to estimate the effects of a change in core inlet temperature, power and power to flow ratio, one needs to relate these variables to the average fuel and sodium temperatures. Since the heat capacity effects associated with the core are small compared to the amount of power produced, an approximate model of the heat transfer in the core based on quasi-steady-state relationships can be used.

If the quasistatic temperatures are expressed in terms of normalized power, power to flow ratio and core inlet temperature, after elimination of average fuel and average core temperatures the following equation for the feedback reactivity is

obtained [64]:

$$\rho_{fd} = \alpha_{T_{in}} \delta T_{in} + \alpha_{pf} \delta \Phi + \alpha_p \delta p \tag{4.2}$$

where $\alpha_{T_{in}}$ is the reactivity coefficient for the inlet temperature, α_{pf} is the reactivity coefficient for the normalized power to flow ratio and α_p is the reactivity coefficient for the normalized power. The normalized power, flow and power to flow ratio are given by

$$p(t) = \frac{P(t)}{P_0} \tag{4.3}$$

$$w(t) = \frac{W(t)}{W_0} \tag{4.4}$$

$$\Phi(t) = \frac{p(t)}{w(t)} \tag{4.5}$$

respectively. The subscript '$_0$' has been used to indicate the initial values. The explicit expressions for the reactivity coefficients of inlet temperature, normalized power and normalized power to flow ratio are

$$\alpha_{T_{in}} = \alpha_d + \alpha_e + \alpha_{Na} + \alpha_s \tag{4.6}$$

$$\alpha_p = \frac{1}{2}(\alpha_d + \alpha_e)\Delta T_{fuel,0} \tag{4.7}$$

$$\alpha_{pf} = \frac{1}{2}(\alpha_d + \alpha_e + \alpha_{Na} + \alpha_s)\Delta T_{core,0} \tag{4.8}$$

respectively. $\Delta T_{core,0}$ is the difference between the core exit and core inlet temperatures at steady-state conditions. $\Delta T_{fuel,0}$ is the temperature drop in the fuel at steady state conditions. In Table 4.4 a comparison of the numerical values for these coefficients for the TR and some other fast reactors is given.

The power coefficient can be considered as the positive reactivity resulting from a unit decrease in the power. The difference between the power coefficients of

Table 4.4: Core inlet temperature, power, and power to flow ratio reactivity coefficients

Mechanism	Reactivity coefficient			
	TRENCH	IFR-Oxide[a]	IFR-Metal[b]	EBR-II[c]
Inlet temperature, $10^{-2}\$/^{o}C$	-0.41	-0.4	-0.3	-0.22
Power to flow ratio, $10^{-2}\$$	-28.70	-40.0	-30.0	-27.30
Power, $10^{-2}\$$	-11.80	-170.0	-15.0	-2.73

[a]900 MW(thermal) power [64].
[b]900 MW(thermal) power [64].
[c]65 MW(thermal) power and metal fuel [65].

metal fueled reactors and oxide fueled reactors is very large. This arises from the $\Delta T_{fuel,0}$ dependence of the power coefficient. Since the temperature drop across a fuel pin, ΔT_{fuel} is proportional to the ratio of the total power to the thermal conductivity of the fuel or in terms of linear power density P_l (W/m)

$$\Delta T_{fuel} = \frac{P_l}{4\pi k_{fuel}} \tag{4.9}$$

For the same linear power density, a higher fuel thermal conductivity will result in a lower temperature drop across the fuel element. For an oxide fuel element the thermal conductivity is $\approx$2 W/m^{o}C whereas for a metal fuel element the thermal conductivity is $\approx$20 W/m^{o}C resulting in an order of magnitude difference in the temperature drop across the fuel element and the power coefficient. Also for a low linear power density, a lower power coefficient results.

The sum of α_p and α_{pf} is the amount of reactivity that is required to bring the reactor to full power from zero power at nominal inlet temperature and flow rate. In order to shut the reactor at constant core inlet temperature and constant core flow rate the amount of reactivity required for the TR is 40.5 cents. In general, with metal fueled cores less reactivity is required to change the power level. Therefore,

the amount of negative reactivity inserted in the core by the control rods can be reduced a great deal in order to decrease the possibility of high positive reactivity insertion accidents.

The effect of core flow rate on reactivity is reflected through the power to flow ratio term. An increase in the core flow rate will result in a $\delta\Phi$ greater than unity. This will introduce positive reactivity. This effect has to be compensated by the changes in the core inlet and power. The change in the core exit temperature can be related to the change in the core inlet temperature and the power to flow ratio by

$$\delta T_{ex} = \delta T_{in} + \delta\Phi\Delta T_{core,0} \tag{4.10}$$

The reactivity coefficient of the core inlet temperature is the only term through which the effects of the secondary systems can be transmitted to the primary system. An increase in the heat removal rate by the secondary systems will reduce the core inlet temperature resulting in a higher power level while increasing core inlet temperature due to decreasing heat removal rate will cause the power to decrease.

The reactivity feedback mechanisms mentioned above do not include some of the feedback mechanisms which were shown to be significant in similar reactor concepts. The control rod drive expansion due to the an increase in the core exit temperature will cause the control rods to be inserted more into the core. This mechanism was found to contribute more than 50 cents of negative reactivity during unprotected loss of flow accident in both PRISM and Westinghouse concepts [17,49].

4.3 Conditions of Inherent Safety

The basic requirement for inherent safety is the ability of the reactor to adjust the power produced so that it matches the amount of heat removed based on only the reactivity feedback mechanisms. The operating conditions during such a transient should be within safe limits. If the heat removal from the primary system is reduced then the reactor power should decrease. For a complete loss of heat removal from the primary system, this condition implies a neutronic shutdown by reactivity feedback mechanisms. In this case the decay heat removal from the reactor core and from the primary system by inherent means should also be sufficiently high to keep the system within safety limits. If the amount of power produced increases then the reactivity feedback mechanisms should cause the reactor power to decrease to match the amount of heat removal available.

The amount of heat removal by the secondary systems and the core flow rate are the major parameters that can cause considerably large deviations in the heat removal rate from the primary system and the reactor core. Assuming a constant core flow rate, the effect of a change in the heat removed from the primary system will be a change in the core inlet temperature. The change in core inlet temperature at the time when the reactor becomes critical can be expressed by using Eq. (4.2) as [64,66]

$$\delta T_{in} = \frac{\alpha_p + \alpha_{pf}}{\alpha_{T_{in}}}(1-p) \tag{4.11}$$

and the corresponding change in the average core outlet temperature is given by

$$\delta T_{ex} = \left(\frac{\alpha_p + \alpha_{pf}}{\alpha_{T_{in}} \Delta T_{core,0}} - 1 \right) (1-p) \Delta T_{core,0} \tag{4.12}$$

where p is the final normalized power which is equal to the heat removed from the primary system.

For a decrease in the heat removal rate Eq. (4.11) shows that the core inlet temperature will increase and reduce the power level. If no heat is being removed by the secondary systems resulting in a loss of heat sink accident, the amount of power will drop to decay heat levels. In this case the mismatch between the decay heat removal and production will cause changes in the core inlet temperature. The maximum increase in the core inlet temperature is limited by the pool temperature. Once this limit is reached, the large heat capacity of the pool and the mismatch between the decay heat removal and production will determine the rate at which the core inlet temperature changes. The increase in the core inlet temperature and consequently the core exit temperature will be reduced for a reactor having a small power reactivity decrement $(\alpha_p + \alpha_{pf})$ and a large inlet temperature coefficient.

On the other hand, if the heat removal rate increases then the core inlet temperature will decrease resulting in a higher power level. This sequence is called overcooling accident. For a given change in core inlet temperature, the final power level can be approximated by using Eq. (4.2) as [66]

$$p = 1 - \left(\frac{\alpha_{T_{in}}}{\alpha_p + \alpha_{pf}} \right) \delta T_{in} \tag{4.13}$$

and the change in core exit temperature will be

$$\delta T_{ex} = \left(1 - \frac{\alpha_{T_{in}} \Delta T_{core,0}}{\alpha_p + \alpha_{pf}} \right) \delta T_{in} \tag{4.14}$$

In order to reduce the increase in the core exit temperature a large power reactivity decrement and a small inlet temperature coefficient are desirable. The maximum

decrease in the core inlet temperature is limited by the secondary sodium temperature which can not go below sodium freezing temperature [66].

If the change in the heat removal rate results from changing core flow rate then the power level reached can be approximated as

$$p = \frac{\left(1 + \frac{\alpha_p}{\alpha_{pf}}\right) - \frac{\alpha_{T_{in}}}{\alpha_{pf}} \delta T_{in}}{\left(\frac{1}{w} + \frac{\alpha_p}{\alpha_{pf}}\right)} \tag{4.15}$$

and then the change in the core exit temperature is given by

$$\begin{aligned} \delta T_{ex} &= \left(\frac{\frac{\alpha_p}{\alpha_{pf}}}{1 + \frac{\alpha_p}{\alpha_{pf}} w} \right) (1 - w) \Delta T_{core,0} \\ &+ \left(1 - \frac{\alpha_{T_{in}} \Delta T_{core,0}}{1 + \frac{\alpha_p}{\alpha_{pf}} w} \right) \delta T_{in} \end{aligned} \tag{4.16}$$

If the flow rate increases at constant core inlet temperature then the core exit temperature decreases. An increase in core flow rate will also result in an increase in the core inlet temperature if the secondary sodium conditions are assumed to be constant. Therefore, this accident sequence will result in reduced temperatures. The maximum flow rate obtainable is limited by the pump capacity and is typically 15 to 20% higher than the nominal flow rate.

If the core flow rate decreases, then the power will decrease and the core exit temperature will increase. The decrease in the power level will be more if the core inlet temperature also increases and less if the core inlet temperature decreases. The minimum flow rate that can be achieved is limited by the natural circulation flow. Assuming a constant core inlet temperature and small final power level and

flow rate ($p \approx w \approx 0$) the change in the core exit temperature will be [66]

$$\delta T_{ex} = \frac{\alpha_p}{\alpha_{pf}} \Delta T_{core,0} \tag{4.17}$$

This indicates that the power coefficient of reactivity should be small and the power to flow ratio coefficient of reactivity should be large.

In the short term, the rate of decrease in the core flow rate is governed by the time constant of the pump (t_p). However, the decrease in the power is controlled by the delayed neutron decay constant (λ) which is larger than the pump time constant. Therefore, the power decrease is slow compared to the flow rate decrease resulting in a peak in the power to flow ratio and consequently in core exit temperature. The peak in the core exit temperature during such a transient can be reduced if [66]

$$t_p \lambda \left(1 + \frac{\alpha_p}{\alpha_{pf}}\right)^2 |\alpha_{pf}| \gg 1\$ \tag{4.18}$$

Thus, in order to reduce the peak during such a transient a large reactivity coefficient of power to flow ratio and a large pump time constant is desirable.

If the amount of power produced increases as a consequence of positive reactivity insertion then assuming that the core inlet temperature and the core flow rate are at their initial value, the increase in the power can be expressed as [66]

$$p = 1 - \frac{\rho_e}{\alpha_p + \alpha_{pf}} \tag{4.19}$$

and the corresponding change in the core exit temperature is given by

$$\delta T_{ex} = -\frac{\rho_e}{\alpha_p + \alpha_{pf}} \Delta T_{core,0} \tag{4.20}$$

where ρ_e is the amount of externally introduced positive reactivity. In order to reduce the increase in the core exit temperature the external positive reactivity source should be small and the power reactivity decrement should be large.

The increase in the power level will eventually cause an increase in the core inlet temperature since the heat removed from the primary system is less than the power produced. The increase in the core inlet temperature will cause the power to return to its initial value. the change in the core inlet and core exit temperatures for this case can be expressed as [66]

$$\delta T_{in} = \delta T_{ex} = -\frac{\rho_e}{\alpha_{T_{in}}} \tag{4.21}$$

In order to reduce the final temperature levels the inlet temperature reactivity coefficient should be large and the externally introduced reactivity should be small. The increase in the core temperature will be slow since the the pool temperature must increase first.

In summary, in order to achieve an inherent shutdown the following conditions must be met [66]:

- Negative power, power to flow ratio and inlet temperature coefficients.
- Small α_p/α_{pf} coefficient in order to limit the long term temperature increase in the loss of flow accidents.
- $\alpha_{T_{in}} \Delta T_{core,0}/\alpha_{pf}$ should lie between 1 and 2 in order to achieve a safe condition during accidents involving loss of heat sink and overcooling of the core.
- $\rho_e/(\alpha_p + \alpha_{pf})$ should be less than 1 in order to limit the consequences of a positive reactivity accident.
- $t_p\lambda(1 + \alpha_p/\alpha_{pf})^2|\alpha_{pf}|$ should be large relative to a dollar of reactivity in order to reduce the peak in a loss of flow accident.

4.4 Transient Model

The simulation of the TR was performed by using Dynamic Simulator for Nuclear Power plants (DSNP) Revision 3.4 [67] code on a Z-248 personal computer. The trade off between describing the reactor components in detail and long running times dictated the complexity of the simulation program. A simulation program which had an execution time of more than 6 hours for 1000 seconds of plant time was considered to have an unreasonably long execution time.

The simulation program can be described as a lumped-parameter model of the primary system. A somewhat more detailed description of the model is given in the Appendix. The thermodynamic and hydrodynamic simulation flow charts are given in Figures 4.1 and 4.2. The reactor core was represented by two core assemblies, one representing the 3 central boxes and the other representing the 2 edge boxes. For each assembly the fuel, cladding, sodium and structure energy equations were solved. Any interaction of these assemblies with each other was neglected. The power generation in the core was modelled with 6-group point kinetics equations for the fission power and a 4-group model for the decay heat. The reactivity feedback mechanisms considered were Doppler, fuel expansion, sodium expansion and structure expansion. The net reactivity feedback was computed as a weighted sum of the individual feedback reactivities of assemblies. The fission gas plenum model associated with each assembly was approximated as sodium flowing in an insulated pipe. The energy equations for the temperatures of sodium and the pipe wall were solved. The pool model was based on the assumption that the hot sodium that exits the core will be fully mixed in the pool. The vessel cooling by natural convection was assumed to be a linear function of the pool temperature, thus

neglecting any time delay due the heat capacity of the vessel and temperature drop between the pool and vessel temperature. The IHX was simulated by a straight shell and tube counterflow heat exchanger model. The pipes to and from the IHX were simulated by using an insulated pipe model containing a metal node representing the structural components and a fluid node representing the coolant.

The simulation of the hydrodynamics of the primary system was also based on a lumped parameter model. The model was based on the assumption that flow reversal will not occur. The pool was represented by an open tank subject to atmospheric pressure at the top, with inlets at the bottom and exits at the top. The IHX and core assemblies were represented by equivalent channels. In calculating the pressure drops, the acceleration pressure drop was included in the total loss coefficient for each channel. The bouyancy terms were based on the average temperatures in each channel. The time rate of change of IHX and core assemblies' flow rates were solved. The pump was modeled by using the homologous pump characteristics covering the possible operating regions expressed in polynomial form as reported in reference [68].

The major deficiencies of the simulation model are the crude representation of the core thermal processes and the assumption of fully mixed pool. The lumped parameter core model does not allow computation of some of the important parameters such as maximum cladding temperature and maximum fuel temperature; these temperatures must be estimated from the core exit temperature and the power produced in the assembly. The decision to use a lumped parameter core model was based on the execution time of the simulation program. The FUELP2 module of the DSNP with 15 axial nodes took approximately 9 minutes for a second of plant

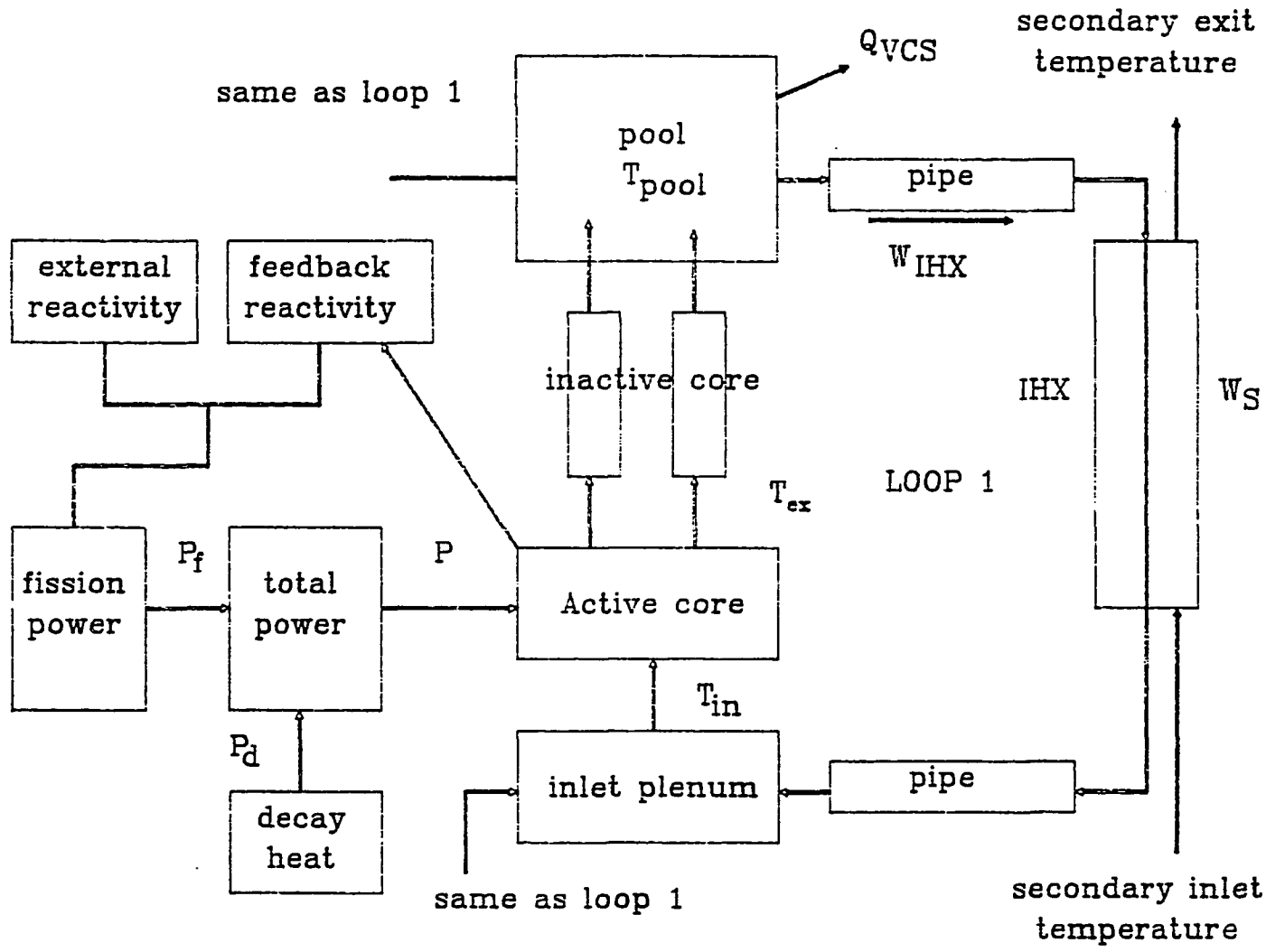

Figure 4.1: Thermal flow chart for the simulation program

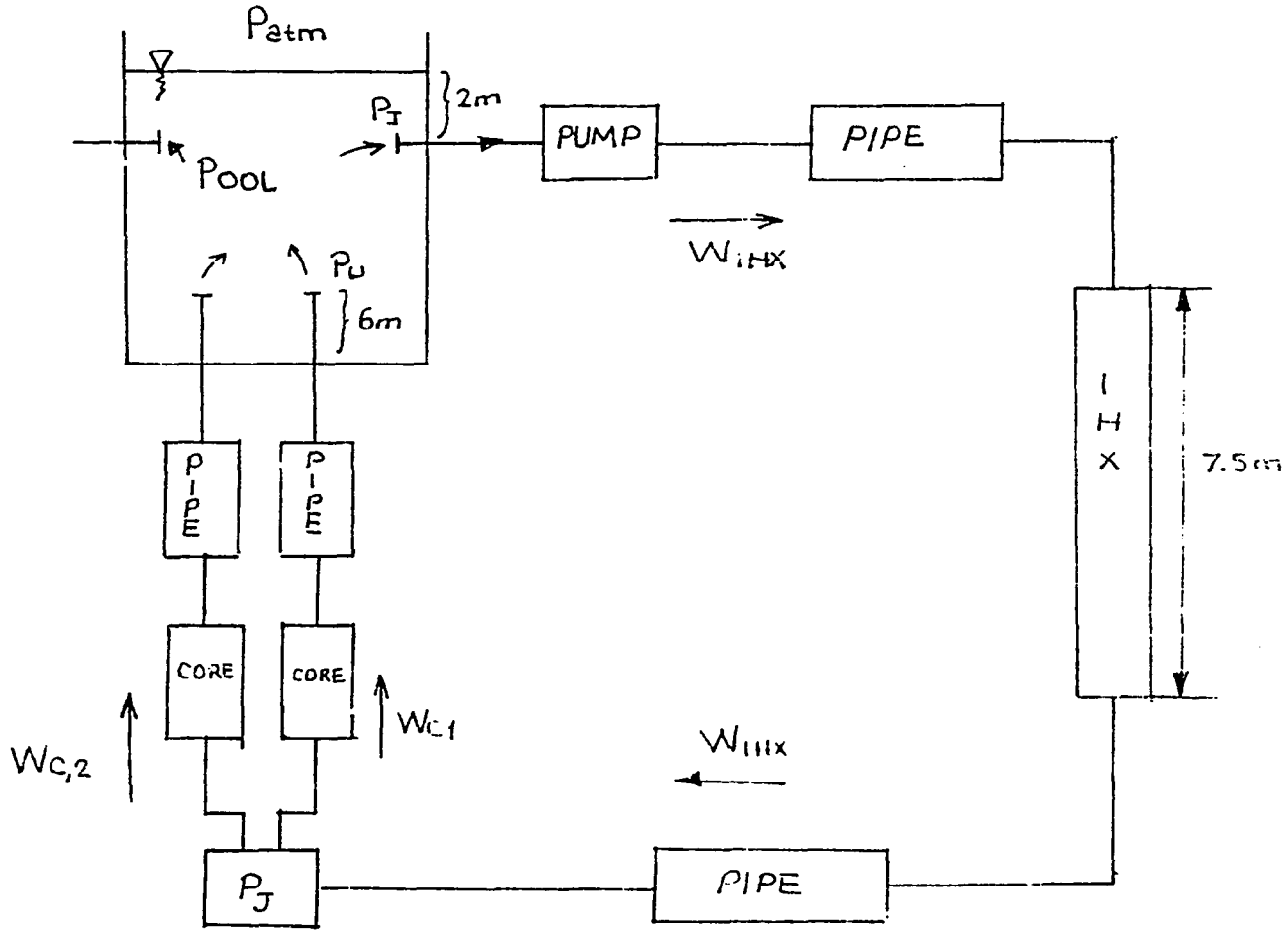

Figure 4.2: Hydraulic flow chart for the simulation program

time. The second major deficiency of the model, namely the assumption of a fully mixed pool, can be justified in terms of good heat transfer characteristics of sodium.

The fact that the secondary loop components were not included explicitly in the simulation program can be justified in terms of the loose coupling between the primary and secondary loop. The secondary loop conditions effect the transient behavior of the plant through their effect on the core inlet temperature. Consider a transient introduced by a malfunction of a component in the secondary loop such as a decrease in heat transfer to water-steam in the steam generator or loss of secondary flow. The temperature and the mass flow rate at the secondary side of the IHX will be affected with a certain time delay. This will change the rate at which the heat is removed from the primary system which will in turn affect the core inlet temperature. Therefore, a detailed knowledge of the transient behavior of the secondary loop is not of major significance to transient behavior of the primary loop as long as the enveloping inlet temperatures at the inlet to the secondary side of the IHX are considered and the delay in the secondary loop is accounted for.

4.5 Loss of Heat Sink Accident

In the loss of heat sink accident (LOHS), it is assumed that the heat removed by the secondary sodium in the intermediate heat exchanger is zero. This implies that the power generated in the reactor core is retained within the primary system boundary except a small portion ($\approx$2% of full power) that is removed from the vessel by natural circulation of the containment atmosphere. Therefore the temperatures within the primary system are expected to rise until the rate of heat produced in the reactor core matches the rate of the heat removal by the vessel cooling system

(VCS).

Numerically, this accident was simulated by reducing the secondary sodium flow rate to 10^{-3} of its initial value at the beginning of the transient. This reduced the rate of heat removal by the secondary sodium to ≈45kW compared to ≈395MW at steady state. The primary pump speeds were kept constant at their steady state value. Only one of the two loops was simulated. The other loop was assumed to behave exactly the same as the simulated loop. As a limiting case, another simulation was performed excluding the IHX. In this case the primary side exit temperature from the IHX was equated to the primary side sodium inlet temperature to the IHX.

A simple description of the transient and the significance of the large heat capacity of the pool can be obtained by considering the pool energy equation and Eq. (4.2). If the heat stored in the reactor core is neglected compared to the large heat capacity of the pool, the energy equation for pool can be expressed as

$$MC_p \frac{dT_{pool}}{dt} = P(t) - Q_{VCS}(t) - Q_{IHX}(t) \tag{4.22}$$

and the variation of core inlet temperature can be approximated by

$$T_{in}(t) = T_{pool}(t - t_d) - \frac{Q_{IHX}(t)}{W(t)C_p} \tag{4.23}$$

where t_d has been used to approximate various time delays between the pool temperature and the core inlet temperature. Since the primary pumps are assumed to be working at their initial speed, the core flow rate is essentially constant implying that the normalized power to flow ratio is equal to the normalized power. The heat removed from the primary through the IHX (Q_{IHX}) vanishes rapidly causing the core inlet temperature to rise rapidly, causing negative reactivity insertion which

can be approximated by (see Eq. (4.2))

$$\rho_{fd} = \alpha_{T_{in}} \delta T_{in}(t) + (\alpha_{pf} + \alpha_p)\delta p(t - t_{pw}) \tag{4.24}$$

where another time delay (t_{pw}) between the variation of core inlet temperature and variation of power has been introduced. As negative reactivity is introduced the power decreases. Since in the TR the heat capacity effects associated with the inlet plenum are small the time delay between the pool inlet temperature and the core inlet temperature is basically the transport time of the sodium from the IHX inlet to the core inlet. Had there been a large heat capacity associated with the lower plenum in the form of a cold pool, such as in EBR-II or SAFR designs, the increase in core inlet temperature will take considerably longer times. If the relative terms in Eq. (4.22) are considered the significance of the large heat capacity of the pool is apparent. Even without any heat removal through the IHX and VCS and neglecting the reactivity feedbacks so that the power is at its initial value the pool temperature will increase by $0.5^oC/s$. If we consider the heat removed by the VCS as

$$Q_{VCS} = aT_{pool} + b \tag{4.25}$$

and neglect the small amount of heat removed through the IHX the pool temperature can be approximated as

$$T_{pool}(t) = T_{pool}(0) + \int_0^t \frac{P(t') - b}{MC_p} \exp\left(-\frac{a}{MC_p}(t - t')\right) dt' \tag{4.26}$$

The numerical values for a and b are $0.04MW/^oC$ and -5.5MW respectively [69]. The pool heat capacity (MC_p) is approximately $1600MJ/^oC$ giving a very small number for the exponential term. Since the core inlet temperature will follow the

pool temperature, the large heat capacity of pool by makes its temperature change very slow and avoids a rapid increase in the core inlet temperature. The importance of a passive VCS can also be inferred from Eq. (4.26). The magnitudes of a and b are insignificant for initial phases of the transient, however; for large times the exponential term will dominate and limit the increase in the pool temperature.

Table 4.5 summarizes the results obtained. The first time value corresponds to the time at which the peak temperature occurs, and the second time value corresponds to the final simulation time. The peak temperatures obtained in both cases are acceptable. At 800 seconds, which is approximately the end of the fast part of the transient the power produced in the reactor is due to decay heat alone. The temperature rise across the core is only 3^oC. The pool and the core inlet temperatures are the same. Hence the primary system is almost isothermal.

The transient response of the reactor can be inferred from Figure 4.3, Figure 4.4 and Figure 4.5. In Figure 4.4 the reactivities are grouped according to the temperature change in the fuel and the coolant (see Eq. (4.1)) so that the fuel feedback reactivity contains the Doppler and fuel expansion coefficients and coolant feedback reactivity contains the contributions from sodium density and structure expansion effects. Figure 4.3 shows the variation of the average core exit,core inlet and pool temperatures.

The transient is driven by the increase in the core inlet temperature. The core inlet temperature increases due to the rapid decay of heat removal from the IHX. Although the secondary flow rate has been reduced to 0.18kg/s which is 0.001 of its initial value, the temperature difference between the primary sodium and tube wall temperatures causes heat to be transferred from the primary sodium to the tubes

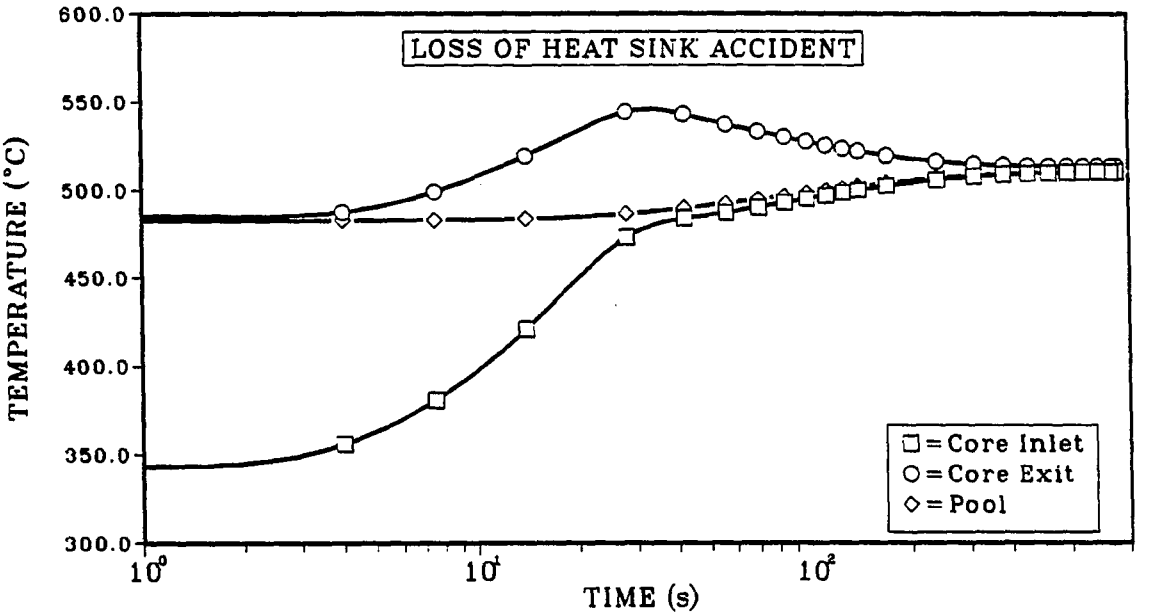

Figure 4.3: Variation of primary sodium temperatures during LOHS accident

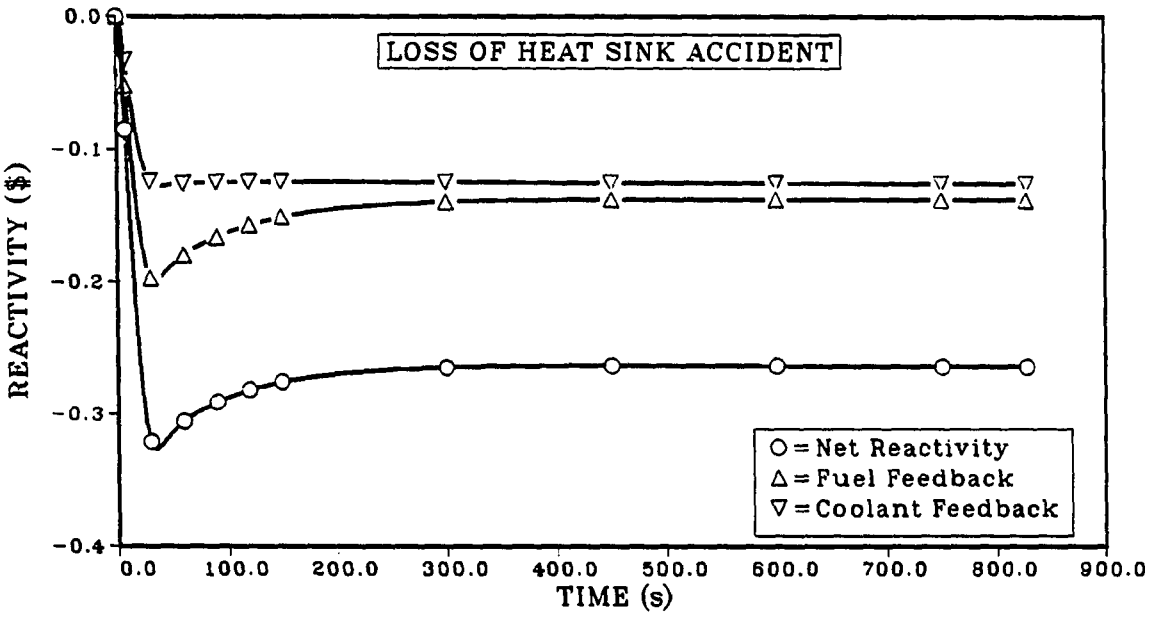

Figure 4.4: Variation of reactivity during LOHS accident

Table 4.5: Results of loss of heat sink accident

	CASE-A[a]		CASE-B[b]	
Time (seconds)	32	800	5.5	800
POWER (MW)				
Fission	329.6	0.14	437.8	0.01
Decay	49.6	16.36	55.8	16.39
Total	379.2	16.50	492.6	16.40
REACTIVITY ($)				
Fuel	-0.1988	-0.1380	-0.2562	-0.1451
Coolant	-0.1259	-0.1259	-0.1443	-0.1291
Net	-0.3247	-0.2639	-0.4005	-0.2742
TEMPERATURE (°C)				
Core Inlet	478.3	510.5	483.2	513.0
Core Exit				
Average	545.7	513.4	568.3	515.9
Central boxes	545.7	513.4	571.3	516.0
Edge boxes	545.6	513.4	560.3	515.9
Pool	487.1	510.5	483.4	513.0

[a]IHX is included in the simulation.
[b]IHX is not included, IHX exit temperature is equal to IHX inlet temperature.

and other structural elements of the IHX. This process continues until the IHX reaches a thermal equilibrium with the primary sodium. Since almost all the power produced in the core is being deposited in the pool, the pool temperature starts to increase, however, the large heat capacity of the pool, ($\approx$1600MJ/^{o}C) limits the rate of temperature increase. Increasing core inlet temperature pushes the core exit temperatures up causing an increase in the average core and fuel temperatures. The increase in the core temperature introduces negative reactivity (Figure 4.4) and a subsequent decrease in the fission power generated (Figure 4.5). Since the core flow rate is essentially constant and equal to its initial value the temperature increase across the core starts to decrease. The maximum core exit temperature is reached

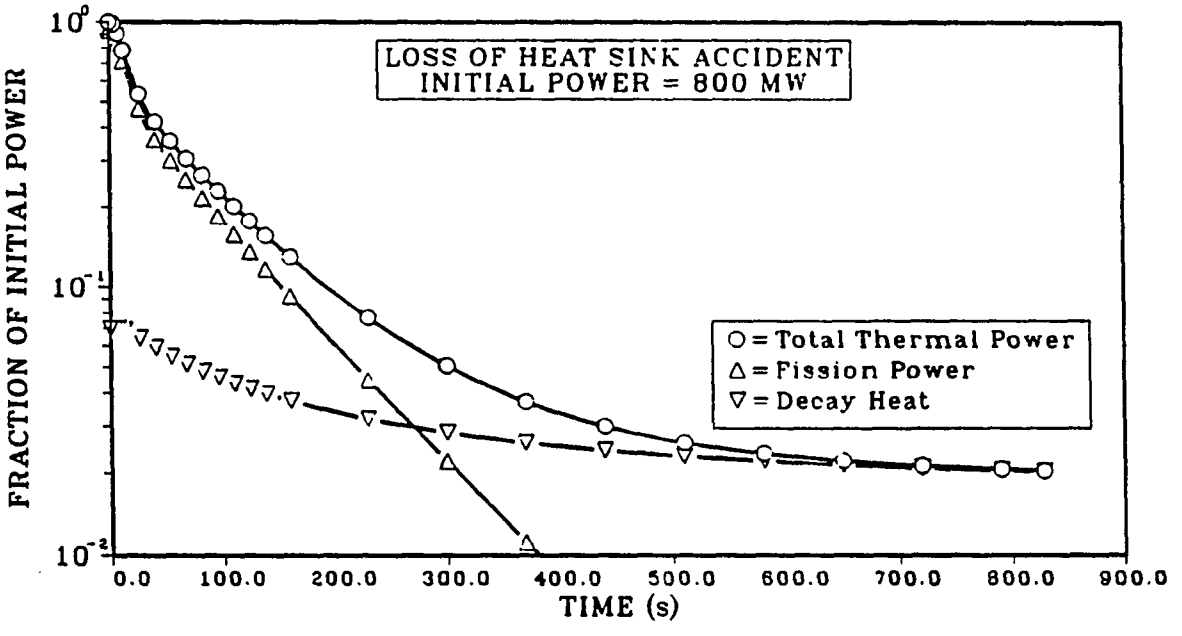

Figure 4.5: Variation of reactor power during LOHS accident

about 32 seconds into the transient. Increasing average core inlet and average temperatures causes more negative reactivity insertion and causes the fission power to drop to 0.01% of its initial value at ≈400 seconds. Then the power from decay of the fission fragments becomes the only source of power production. The elevated temperatures introduce ≈-25 cents of negative reactivity causing the reactor to remain in a subcritical state. The difference between the decay heat production rate and the heat removal rate of the VCS is the driving force for the transient after this stage. The mismatch between these two mechanisms which is of the order of a few MW will cause the pool temperature to change. The time scale of the subsequent changes in temperatures will be determined by the change in the pool temperature. Due to the large heat capacity of the pool and relatively small magnitude of the driving force the pool temperature will change very slowly ($\approx 1^{o}C$

per 800 seconds). This allows more than enough time for any corrective action to be decided upon and implemented to terminate the accident permanently.

The TR responds to the LOHS accident considerably faster than the other pool type fast reactor concepts. The elimination of the cold pool to serve as an inlet plenum to the core allows the core inlet temperature to follow the primary side IHX exit temperature closely. Therefore, the effect of the core inlet temperature associated feedbacks are felt early in the transient causing the power to decrease. The results of a comparable LOHS accident reported in reference [64] show that the reactivity feedbacks are not felt after $\approx$ 80 seconds into the transient. However, in the TR at 80 seconds the reactor thermal power has dropped to approximately 30% of its initial value. It can be argued that such a rapid response may be undesirable. However, the temperature levels associated with the LOHS accident are not near the temperature limits.

If the heat removal rate from the IHX is identically zero, then the above description of the accident is still valid with minor differences. In this case the accident proceeds more rapidly due to an almost instantaneous increase in the core inlet temperature. Therefore the core exit temperature rises more rapidly and reaches its peak value at 5.5 seconds compared to 32 seconds in the previous case. This rapid increase causes a large negative feedback reactivity causing the power to decrease and core exit temperature to increase. The final pool temperature is $\approx 3^{o}$C higher than the previous case.

Further insight to the initial and final stages of the transient can be obtained by considering Eq. (4.2) which relates the changes in core inlet temperature, power to flow ratio and power to the feedback reactivity. Without forgetting the approximate

nature of this relationship in fast transients, we can infer that the reactivity in the core is determined by the competition between the negative feedback effect of the increase in the core inlet temperature and the positive feedback effect of the decreasing power. Since the core flow rate is kept at its initial value, normalized power to flow ratio is equal to the normalized power, that is $\Phi(t) = p(t)$. In this case for the feedback reactivity to be negative the following inequality must hold:

$$\delta T_{in} \geq \frac{\alpha_{pf} + \alpha_p}{\alpha_{T_{in}}} |\delta p| \tag{4.27}$$

In other words, the increase in the core inlet temperature must be high enough to compensate for the positive feedback effects of a unit decrease in the power. For a 1% decrease in power the above equation gives a core inlet temperature increase of $\approx 1^oC$. Since the change in the core inlet temperature is the driving force for the transient and the power induced feedback component will lag behind the inlet temperature induced feedback component, the net reactivity will be negative.

For the reactor to become critical at zero power, the inlet temperature must be approximately 100^oC above its steady state value. Since the pool and the core inlet temperature will remain approximately equal, the time when the reactor will become critical again will depend on the time to cool the pool from 510.5^oC to 443^oC. If no heat were removed from the pool, the pool temperature will rise slowly and the reactor will remain subcritical all the time.

The peak temperatures predicted and the final state that the reactor reaches in the LOHS accident, shows that the reactor is *inherently safe* in the case of a LOHS accident without scram. The passive VCS heat removal rate is important in order to limit the increasing pool temperature, but does not have any effect on the peak core exit temperatures. If the VCS were to fail there is ample time to

take corrective action to terminate the accident permanently without any damage to primary system components.

4.6 Loss of Flow Accident

In the loss of flow accident (LOF), it is assumed that the electrical power to the primary pumps is lost. The resulting transient is due to a gradually decreasing primary flow rate. After the primary pumps stop, the only driving force left for a flow to be established is bouyancy from temperature differences. During such a transient several assumptions can be made regarding the secondary sodium flow rate. One limiting case is to assume that the secondary sodium pumps are at constant speed. The other limiting case can obtained by assuming that the secondary sodium flow rate is zero, hence, resulting in a coupled LOHS-LOF accident. In general these two cases will envelope the possible influences of the secondary sodium flow rate. The inlet temperature of the secondary sodium to the IHX will be important in cases where the secondary flow rate is high. This parameter is also treated parametrically.

In numerical simulation, the transients were introduced by decreasing the pump speed as a function of time:

$$\Omega(t) = \frac{\Omega(0)}{1 + \frac{t}{t_p}} \tag{4.28}$$

where Ω is the pump speed and t_p is the pump time constant. This equation assumes that the kinetic energy is proportional to Ω^2 and friction losses are proportional to Ω^3 [70]. Several values of pump time constant were considered. The secondary flow rate was either kept constant at its initial value or at 10^{-3} of its initial value. In the following discussion, I will use case-A to denote the transients in which the

secondary sodium is at zero flow and case-B to denote the transients during which the secondary sodium flow rate was kept constant at its initial value. In both cases the inlet temperature to the IHX at the secondary side was kept constant at its initial value. Table 4.6 and Table 4.7 summarize the results for both cases for various values of pump time constant.

Figures 4.6-4.8 show how the transient develops for case-A. The decreasing pump speed causes the core flow rate to decrease, and the loss of heat removal from the IHX cause an increase in the IHX exit temperature on the primary side followed by an increase in the core inlet temperature. Decaying flow rate and increasing core inlet temperature result in an increase in the average core temperature and core exit temperatures. The fuel with its low heat capacity and high thermal conductivity is able to follow the increase in the core sodium temperature. Increasing core temperatures introduce negative feedback reactivity and start to pull the reactor power down. The mismatch between decreasing power and more rapidly decreasing flow rate and increasing core inlet temperature causes a peak in the core exit temperatures. After this initial peak, core inlet temperature stabilizes and the core exit temperatures start to decrease. The fission power decreases faster than a LOHS case due to the combined negative feedback effects of power to flow ratio and core inlet temperature. After the fission power has dropped to small levels, the transient is governed by the competition between the decay heat produced and heat removed by the VCS.

The long term temperature variation can be seen in Figure 4.9. The core exit temperatures increase because of the reduced flow rate which is due to natural circulation alone. The core exit and pool temperatures reach another peak and then

Table 4.6: Results of loss of flow accidents for case-A type transients

	Pump time constant (seconds)							
	10		20		30		40	
Time (seconds)	78	1000	78	1000	70	1000	64	1000
POWER (MW)								
Fission	103	0	123	0	152	0	175	0
Decay	36	16	37	16	39	16	41	16
Total	139	16	160	16	191	16	216	16
REACTIVITY ($)								
Fuel	-.342	-.261	-.289	-.257	-.259	-.242	-.243	-.227
Coolant	-.212	-.183	-.185	-.181	-.168	-.173	-.158	-.167
Net	-.555	-.443	-.474	-.437	-.428	-.415	-.401	-.394
TEMPERATURE (^oC)								
Core Inlet	454	495	478	500	482	502	483	504
Core Exit								
Average	700	616	635	607	607	594	591	581
Central Boxes	711	620	641	612	610	599	593	586
Edge Boxes	675	605	624	597	600	583	586	572
Pool	492	500	493	503	493	504	493	505
NORMALIZED								
Flow	0.101	0.023	0.182	0.026	0.275	0.030	0.360	0.036
Power to flow ratio	1.722	0.850	1.098	0.755	0.870	0.644	0.751	0.549
Core ΔT	1.732	0.854	1.112	0.757	0.882	0.642	0.763	0.547
IHX ΔT	0.262	0.033	0.106	0.017	0.078	0.011	0.067	0.008

Table 4.7: Results of loss of flow accidents for case-B type transients

	Pump time constant (seconds)							
	10		20		30		40	
Time (seconds)	80	1000	118	1000	160	1000	190	1000
POWER (MW)								
Fission	207	56	233	60	237	65	253	71
Decay	40	19	39	19	38	19	38	20
Total	247	75	272	79	275	84	291	91
REACTIVITY ($)								
Fuel	-.159	0.041	-.087	0.040	-.053	0.038	-.036	0.036
Coolant	-.117	-.041	-.082	-.042	-.067	-.042	-0.58	-.042
Net	-.276	0.000	-.170	-.002	-.120	-.004	-.094	-.006
TEMPERATURE (^{o}C)								
Core inlet	293	293	293	293	293	293	293	293
Core exit								
Average	710	592	657	592	633	592	620	593
Central boxes	728	610	672	611	647	612	632	612
Edge boxes	672	555	626	553	605	554	593	554
Pool	493	505	496	510	500	514	502	518
NORMALIZED								
Flow	0.107	0.045	0.134	0.047	0.145	0.050	0.159	0.054
Power to flow ratio	2.900	2.104	2.542	2.103	2.380	2.107	2.291	2.107
Core ΔT	2.942	2.111	2.570	2.110	2.402	2.114	2.308	2.116
IHX ΔT	1.434	1.526	1.460	1.561	1.485	1.590	1.501	1.614

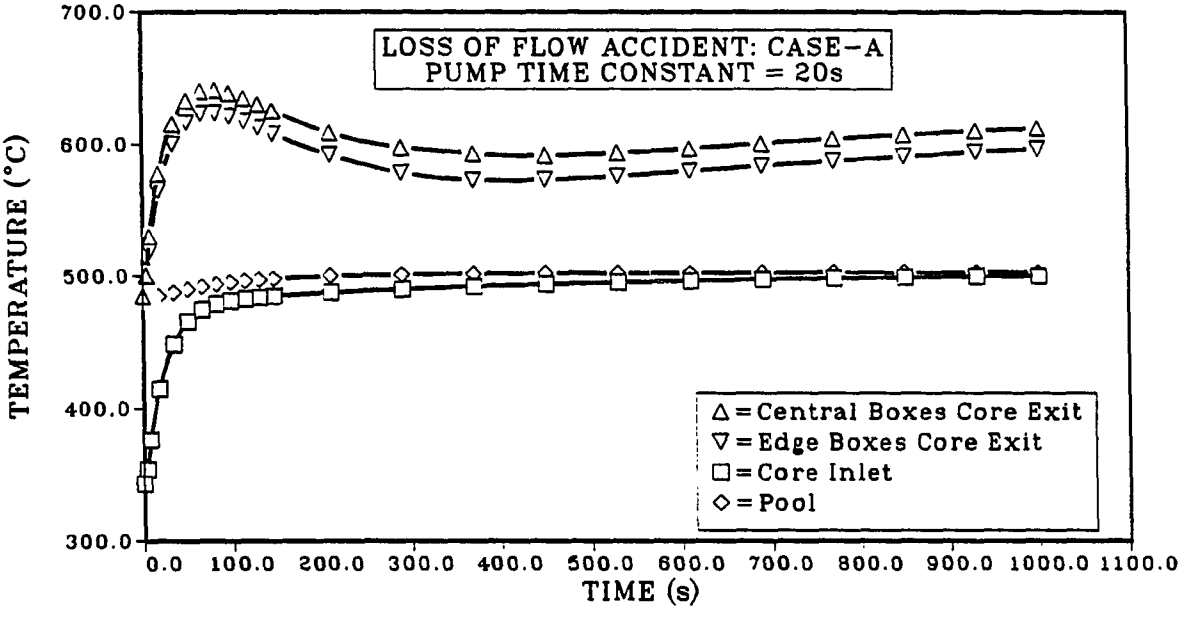

Figure 4.6: Variation of primary sodium temperatures during case-A type LOF accident

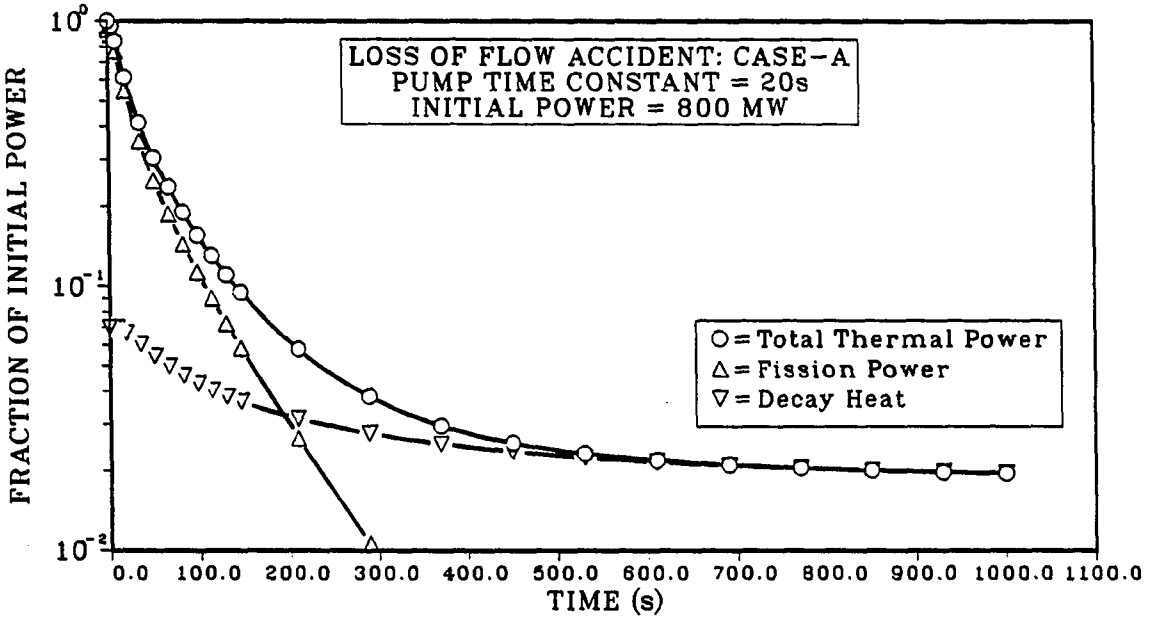

Figure 4.7: Variation of reactor power during case-A type LOF accident

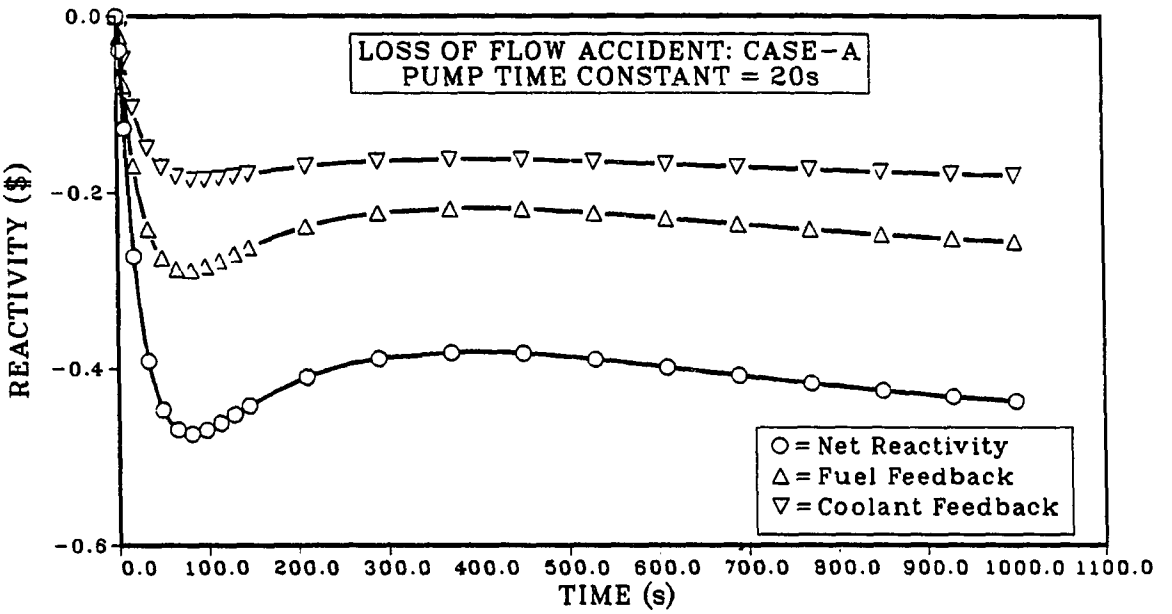

Figure 4.8: Variation of reactivity during case-A type LOF accident

start to decrease due to the heat removed by the VCS. The elevated temperatures, by introducing negative reactivity, cause the reactor to stay in a subcritical condition. The rest of the transient proceeds as LOHS accident with a reduced flow rate.

For case-B, the transient develops in a different manner. Figure 4.10 shows the variation of core exit, pool and core inlet temperature. Decreasing core flow rate cause the primary exit temperature from the IHX to reach the secondary inlet temperature to the IHX asymptotically. In this case, the negative feedback due to the increase in the power to flow ratio has to compensate for both the positive feedbacks from decreasing core inlet temperature and decreasing power. Since a unit increase in power to flow ratio introduces more negative reactivity than the combined effect of decreasing core inlet temperature and power, the net reactivity

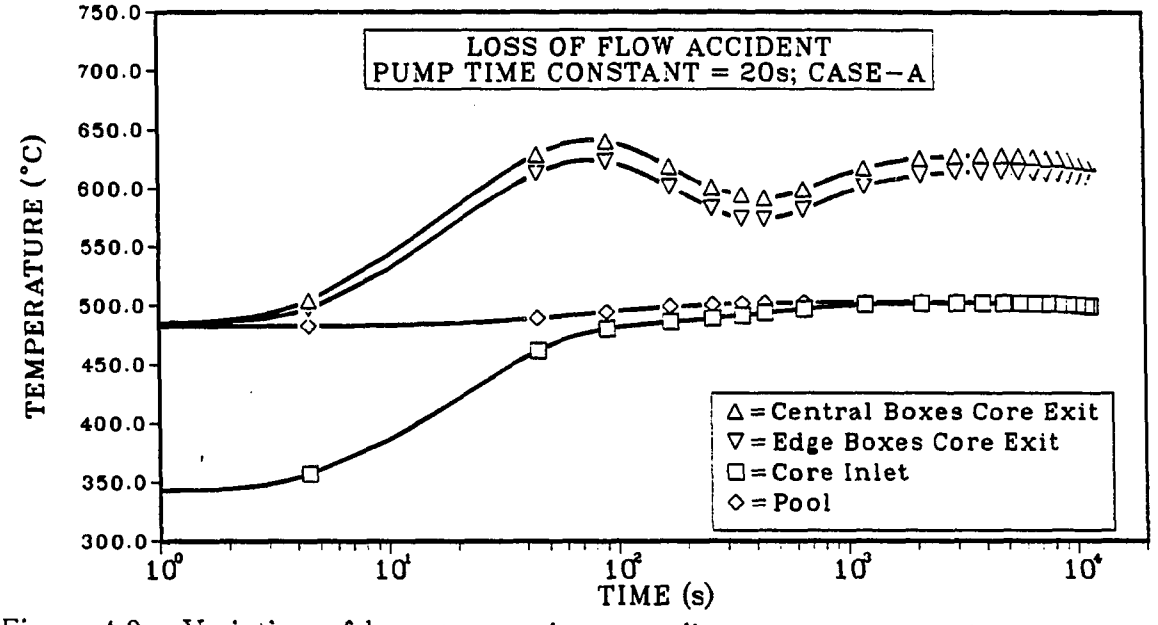

Figure 4.9: Variation of long term primary sodium temperatures during case-A type LOF accident

is negative (Figure 4.11).

The core exit temperatures reach a peak as the core inlet temperature reaches the secondary sodium IHX inlet temperature. As the natural circulation flow is established the core exit temperatures start to decrease, reducing the amount of negative reactivity. Since the initial stored energy in the fuel is small, the fuel temperature follows the power change closely, resulting in a decreased fuel temperature. The fuel feedback effects start to decrease in magnitude and finally become positive. However the mismatch between the power and flow keeps the core coolant temperature at a higher level than its initial steady-state value. These two effects compensate for each other and the net reactivity approaches zero putting the reactor into a critical state at low power (Figure 4.12). Since the natural circulation

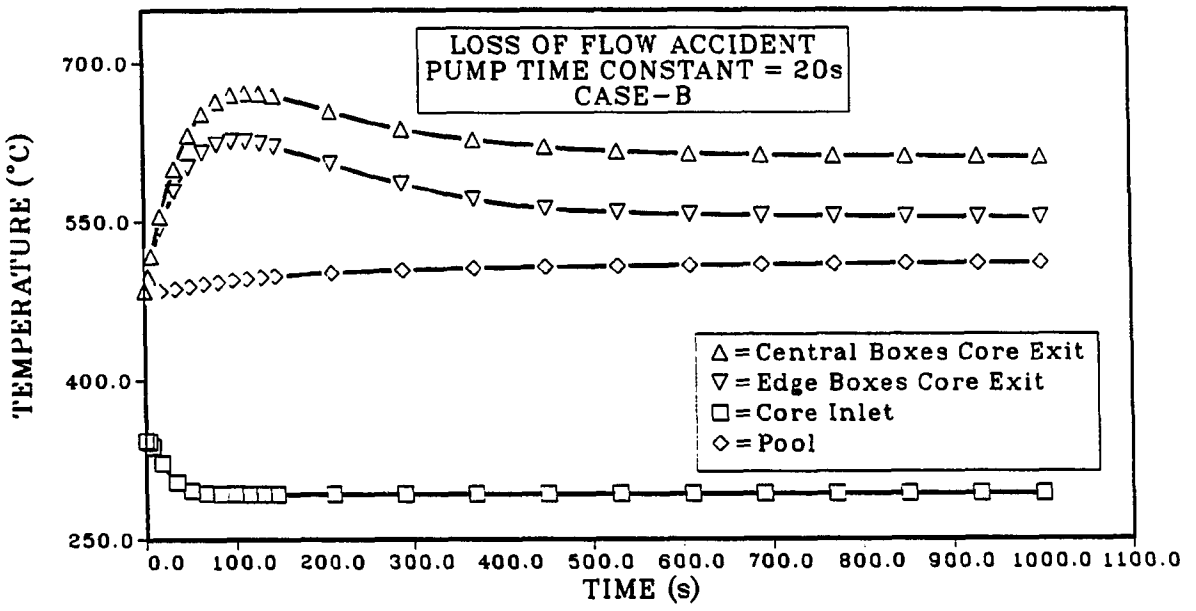

Figure 4.10: Variation of primary sodium temperatures during case-B type LOF accident

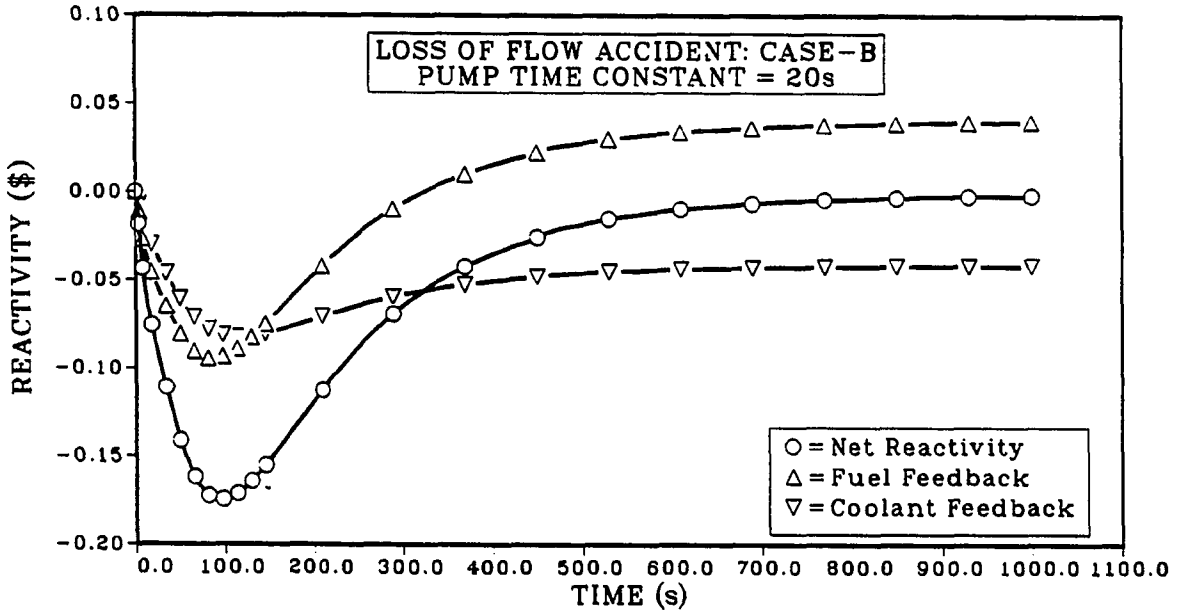

Figure 4.11: Variation of reactivity during case-B type LOF accident

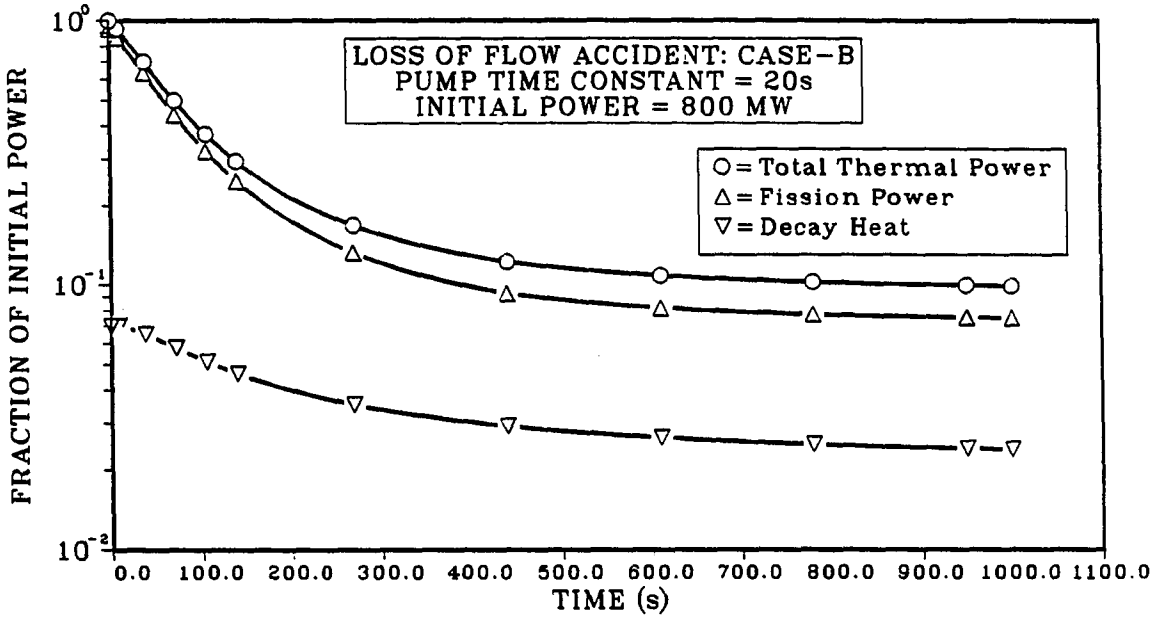

Figure 4.12: Variation of reactor power during case-B type LOF accident

flow has been established and the core inlet temperature has reached its asymptotic value, the heat production rate in the reactor and heat removal rate through the IHX and VCS are in balance and the reactor will remain in this critical state unless another major perturbation occurs.

Figure 4.13 compares the average core and pool temperatures for both cases. It can be observed that the core inlet temperature reaches its asymptotic value faster in case-B then it does in case-A. This is simply because the limiting temperature in case-B (IHX secondary inlet temperature) is closer to the initial core inlet temperature than the limiting temperature in case-A (pool temperature). The peak in the core exit temperature occurs earlier in case-A due to the combined effect of increasing core inlet temperature and increasing power to flow ratio whereas in case-B the decreasing core inlet temperature causes this peak to occur later. The

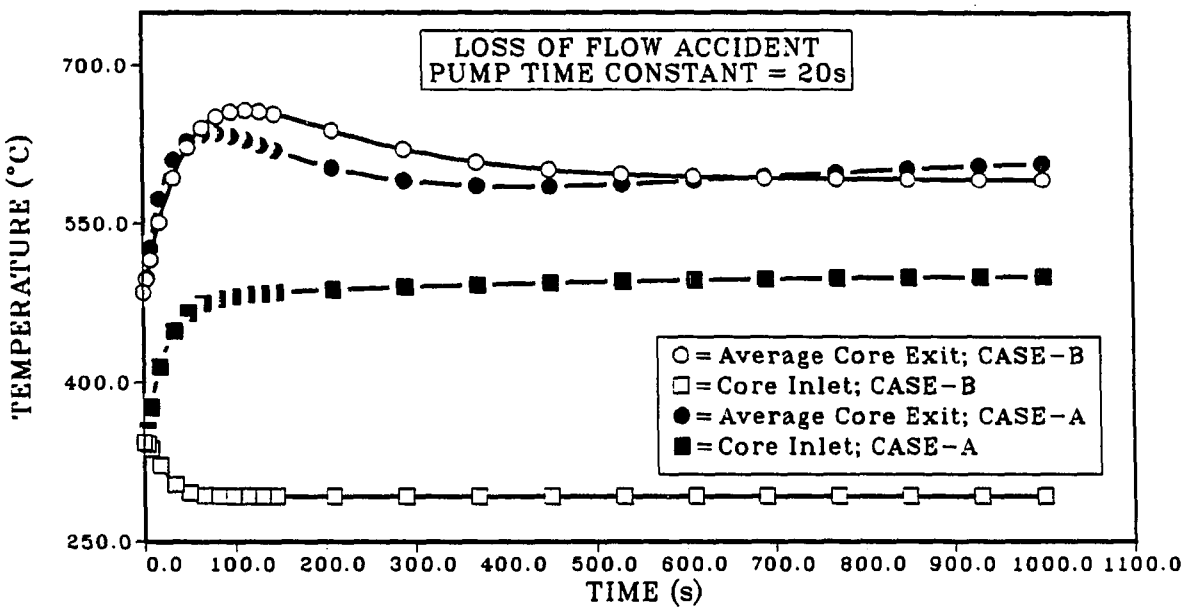

Figure 4.13: Comparison of primary sodium temperatures during case-A and Case-B type LOF accidents

magnitude of the peak in case-B is larger than it is in case-A, because less negative reactivity is introduced, hence the power is higher resulting in a higher power to flow ratio which is basically the fundamental parameter that determines the core exit temperature. The core exit temperatures and the pool temperature are increasing in case-A because the only heat that is being removed from the primary system is by the VCS. On the contrary, in case-B the IHX is removing all the heat that is produced in the core. Finally, at 1000 seconds the fission power, although a fraction of its initial value, is the major source of heat production in case-B whereas in case-A the power produced is due to decay heat alone.

The pump time constant is an important parameter in the transient response of the reactor. Table 4.6 and Table 4.7 give the numerical results at selected values

for various pump time constants for both case-A and case-B. This parameter has different effects for case-A and case-B type transients. If case-A type transients are considered one can identify two limiting cases. The first limiting case corresponds to a very small pump time constant ($t_p \rightarrow 0$) so that core flow rate drops instantaneously to its asymptotic natural circulation value, assuming that flow reversal will not occur. The second limiting case can be obtained by assuming $t_p \rightarrow \infty$ so that core flow rate is at its initial value. This corresponds to the LOHS accident. The maximum core exit temperature decreases with increasing t_p and is at its minimum for LOHS accident. The time at which the peak temperature occurs is also earlier for increasing t_p for all the t_p values considered in this study. However, if $t_p \rightarrow 0$ the core exit temperature will increase almost instantaneously indicating that the curve, time when the peak temperature occurs versus t_p, will have a peak for small t_p and then decrease monotonically, finally reaching the LOHS value.

For case-B type transients, increasing t_p results in reduction in the peak temperature and delays the time at which the peak temperature occurs. For a four-fold increase in t_p the peak temperature is reduced by approximately 100^oC and the time the peak occurs is twice as late. Since core exit temperature is basically determined by the power to flow ratio, the effect of t_p can be seen from Figure 4.14. The overshoot in the Φ is less for higher t_p values. Also, the slope of the $\Phi(t)$ curve is smaller indicating a milder increase in the core exit temperature.

Figure 4.15 compares the variation of net reactivity and Figure 4.16 shows the variation of normalized total reactor power for various t_p values for both cases. The effect of pump time constant on the decay of total power is more pronounced for case-B type transients then it is for case-A transients, causing a slower decay

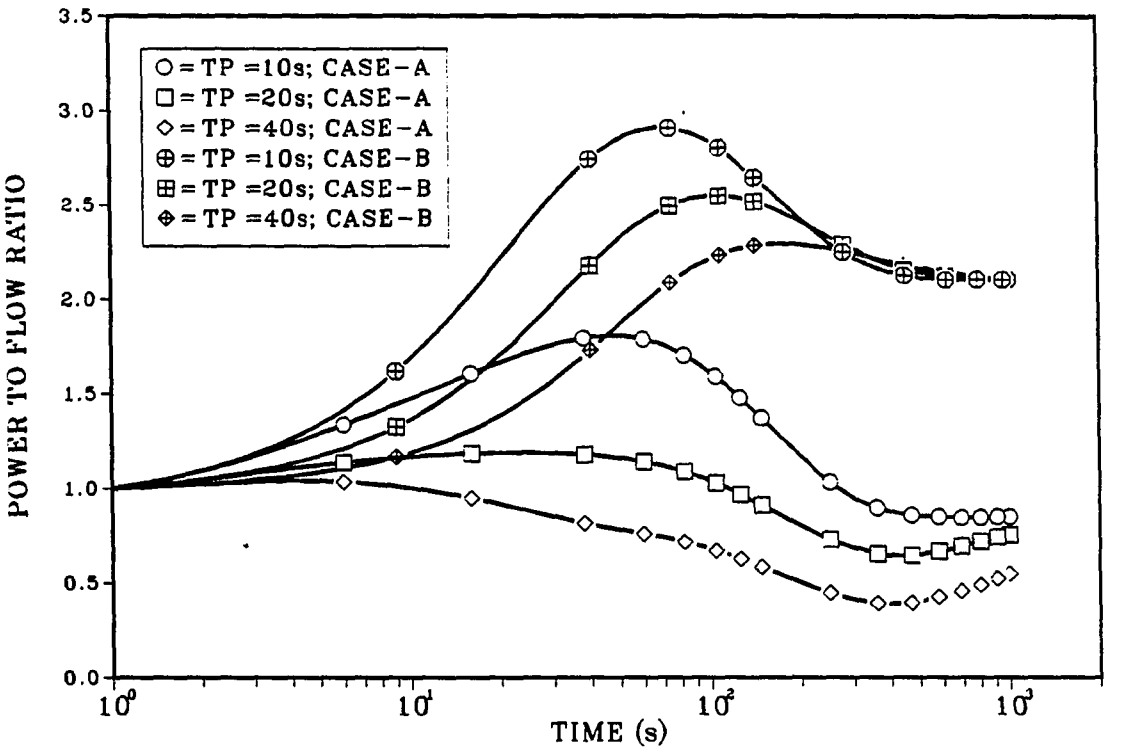

Figure 4.14: Comparison of the effect of primary pump time constant and secondary flow rate on the power to flow ratio during LOF accident

of fission power with increasing t_p. However, its effect on the final power level (at 1000 seconds) is small. The reason for this can be inferred from the net feedback reactivity variation (Figure 4.15). After ≈300 seconds into the transient the feedback reactivities are almost same for all the t_p values considered. On the contrary, for case-A transients the feedback reactivity is almost independent of t_p in the initial stages of the transients resulting in uniform decay of reactor thermal power causing it to drop to decay heat levels.

In general, case-B transients are more severe than the case-A transients due primarily to the way the core inlet temperature responds to the decrease in core

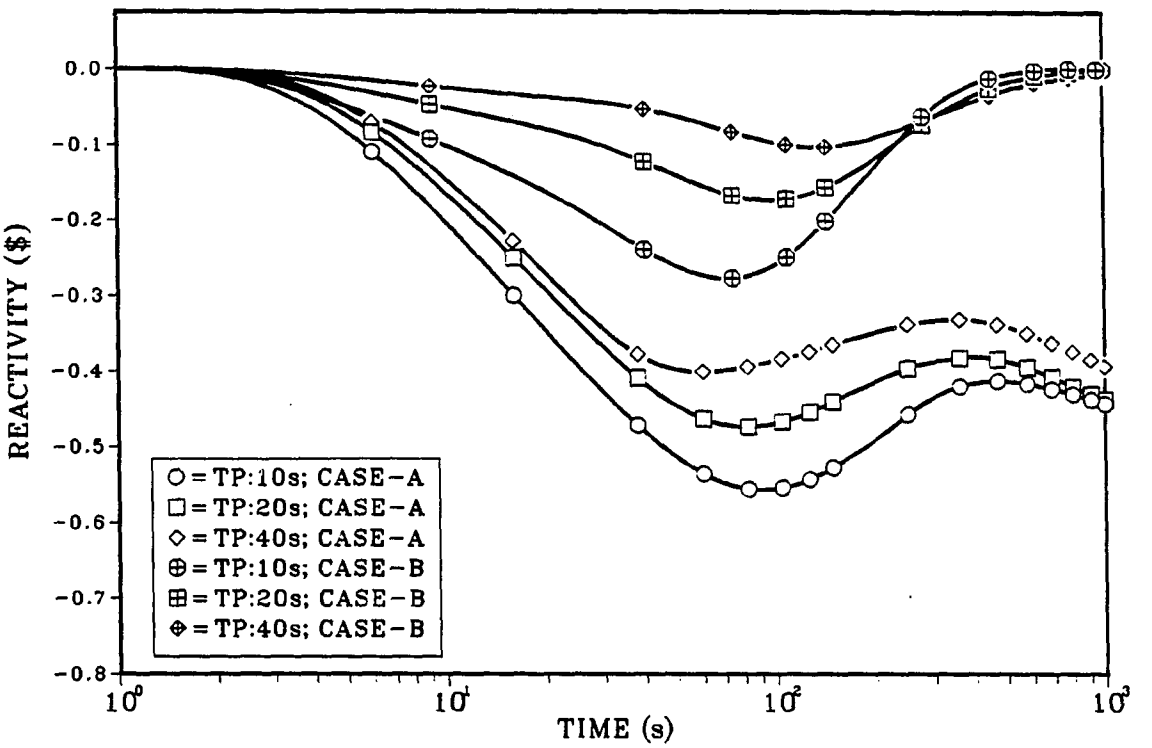

Figure 4.15: Comparison of the effect of primary pump time constant and secondary flow rate on net reactivity during LOF accident

flow rate. Since there are negligible heat capacity effects associated with the cold side of the primary system, the core inlet temperature can be adversely affected by the secondary loop conditions (decrease to introduce positive feedback reactivity). If the primary system and the secondary system are isolated from each other during a transient which was the case in LOHS and LOF-LOHS accidents the transients are less severe. However, in case-B type accidents the secondary loop conditions affected the primary system through their effect on the core inlet temperature. If one were to put a large heat capacity in the form of a cold sodium pool the coupling between the core inlet temperature and the primary sodium exit temperature from

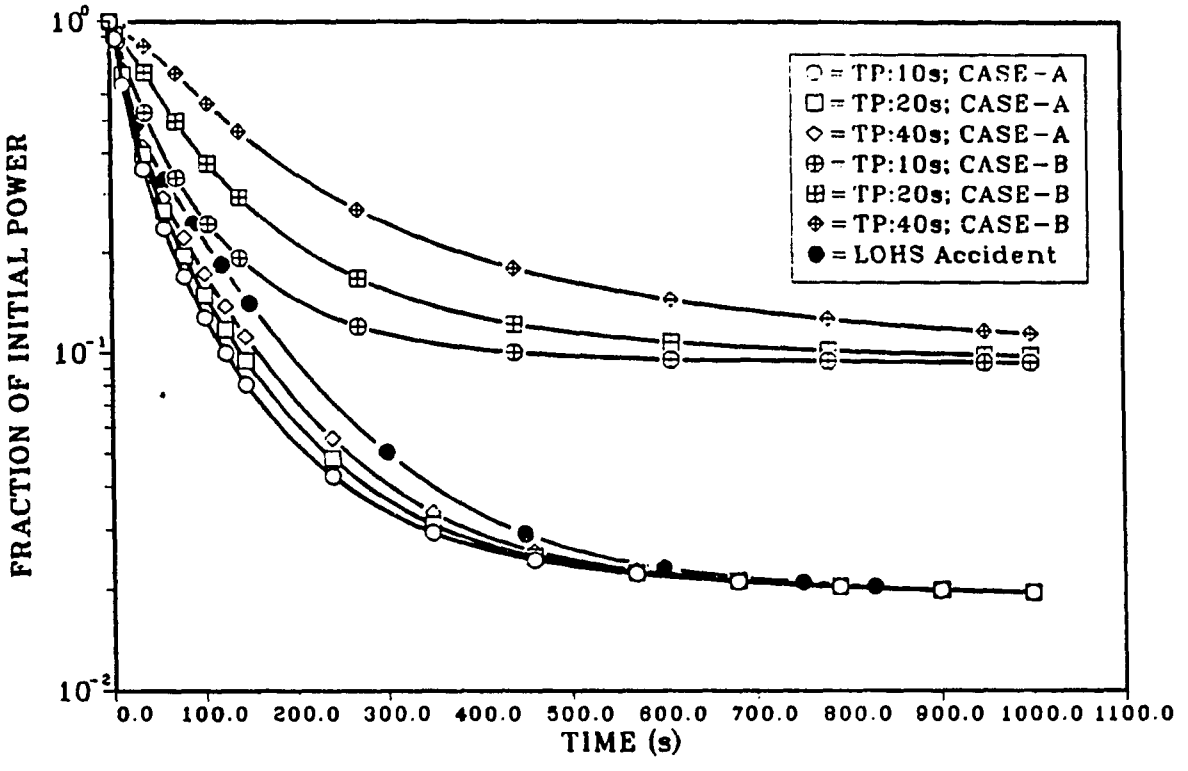

Figure 4.16: Comparison of the effect of primary pump time constant and secondary flow rate on the normalized power during LOF accident

the IHXs hence from the secondary loop conditions would be weakened.

The effects of the heat capacity associated with core inlet temperature can be observed by using a simple model for case-B type transients. The energy equation for the core inlet temperature can be approximated as

$$\frac{dT_{in}}{dt} = \frac{W(0)C_p}{MC_p} w(t)(T_{IHX} - T_{in}) \tag{4.29}$$

where T_{IHX} is the IHX exit temperature. The core flow rate in the initial stages of the transient can be approximated closely by

$$w(t) = \frac{1}{1 + \frac{t}{t_p}} \tag{4.30}$$

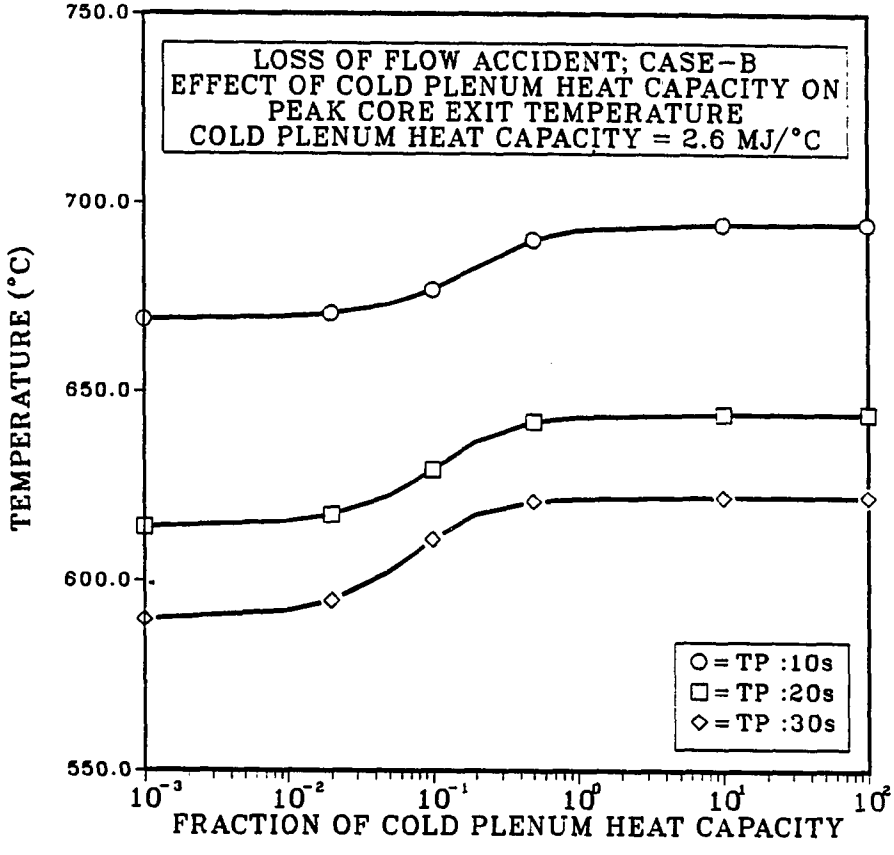

Figure 4.17: Effect of inlet plenum heat capacity on peak temperatures during case-B type LOF accident

The point kinetics equations with feedback reactivity given by Eq. (4.2), decay heat equations, a quasi-steady model of the IHX, and the pool energy equation (Eq. (4.22)) were solved to observe the effects of cold plenum heat capacity. The average core exit temperature was approximated with

$$T_{ex}(t) = T_{in}(t) + \Phi(t)\Delta T_{core,0} \tag{4.31}$$

Although the temperatures computed with this model are not as accurate as those from the more detailed simulation program the trends are predicted fairly well.

Figure 4.17 shows the average core exit peak temperatures as a function of the cold pool heat capacity for case-B type LOF accidents. The hot pool capacity was kept at its nominal value. The peak temperatures are reduced greatly if the amount of heat capacity associated with the core inlet temperature is increased. The large time constant associated with a large heat capacity avoids or delays the possible reduction in the core inlet temperature hence eliminating the positive reactivity feedback of a decrease in the core inlet temperature. In the case of a large cold pool, both case-A and case-B transients will be similar, at least at the initial stages of the transient, because the core inlet temperature will remain relatively constant for long periods. However, from Figure 4.17 one can observe that the pump time constant has a more pronounced effect than the heat capacity of the core inlet. Increasing the pump time constant by two-fold is more effective than increasing the cold plenum heat capacity by a factor of thousand. For the TR the pool heat capacity is roughly a thousand times the cold plenum heat capacity, that is the primary vessel needs to be doubled in size to include a cold plenum that has a heat capacity as much as the pool has. A large vessel will probably introduce more problems than it will help to solve. Since the primary pumps can be designed to have the desired pump coastdown characteristics, it is more desirable to require a long pump coastdown time than to require a larger vessel.

If the pump coastdown is not smooth but changes abruptly then the transition to natural circulation will reflect the sudden change in the pump speed. In order to simulate such a situation the pump speed was assumed to drop to zero instantaneously after it has dropped to 7% of its initial value. The result of this sudden change is another peak in core exit temperatures for both case-A (Figure 4.18) and

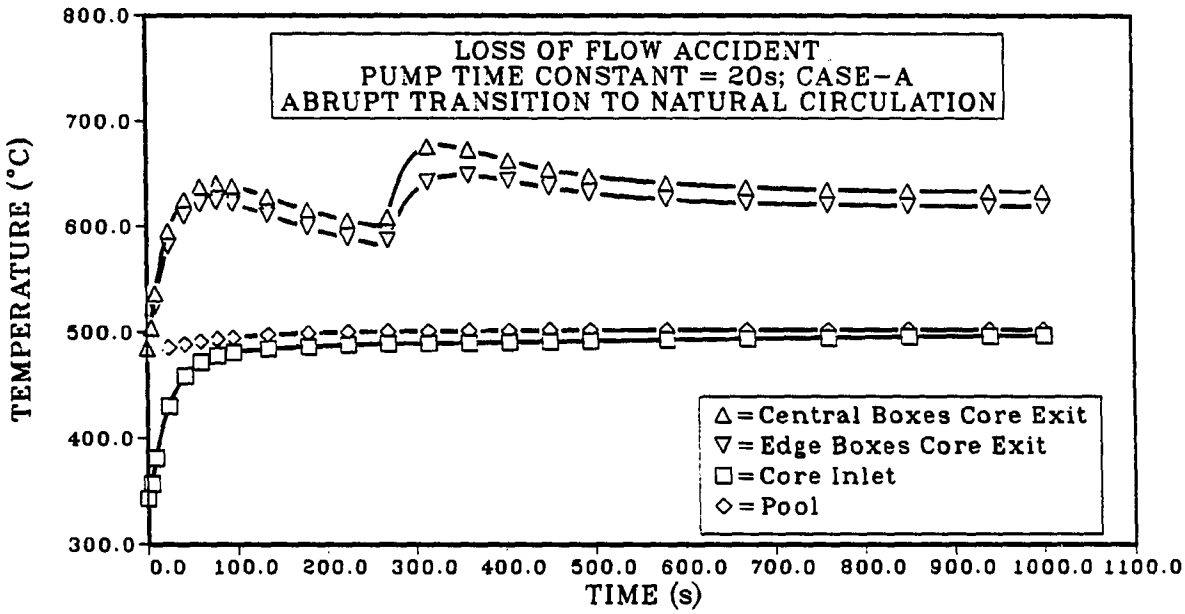

Figure 4.18: Variation of primary sodium temperatures during case-A type LOF with abrupt transition to natural circulation

case-B (Figure 4.19) because of the increase in power to flow ratio. For case-B the magnitude of the peak is larger and occurs earlier than case-A. The increase in temperature is followed by an increase in the magnitude of the negative feedback reactivity introduced. For case-B (Figure 4.20) the variation of reactivity due to the rapid change in the flow is more pronounced. Since the fission power still constitutes a major fraction of the total reactor thermal power, the rapid insertion of negative reactivity causes the power to drop more rapidly (Figure 4.21). On the other hand for case-A, at the time when the flow perturbation occurs the fission power has dropped to a small fraction of the total power, therefore, the effect of the sudden increase in negative feedback reactivity is not significant on total power (Figure 4.21).

Table 4.8: Results of loss of flow accident with $t_p = 20s$ and abrupt transition to natural circulation

	CASE-A[a]		CASE-B[b]	
Time (seconds)	330.0	1000.0	285.0	1000.0
POWER (MW)				
Fission	4.02	0.00	75.29	53.50
Decay	21.00	15.66	27.32	18.65
Total	25.02	15.66	102.64	72.14
REACTIVITY ($)				
Fuel	-.3290	-.2821	-.1092	0.0421
Coolant	-.2143	-.1926	-.1062	-.0413
Net	-.5433	-.4748	-.2154	0.0008
TEMPERATURE (°C)				
Core Inlet	489.7	497.1	292.9	292.8
Core Exit:				
Average	668.2	628.8	689.6	592.2
Central boxes	677.4	633.1	715.4	609.5
Edge boxes	647.4	619.2	637.3	557.2
Pool	501.1	502.4	503.8	508.3
NORMALIZED[c]				
Flow	0.0247	0.0214	0.0451	0.0428
Power to flow ratio	1.2650	0.9171	2.8460	2.1060
Core ΔT	1.2600	0.9290	2.7990	2.1130
IHX ΔT	0.0762	0.0354	1.5140	1.5460

[a]Secondary flow rate is 0.18kg/s.
[b]Secondary flow rate is constant at 1800kg/s.
[c]Normalized with respect to initial value.

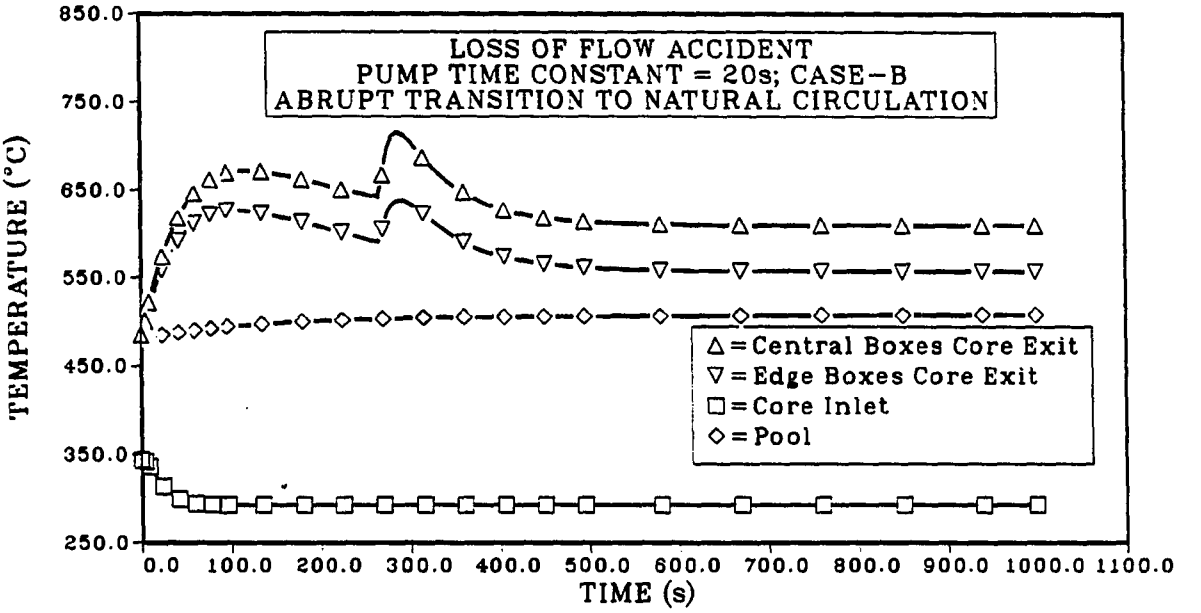

Figure 4.19: Variation of primary sodium temperatures during case-B type LOF with abrupt transition to natural circulation

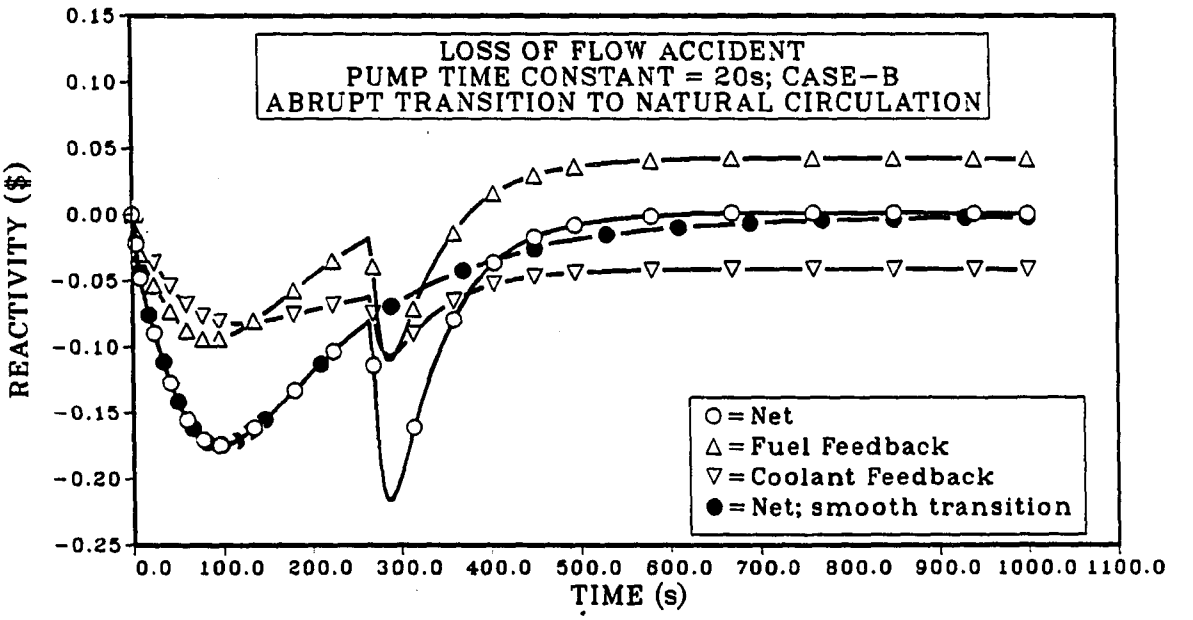

Figure 4.20: Variation of reactivity during LOF accident with abrupt transition to natural circulation

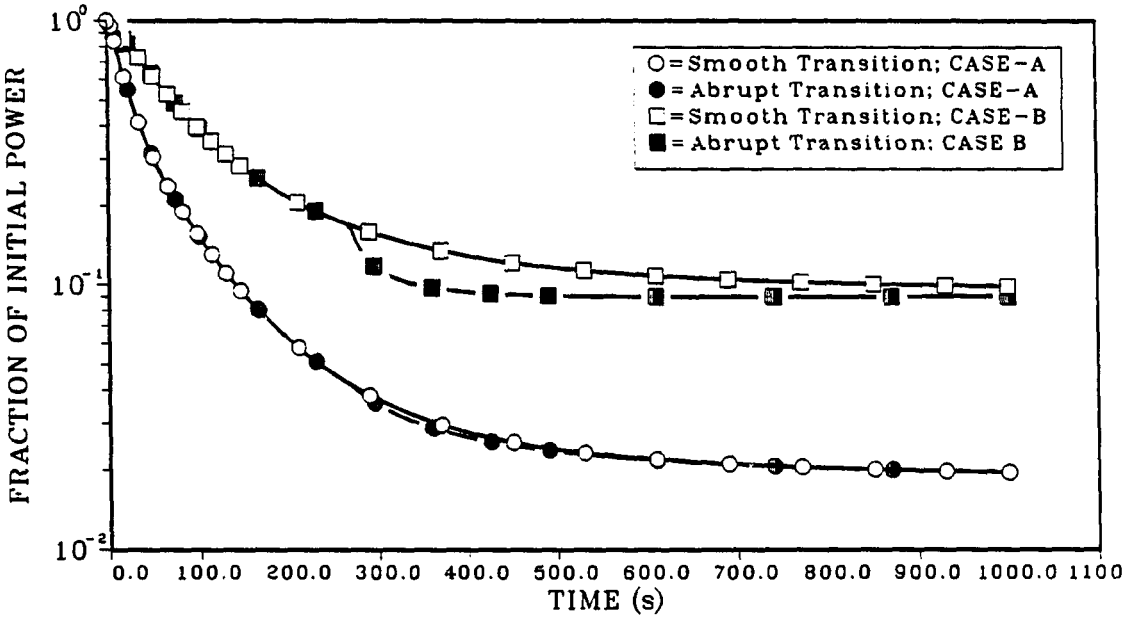

Figure 4.21: Variation of reactor power during LOF accident with abrupt transition to natural circulation

For case-B type transients, the secondary inlet temperature to the IHX is an important parameter because of its effect on the core inlet temperature. As mentioned earlier the secondary inlet temperature to the IHX is the limiting temperature for the core inlet temperature. The decrease in the core inlet temperature introduces positive feedback, hence is not desirable. The case-B transients so far have assumed that the secondary inlet temperature was constant at its initial value and the secondary flow rate was constant. The limiting secondary inlet temperatures are hard to establish. If heat removal from the secondary loop is neglected completely then the pool temperature is an upper bound for the secondary sodium inlet temperature. However, in this case the time delay in the secondary loop must be accounted for; otherwise the secondary sodium will heat the primary sodium. As a lower limit one can consider the feedwater temperature which is 237^{o}C. This limiting case is

extremely unlikely since the secondary flow rate is assumed to be at its initial value so that the steam generator units will have to remove more than their designed capacity at a lower temperature difference between the sodium and water sides.

If we consider the long term outcome of these accidents the effect of the final state of the core inlet temperature can be observed from Eq. (4.2). It can be shown that the asymptotic natural circulation rate can be related to the power produced in the core by [71]

$$w_\infty = K_w p^{1/3} \tag{4.32}$$

For the reactor to become critical again the sum of the feedback reactivities has to be zero. Combining Eq. (4.2) and Eq. (4.32) one gets

$$0 = \alpha_{T_{in}} \delta T_{in} + \alpha_{pf}\left(\frac{p}{K_w p^{1/3}} - 1\right) + \alpha_p(p-1) \tag{4.33}$$

For a known change in core inlet temperature Eq. (4.33) can be solved for the normalized power p. Figure 4.22 shows the variation of the asymptotic value of the core power as a function of a change in the core inlet temperature. It should be noted that this figure does not give any information about the initial stages of the transient. We see that the core inlet temperature determines basically the final power level. If the secondary sodium loop conditions are such that the core inlet temperature is lower than its initial value of 343^oC the resulting power level is higher than if the core inlet temperature were to approach the pool temperature as in case-A type transients. Since the secondary inlet temperature to the IHX is important only through its effect on the core inlet temperature and primary pump time constant is basically the design controllable variable that limits the peak temperatures during a LOF transient, Figure 4.22 shows that the reactor will reach

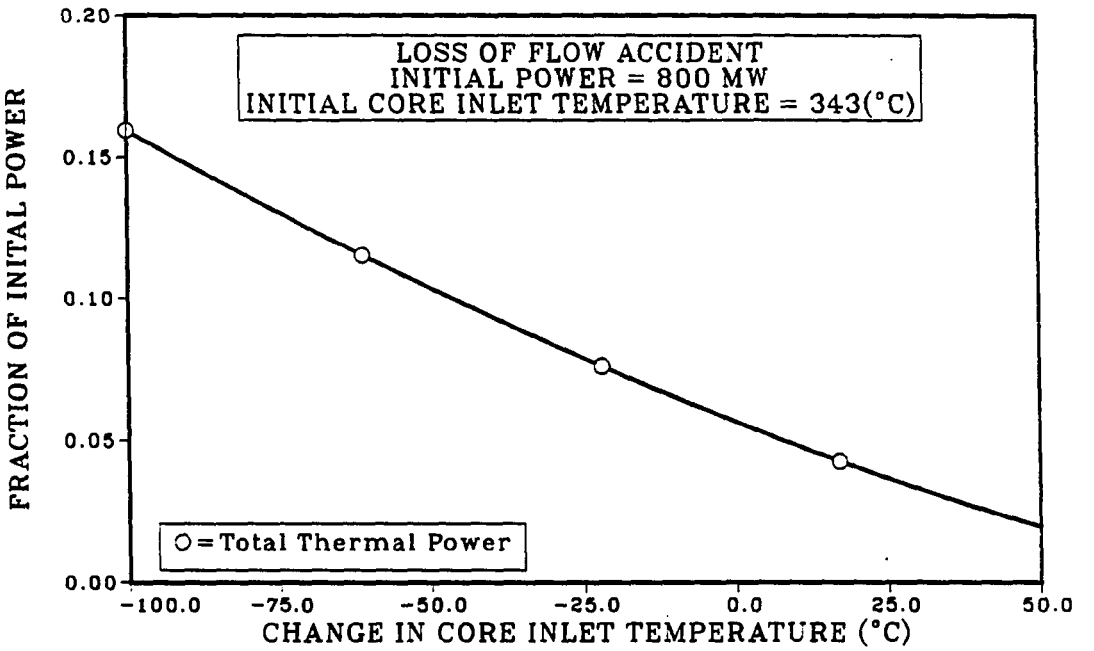

Figure 4.22: Asymptotic power level as a function of change in core inlet temperature for LOF accident

a low power critical condition for the ranges of core inlet temperature considered.

The above discussion indicates that the reactor will respond to the LOF accident in two substantially different manners. The first one which is the coupled LOF-LOHS accident (case-A) results in a *subcritical* state in which the long term response of the reactor is governed by the changes in decay heat generated in the core and the heat removed from the vessel by the VCS. The second one which is a coupled LOF and overcooling accident (case-B) results in a low power *critical* state in which the power generated in the core and the heat removal from the IHX are in balance. The time duration of the initial phase of the transient (transition to natural circulation in the primary system) for both cases is governed by the pump time constant. Coupled LOF-LOHS accident and LOHS accident results indicate that the primary system when decoupled from the secondary system behaves in an

inherently safe manner. From the results of coupled LOF and overcooling accidents, it has been shown that although the fission power will not die away the inherent reactivity feedback effects will bring the reactor into a critical stable state. The conditions that sustain this state develop inherently and will exist unless another disturbance in the balance of the reactor is introduced. Therefore, we can conclude that with regards to the final state of the reactor case-B transients also give an *inherently safe* behavior. In terms of the damage to the primary system components, the hydraulic profile of the primary system allows the pump coastdown characteristics to be selected so that the damage to the primary system components can be avoided. From the above results a pump time constant higher than 30 seconds is necessary.

The more limiting type of the LOF accident was based on the assumption that the secondary pumps were working at their initial speed when the primary pumps were coasting down. A very simple and effective method of avoiding such an accident is to make sure that the the secondary pumps also start to coast down after the power to primary pumps is lost. This scenario is more likely to happen in real life if the cause of the LOF accident is loss of electrical power. In this case the accident will be less severe, since the inlet temperature to the core will eventually increase and introduce negative feedback reactivity and will cause the power to decrease.

4.7 Transient Overpower Accident

In the transient overpower accident (TOP), it is assumed that positive reactivity is inserted into the core and the plant protection and control systems fail to respond. TOP accidents are different from the LOHS or LOF accidents in the sense

that an external disturbance is not only required to initiate the accident but to keep the accident going on whereas, in a LOHS or LOF accident, once the accident is initiated it develops without requiring the existence of any external source. The source of the positive reactivity that will be inserted accidentally comes from the control elements in the reactor core.

Numerically this accident was simulated as step reactivity insertion. Reactivity insertions of 0.25 and 0.50 dollars were considered. Table 4.9 gives the numerical results for the peak temperatures and temperatures at the final simulation time for step reactivity reaction alone and coupled with LOHS and LOF accidents. The primary pump speed, secondary loop IHX inlet temperature and flow rate were kept at their initial values.

Variation of average temperatures, total thermal power and reactivities for the 0.5$ case are shown in Figure 4.23, Figure 4.24 and Figure 4.25, respectively. The 0.25$ step reactivity insertion case behaves in a similar manner but the magnitudes of the variables are less. After a jump to approximately twice its value the power starts to decrease due to the effect of negative feedback reactivities, first from the fuel temperature associated component then from the coolant temperature associated component. The net reactivity for this case becomes zero at approximately 140 seconds. The increase in power causes the core exit, pool and core inlet temperatures to increase. The final stage is steady operation at a higher power level with increased temperatures. The variations in the flow level are due to the change in the density of sodium with increased temperatures.

Although highly improbable, a reactivity insertion accident may occur with other types of accidents such LOHS or LOF. These accidents should be considered

Table 4.9: Results of transient overpower accidents for step reactivity insertion

	TOP				TOP-LOHS		TOP-LOF			
							t_p=30 seconds			
							CASE-A		CASE-B	
ρ_{ext} (\$)	0.25		0.50		0.50		0.50			
Time (seconds)	220	500	180	500	31	500	94	500	170	500
POWER (MW)										
Fission	1107	1052	1514	1376	795	51	263	17	391	184
Decay	73	72	90	90	62	23	43	20	47	29
Total	1180	1124	1604	1466	857	74	306	37	438	213
REACTIVITY (\$)										
Fuel	-.193	-.190	-.383	-.376	-.394	-.378	-.475	-.369	-.389	-.322
Coolant	-.059	-.062	-.119	-.127	-.183	-.234	-.264	-.232	-.211	-.196
Net	-.002	-.002	-.003	-.002	-.077	-.112	-.239	-.101	-.100	-.018
TEMPERATURE (^oC)										
Core Inlet	354	361	362	379	479	589	491	525	293	293
Core Exit										
Average	566	563	652	646	633	603	745	660	855	830
Central Boxes	565	563	651	645	633	603	751	669	876	854
Edge Boxes	566	564	654	648	634	603	729	643	809	780
Pool	528	551	566	625	498	590	514	539	537	571
NORMALIZED										
Flow	0.996	0.993	0.991	0.984	0.998	0.985	0.218	0.050	0.140	0.071
Power to flow ratio	1.481	1.416	2.024	1.862	1.073	0.094	1.756	0.929	3.897	3.737
Core ΔT	1.490	1.425	2.046	1.883	1.084	0.096	1.788	0.956	3.967	3.794
IHX ΔT	1.249	1.364	1.466	1.764	0.126	0.007	0.164	0.095	1.756	1.998

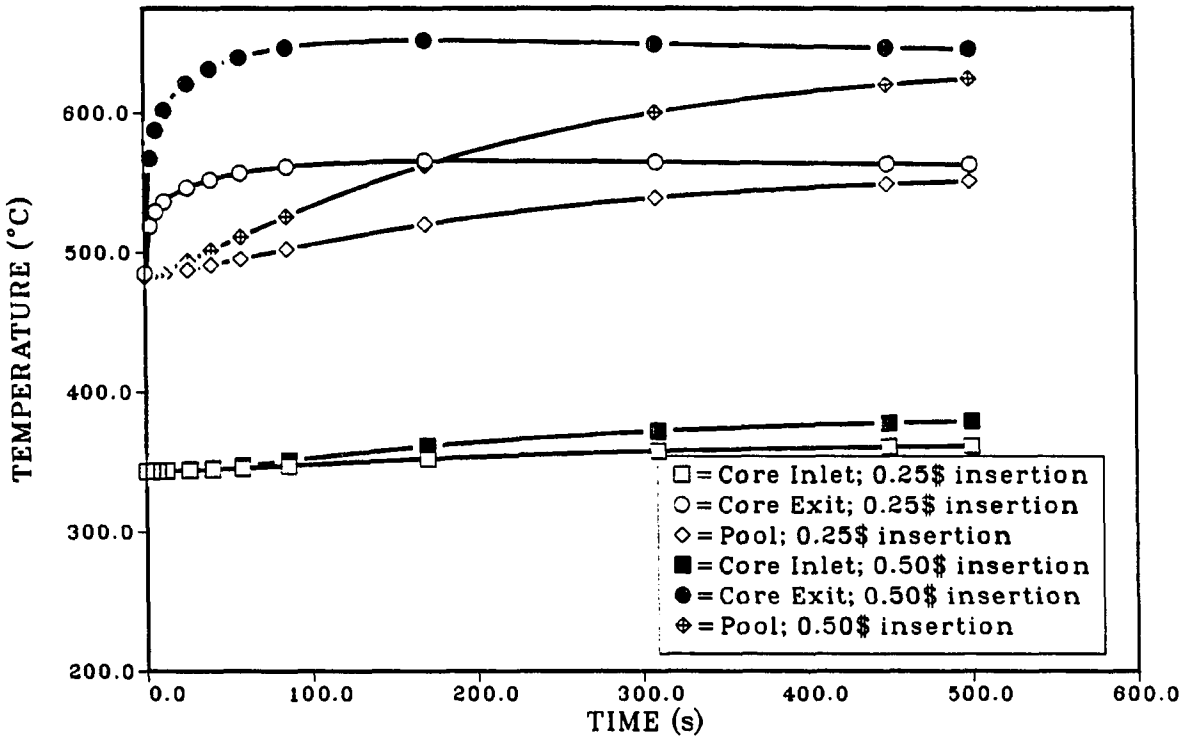

Figure 4.23: Variation of primary sodium temperatures during TOP accident

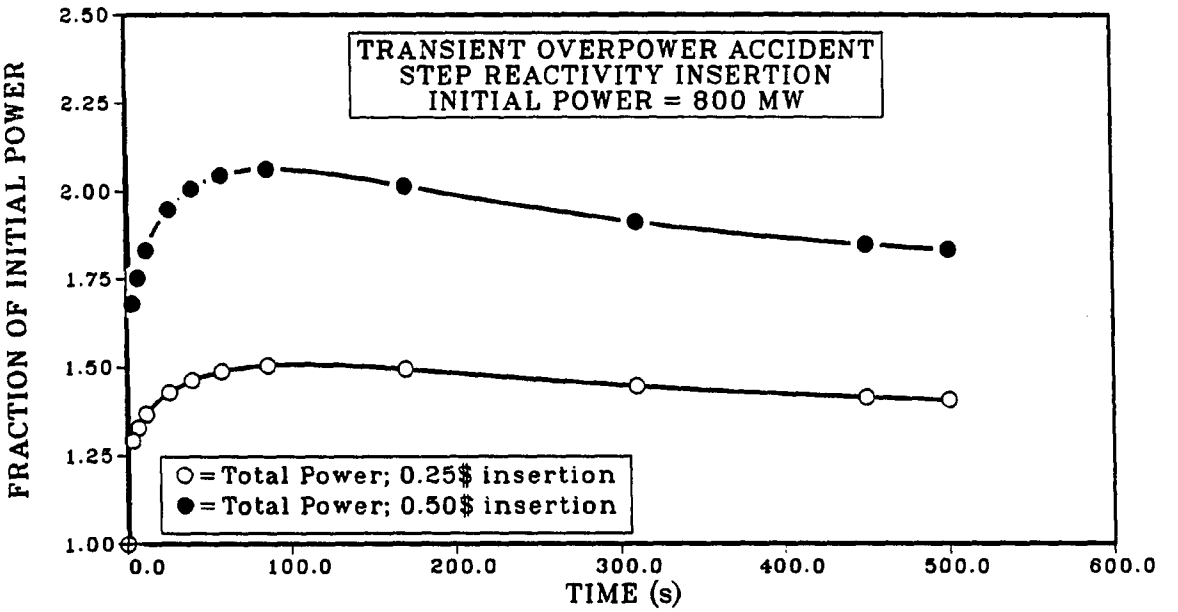

Figure 4.24: Variation of reactor power during TOP accident

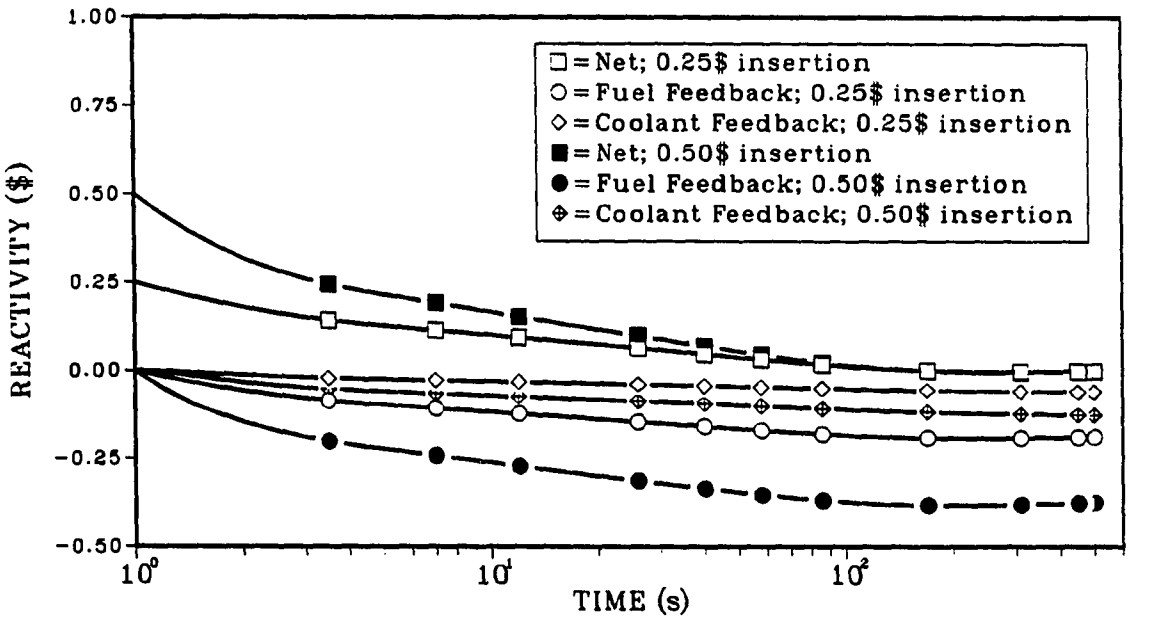

Figure 4.25: Variation of reactivity during TOP accident

as two infrequent events occurring at the same time. In a combined LOHS and TOP accident the reactor response is very similar to the LOHS accident. The temperatures and power levels are higher due to the additional reactivity introduced. Table 4.9 gives the results of this accident for a step reactivity insertion of 0.5 dollars. Figure 4.26, Figure 4.27 and Figure 4.28 show the variation of temperatures, power and reactivity components for this accident. The increase in power due to reactivity insertion causes the fuel temperature and fuel temperature associated negative feedbacks to increase. The loss of heat removal from the IHX results in higher core inlet temperatures introducing more negative feedback reactivity. Even though the core exit temperature is higher, introducing hotter sodium into the pool, the pool temperature rises slowly compared to the core inlet temperature. Therefore, the peak temperatures occur at a time similar to that would happen on a LOHS accident alone. However, the peak temperature is higher due to the increased power level. The peak core exit temperatures are approximately 100^oC higher than a LOHS accident whereas the core inlet temperatures are the same for both cases. The negative feedbacks compensate for the inserted reactivity and cause the reactor to remain in a subcritical condition.

The combination of LOF and TOP accident is clearly the worst accident that can be considered. Since in LOF accidents the secondary loop conditions influence the outcome of the accident through their effect on the core inlet temperature the two limiting cases that were considered in Section 4.6 were considered. Table 4.9 lists the results of this accident for pump time constant of 30 seconds and 0.5 dollars step reactivity insertion. The response of the reactor to the coupled TOP-LOF accident and to LOF accident alone are very similar. Again the accident proceeds as it would

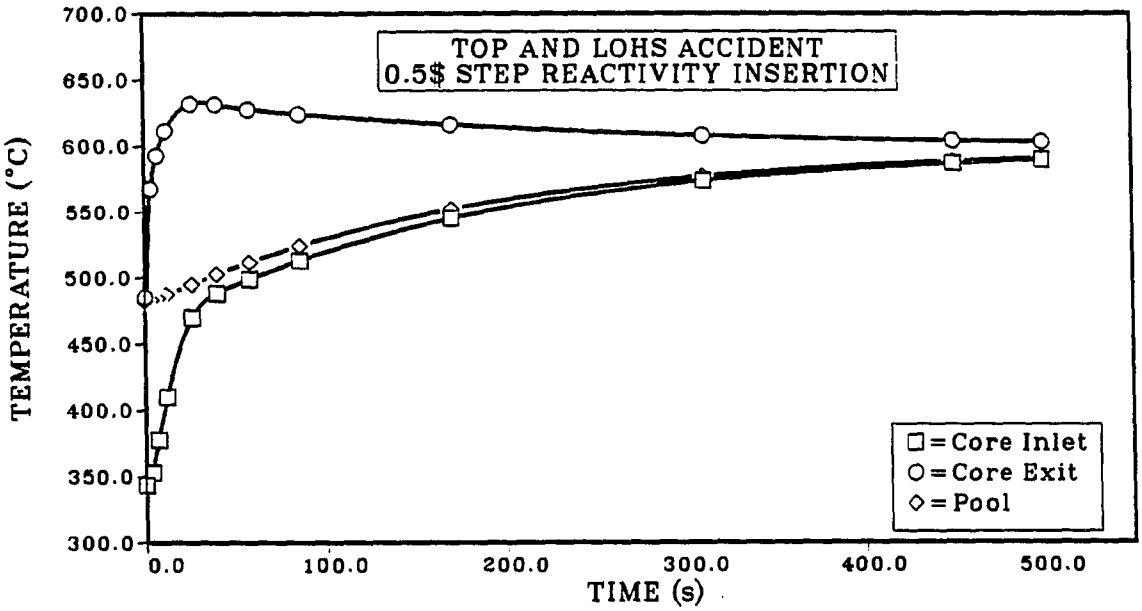

Figure 4.26: Variation of primary sodium temperatures during TOP-LOHS accident

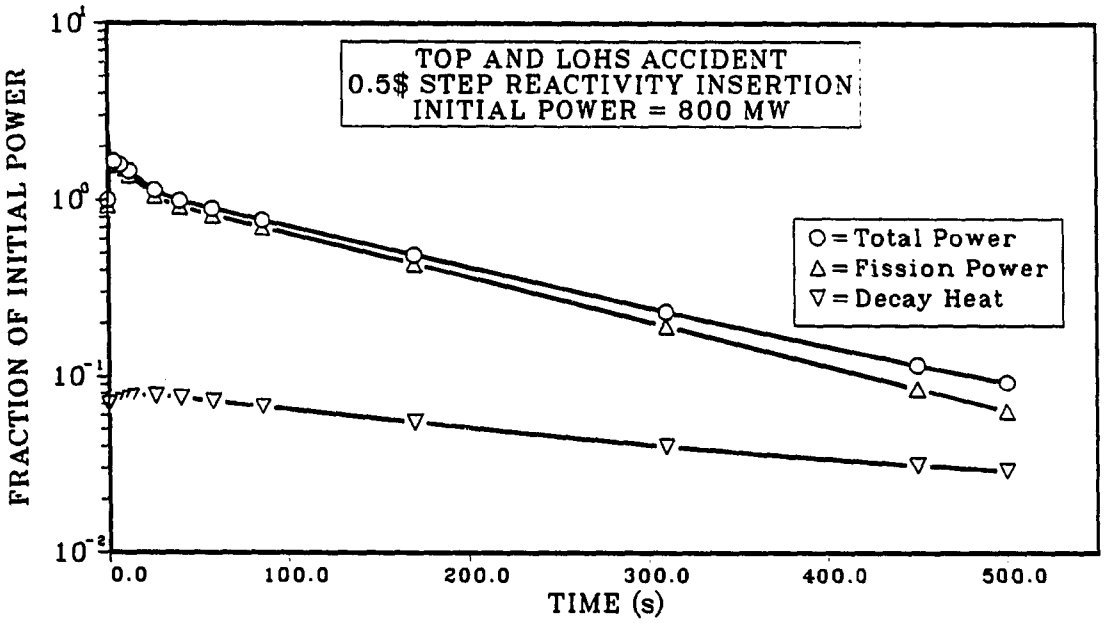

Figure 4.27: Variation of reactor power during TOP-LOHS accident

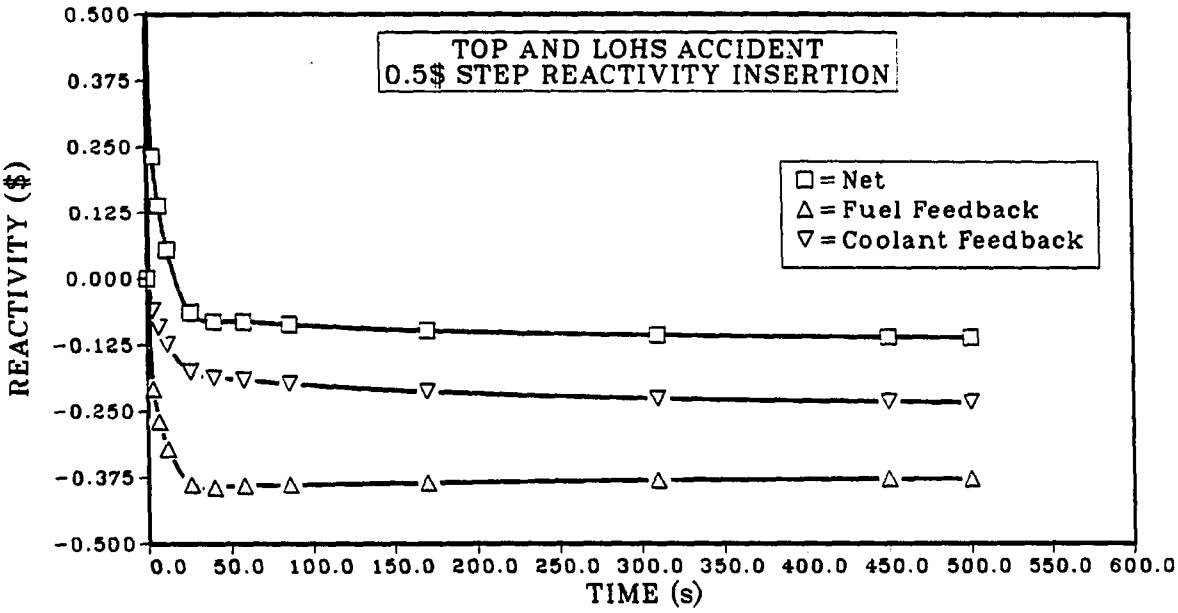

Figure 4.28: Variation of reactivity during TOP-LOHS accident

be in the case of a LOF accident; however, the severity of the accident has increased due the the increased power level as a result of the reactivity insertion. At the time at which the peak temperature occurs the core inlet temperatures for the coupled TOP-LOF and LOF accident are very close to each other; however, the core exit temperatures differ by approximately 150^{o}C. This indicates that the dynamics of the accident is governed by the LOF accident dynamics and the effect of reactivity insertion is merely to increase the power and temperature levels as was observed in the coupled TOP-LOHS accident case. This behavior of the reactor is due to the large heat capacity hence, the large time constant of the pool. The pool dampens the rapid increase in the core exit temperature. The case in which the secondary loop flow rate is assumed to be in its initial flow rate and temperature (case-B) is more limiting than the other case in which the secondary loop flow rate is reduced

to 0.001 of its initial value. The same arguments that were presented in Section 4.6 apply to the coupled TOP-LOF accident as far as the qualitative characteristics of the effects of pump time constant, transition to natural circulation and secondary sodium inlet temperature to the IHX.

The average core and pool temperatures resulting from a TOP accident alone or coupled with a LOHS accident are within the accepted safety limits. The coupled TOP-LOF accident with the secondary sodium assumed to be in its initial conditions which can be considered as a coupled TOP-LOF-OCL accident for average central boxes exit temperature gives only 5^{o}C margin to sodium boiling which implies that this accident, under postulated conditions, will cause sodium boiling for much of the core and, if allowed to continue, will cause severe damage to core. In this case the pool temperature is well below the safety limits eliminating a short term vessel failure. In the case of step reactivity insertion alone, the exit temperatures are within the limits and no widespread damage to the core will occur. However, the primary system which is designed for 800MW is now working at higher levels with the excess power being deposited in to the pool resulting in increasing pool temperature. Since the vessel is not pressurized, the stress levels on the vessel are small, and the time to failure of the vessel is of the order of hours. Hence TOP is the most severe accident threatening the primary vessel integrity. The coupled TOP and LOF or LOHS accidents threaten the sodium boiling limit in the short term, however, the vessel integrity is not challenged.

4.8 Overcooling Accident

In the overcooling accident (OCL), the effects of a decrease in the reactor inlet temperature are of concern. Such an accident will most probably be caused by an increase in heat removal in the steam generator (SG). If the amount of feedwater that is being pumped into the SG increases or the pressure at which evaporation takes place decreases the outlet temperature of the secondary sodium in the SG will decrease. Since a once through steam generator concept is being used in the TR, a decrease in the evaporation pressure will result in a dry-out in the steam generator due to the small amount of liquid inventory causing the accident to become a partial loss of heat sink. Other events that may cause an OCL accident are an increase in the primary or secondary sodium flow rate.

Numerically this accident was simulated as a ramp change in the secondary inlet temperature to the IHX. The secondary inlet temperature was reduced to the feedwater temperature which is 237^{o}C. The numerical results are summarized in Table 4.10. As can be seen this accident is very minor in terms of the temperature levels achieved. The increase in the reactor power level is due to the positive feedback reactivity introduced by the decrease in the core inlet temperature which is then compensated by the feedback reactivity from the fuel temperature associated feedbacks. Figure 4.29, Figure 4.30 and Figure 4.31 show the variation of average primary system temperature, reactor thermal power and reactivity components. The overcooling accident can be considered as a small positive reactivity input due to the chilling of the core.

Since overcooling events that originate from the steam side of the steam generator transform into overheating events for a once-through steam generator type

Table 4.10: Results of overcooling accident

	CASE-A[a]		CASE-B[b]		OCL-LOHS	
Time (seconds)	375	1000.0	390.0	1000.0	130.0	1000.0
POWER (MW)						
Fission	1023	1013	1023	1013	421	0
Decay	70	70	70	71	56	16
Total	1093	1083	1093	1084	477	16
REACTIVITY ($)						
Fuel	-.017	-.016	-.017	-.016	-.193	-.150
Coolant	0.016	0.016	0.016	0.016	-.116	-.131
Net	-.000	-.000	-.000	0.000	-.309	-.282
TEMPERATURE (^oC)						
Core Inlet	305	306	305	306	462	515
Core Exit:						
Average	498	497	498	497	547	518
Central boxes	498	498	498	497	547	518
Edge boxes	498	497	498	497	547	518
Pool	491	495	491	495	489	515
NORMALIZED[c]						
Flow	0.999	0.999	1.000	0.999	0.999	0.995
Power to flow ratio	1.367	1.354	1.366	1.355	0.597	0.020
Core ΔT	1.363	1.352	1.363	1.352	0.599	0.020
IHX ΔT	1.337	1.356	1.337	1.356	0.192	0.000

[a]Secondary loop inlet temperature to IHX drops to 237^oC in 33s.
[b]Secondary loop inlet temperature to IHX drops to 237^oC in 56s.
[c]Normalized with respect to initial value

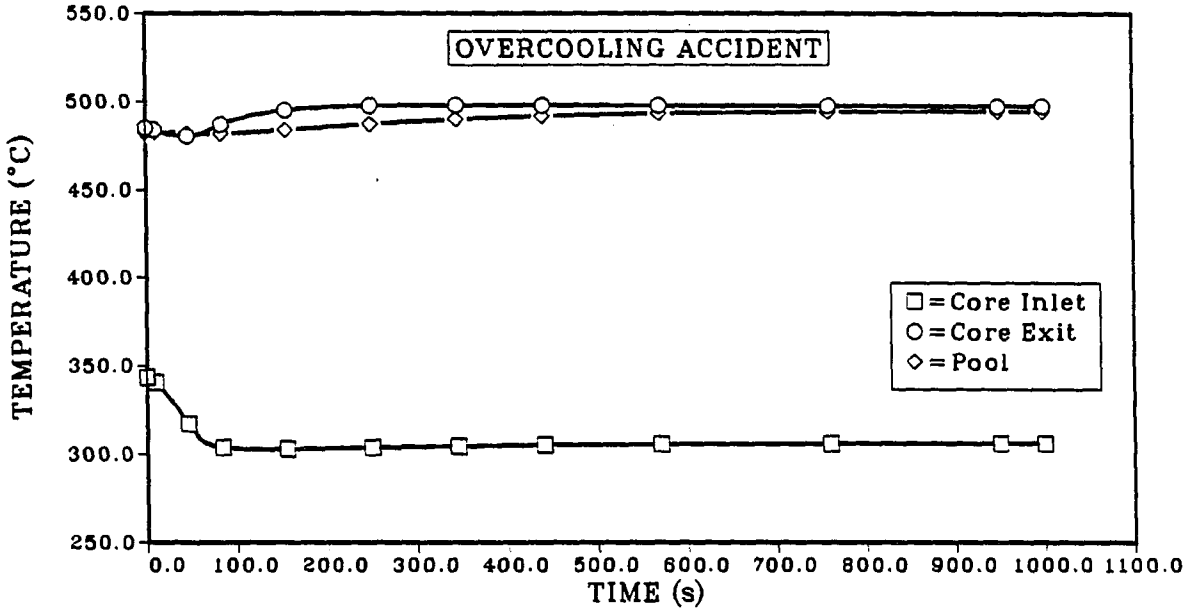

Figure 4.29: Variation of primary sodium temperatures during OCL accident

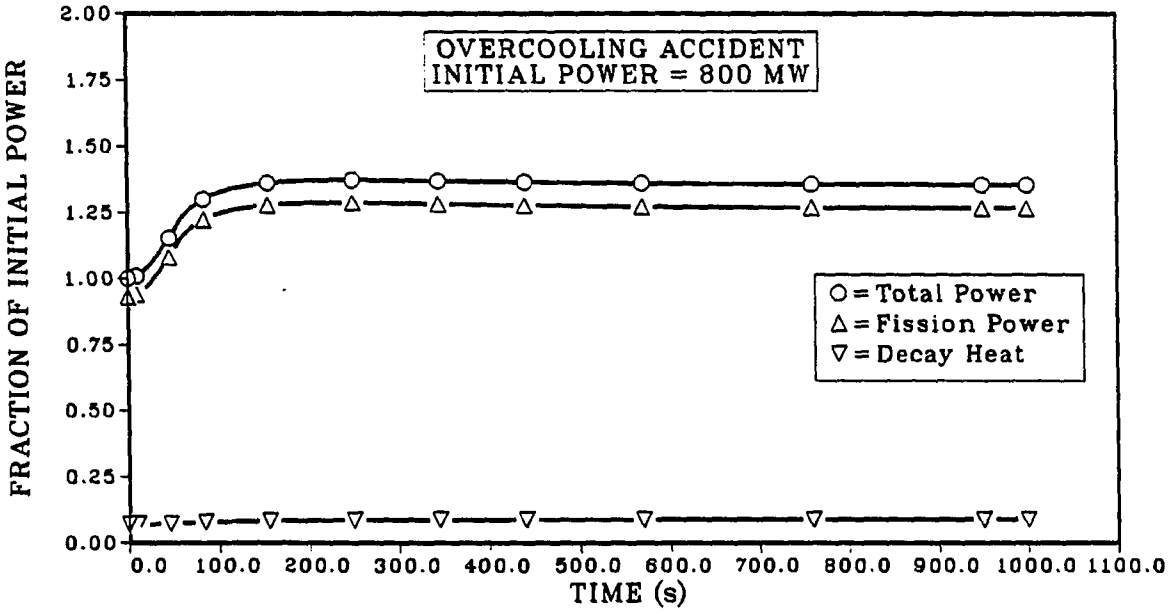

Figure 4.30: Variation of reactor power during OCL accident

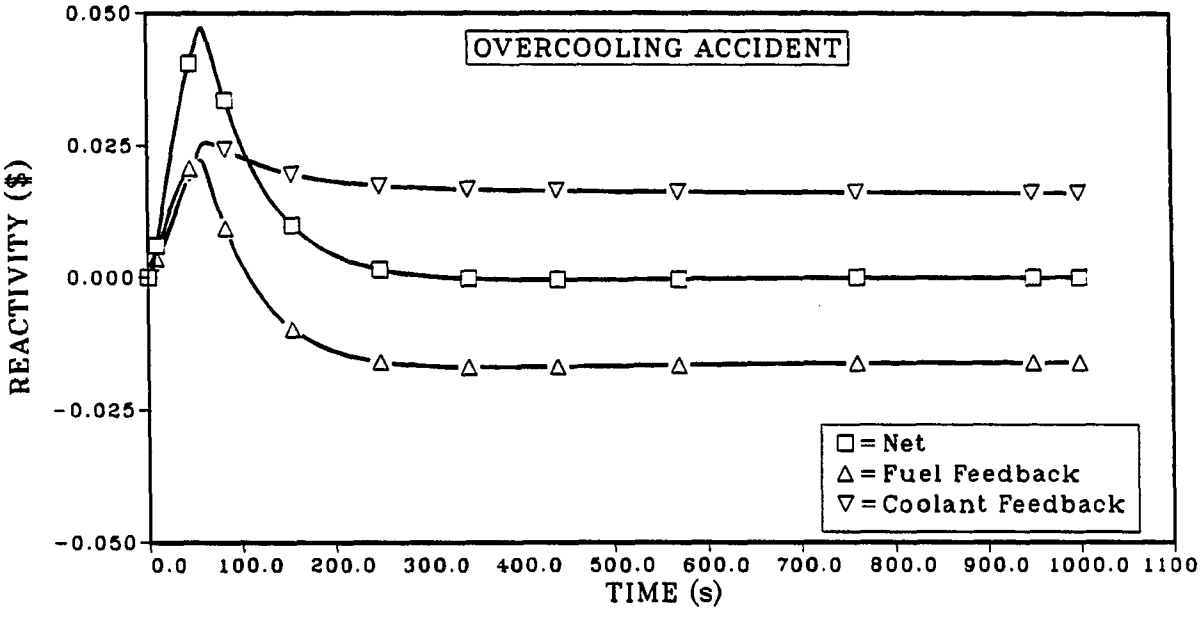

Figure 4.31: Variation of reactivity during OCL accident

in a short time, the secondary sodium temperature will start to increase after decreasing. To simulate such an accident, the secondary sodium inlet temperature at the IHX was first reduced to 237^{o}C then increased to the exit temperature from the secondary side of IHX. This assumption implies that there is no heat transfer to water-steam in the steam generator and therefore that all the heat transferred to the secondary sodium loops remains in the secondary sodium loops. The variations of average primary loop temperatures, power and reactivity components are shown in Figure 4.32, Figure 4.33 and Figure 4.34. This accident can be considered as an OCL accident followed by a LOHS accident. As can be seen from Figure 4.32 the peak temperatures are acceptable. The increasing secondary inlet temperature to the IHX by causing the the core inlet temperature to increase results in an increase in the core exit temperature. The power rapidly drops to decay heat levels due to

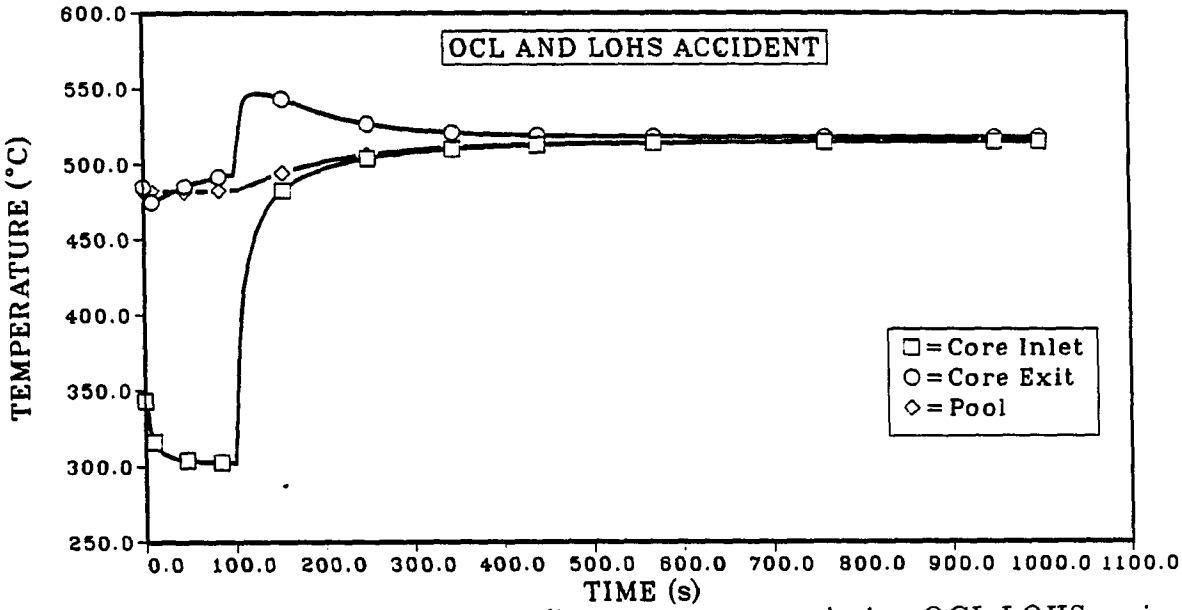

Figure 4.32: Variation of primary sodium temperatures during OCL-LOHS accident

the increased negative feedback. Again the large heat capacity of the pool and the low heat capacity of the inlet plenum has important effects on the transient. The core inlet temperature increases rapidly up to pool temperature causing the core exit temperatures to increase and consequently introducing more negative feedback reactivity, yet the pool limits the increase in the core inlet temperature avoiding damage to the core.

Neither of the two variations of this accident is challenging either to the short term or long term safety limits. Had there been a large cold pool associated with the reactor the OCL accident would have acted on a longer time scale determined primarily by the time constant of the cold plenum. Since the driving force for the accident is the core inlet temperature change the magnitudes of the peak exit temperatures are determined primarily by the changes in the inlet temperature.

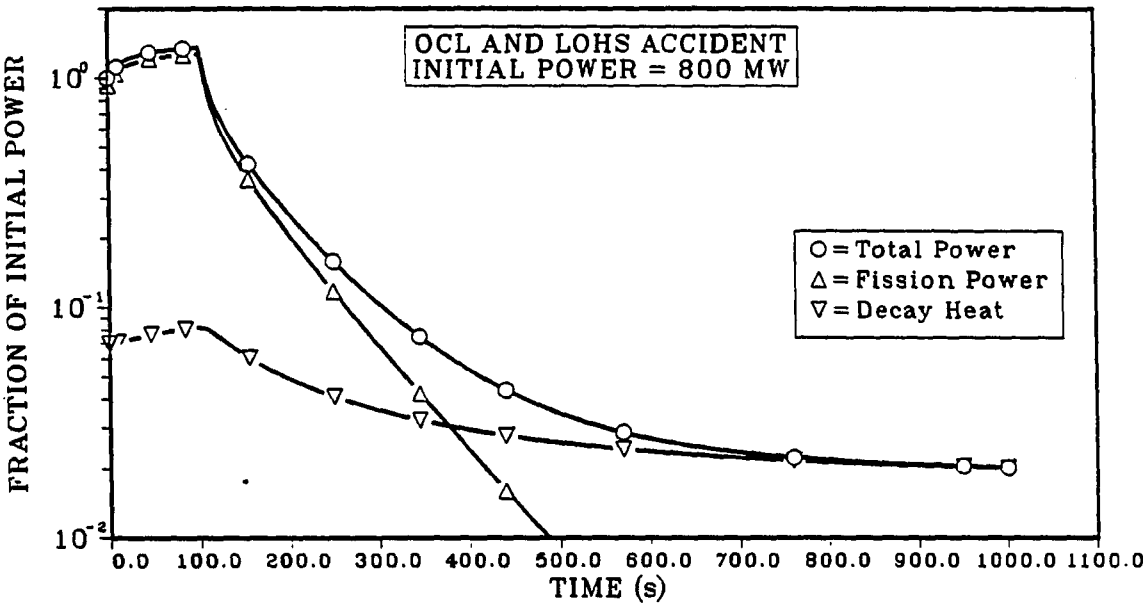

Figure 4.33: Variation of reactor power during OCL-LOHS accident

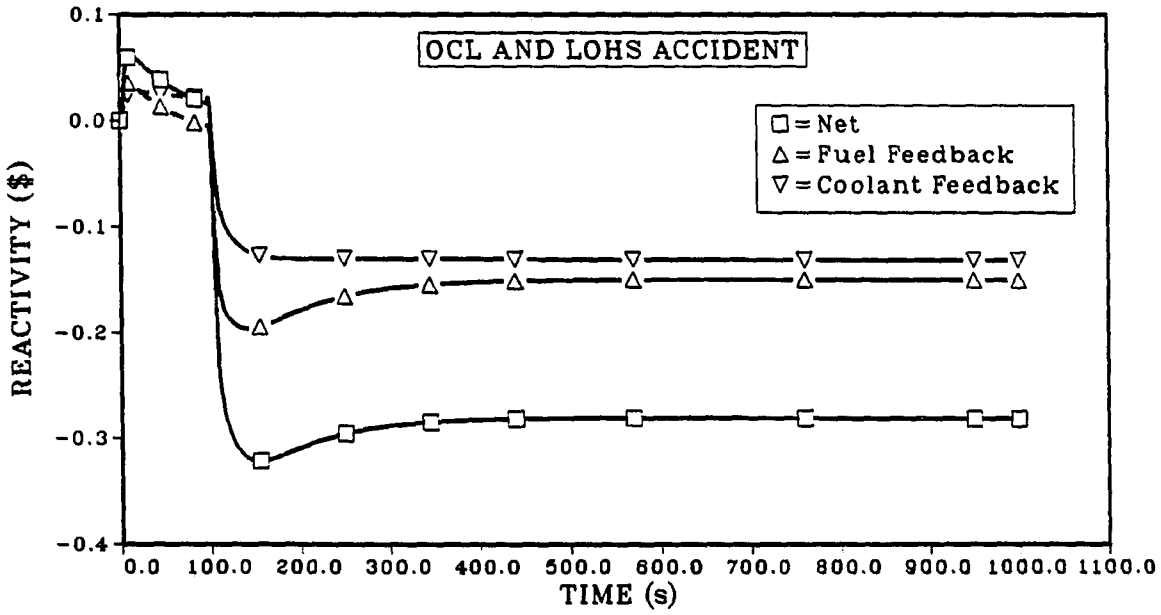

Figure 4.34: Variation of reactivity during OCL-LOHS accident

For the same resulting inlet temperature change, the resulting conditions at the termination phase of the accident will be approximately the same.

4.9 Cladding Damage Estimates

In order to estimate the damage to the cladding the cumulative damage fraction method was used as described in Section 2.1.1.2. The results of the estimates are given in Table 4.11. The failure mechanisms considered are eutectic penetration of the cladding, fission gas pressure loading and thermal stresses. The cladding is assumed to fail if either the cumulative damage fraction is greater than 1.0 or if the equivalent stress is greater than the yield stress of the cladding. The beginning of life fuel properties was used in the analysis. Although the fuel thermal conductivity decreases with increasing burnup resulting in higher fuel centerline temperatures the power density also decreases; hence the beginning of life conditions are limiting. The hot spot factors of Table 3.2 were used to compute the peak temperatures with 3σ uncertainty factors. The hot spot factor for the temperature increase in the cladding due to wire wrap was also used to compute the fuel centerline and surface temperatures; hence the fuel centerline predictions are highly conservative. The instantaneous core inlet, core flow rate, central boxes core exit, and power were obtained from the results of the transient simulation program. Since the peak fuel temperatures do not occur at the top of the fuel pin 34 axial nodes was used to predict the peak fuel temperatures. In the radial direction three nodes in the fuel, one bond in the node, two nodes in the cladding and one node in the coolant were used. The flow redistribution in a core boxes among the fuel pins was neglected to be conservative. Although the cladding and coolant temperatures peak at approxi-

mately the same time, the time at which the fuel temperature peaks is earlier. The core box design in the TR allows a uniform temperature distribution in each core box by not dividing the fuel pins in subassemblies. For the transients considered in this section flow redistribution due to buoyancy effects is not significant at the time when the peak temperatures occurs; however, neglecting this effect results in higher cumulative damage fractions for the hottest pin due to the application of uncertainty factors to temperature increases that are higher than the nominal. This assumption had to be made partially due to the lack of analytical tools to estimate the flow distribution among the various coolant subchannels associated with fuel pins having different power fractions.

An investigation of Table 4.11 shows that the LOHS and OCL accidents are of minor importance in terms of damage to the cladding. In fact, these two accidents need not be considered as accidents but merely as operational transients. The case-A type LOF accidents with a pump time constant greater than 20 seconds are also acceptable. The case-B type LOF accidents result in permanent damage to the cladding of the hottest fuel pin for all the pump time constants considered. The damage mechanism is due to eutectic formation and as the pump time constant is increased the time spent above the eutectic temperature increases. However, for eutectic penetration, the important factor is the time spent at a temperature. Since increasing pump time constant results in lower temperature levels the damage fractions decrease with increasing pump time constants. Figure 4.35 shows the cladding thinning for the cases considered in case-B type LOF transients.

The 25 cent step reactivity insertion does not result in cladding failure or damage. However, step reactivity insertion of 50 cents results in violation of fuel

Table 4.11: Transient cumulative damage fractions for the unprotected accidents

Accident	Temperature (°C)			Cumulative Damage Fraction	Violation
	Fuel Centerline	Clad Inner Surface	Coolant Core Exit		
LOHS	722	548	547	$2.0\ 10^{-9}$	None
	(923)[a]	(611)	(585)	$1.4\ 10^{-7}$	None
LOF, Case-A	730	711	711	$3.7\ 10^{-6}$	None
t_p=10s	(853)	(834)	(834)	$3.6\ 10^{-3}$	E[b]
LOF, Case-A	725	642	641	$4.2\ 10^{-7}$	None
t_p=20s	(827)	(721)	(719)	$9.5\ 10^{-6}$	None
LOF, Case-A	724	610	610	$1.6\ 10^{-7}$	None
t_p=30s	(824)	(677)	(673)	$1.8\ 10^{-6}$	None
LOF, Case-A	723	595	595	$8.1\ 10^{-8}$	None
t_p=40s	(822)	(853)	(648)	$6.9\ 10^{-7}$	None
LOF, Case-B	739	728	728	$3.1\ 10^{-6}$	None
t_p=10s	(947)	(920)	(920)	$1.1\ 10^{-2}$	E and B[c]
LOF, Case-B	723	672	672	$6.2\ 10^{-7}$	None
t_p=20s	(878)	(841)	(841)	$8.8\ 10^{-4}$	E
LOF, Case-B	722	647	647	$3.5\ 10^{-6}$	None
t_p=30s	(855)	(806)	(806)	$4.5\ 10^{-3}$	E
LOF, Case-B	721	633	633	$2.6\ 10^{-6}$	None
t_p=40s	(846)	(786)	(786)	$3.1\ 10^{-4}$	E
TOP	677	581	586	$2.3\ 10^{-6}$	None
25 cents	(1021)	(698)	(675)	$1.8\ 10^{-5}$	None
TOP	1030	673	652	$6.0\ 10^{-6}$	None
50 cents	(1223)	(834)	(801)	$3.6\ 10^{-3}$	F[d]
TOP -LOHS	991	646	635	$8.7\ 10^{-7}$	None
50 cents	(1174)	(693)	(762)	$1.9\ 10^{-5}$	None
OCL	803	512	499	$1.4\ 10^{-9}$	None
	(935)	(617)	(597)	$7.4\ 10^{-7}$	None

[a]Numbers in parantheses are 3σ temperatures.
[b]Eutectic formation
[c]Sodium boiling
[d]Fuel melting

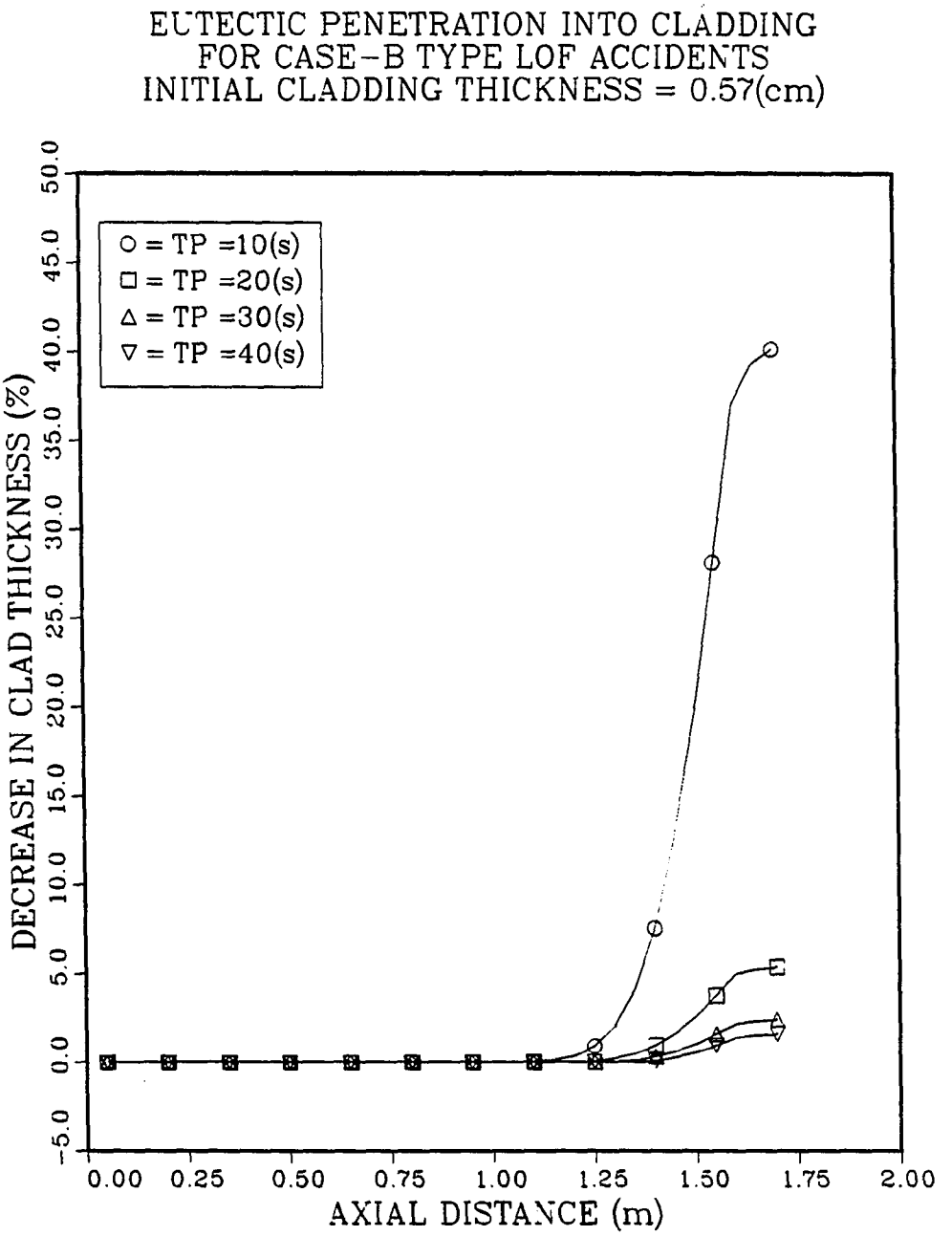

Figure 4.35: Eutectic penetration into the cladding for case-B type LOF accidents

melting for approximately 200 seconds and considerable damage to the cladding due to eutectic formation for the 3σ temperatures. Since the molten fuel cladding interaction was not modelled in these calculations the cladding damage fraction is underestimated. However, since the fuel centerline temperature is computed overly conservatively due to the inclusion of the hot spot factor from the wire wrap, and the peak fuel temperature is only $23^{o}C$ over the nominal fuel melting temperature fuel melting may not occur at all. Also, in calculating the fuel centerline temperature no credit was taken for the increase in the fuel melting due to restructuring of the fuel. The TOP accident with 50 cent reactivity insertion and combined with LOF accident results in complete failure due to sodium boiling initiation first and then cladding and fuel failures. The core will melt upon such an accident; hence the combined TOP-LOF accidents pose the greatest threat to the reactor.

4.10 Discussion

The results of the accidents simulated in this chapter indicate that the TR reactor can mitigate the consequences of a wide range of accidents without causing damage to the plant in the absence of any favorable action from the plant control and protection system. The important characteristics of the TR that led to this favorable response were the large heat capacity associated with the hot sodium pool, the reactivity feedback mechanisms from the coolant temperature and the metallic fuel and the large initial margins to failure. Even with conservatism applied in the both the simulation program and in estimating the worst conditions, the results of most of these accidents are not damaging to either the primary system components or to the core.

The TOP accident with 50 cent or more positive reactivity insertion and its combination with other accidents seem the only accident sequences during which major damage can be expected. However, as mentioned earlier both the fuel management strategy adopted for the TR and the favorable reactivity change that can be achieved with the use of metal fuel makes the step insertion of 50 cents of reactivity as an upper bound. The control rods employed in the TR will not contain this much reactivity and and most of them will not be inserted completely throughout most of the lifetime of the reactor core eliminating the possibility of such a large amounts of positive reactivity insertion. As mentioned earlier, the combination accidents, for example TOP-LOF, are very low probability events so that the consequences of such accidents should not be of major concern.

Two of the neglected feedback mechanisms should reduce the power and temperature levels calculated in during the accidents. The first one of these is the relative thermal expansion of the control rods with respect to the core. This effect was found to introduce large amounts of negative feedback reactivity in the numerical simulations done with the current fast reactor concepts such as PRISM and SAFR. In particular, this effect will be effective in transients during which the increase in the core exit temperature is higher than the increase in the core inlet temperature. The other feedback mechanism which will be effective during a TOP accident is the rapid transient swelling of the metallic fuel elements. If this feedback mechanism is as high as the value estimated in reference [23] which is approximately 2 cents per ^{o}C increase, then this effect alone will be able to compensate for the step positive reactivity insertion.

It can be concluded that under the postulated accident conditions the TR

responds in an inherently safe manner to LOHS, LOF, OCL and TOP accidents with 25 cents of reactivity insertion. The characteristics that cause such inherently safe behavior are the properties of the materials and the configuration of the reactor primary system, even without any activated safety devices.

5 CONTROL AND PROTECTION SYSTEM CONCEPTS

5.1 Control Modes

The results of the last chapter have shown that the only accident sequence that may lead to substantial damage to the primary system components is initiated by introducing a large amount of positive reactivity. The most probable source of such large amounts of reactivity is the control rods. It is therefore desirable to limit the amount of reactivity contained in control rods, limit the number of control rods and increase the reliability of the control rod system. These can be achieved by limiting the use of control rod to control the power changes caused by burnup during the lifetime of the core. This implies a plant control system that does not use the control rods. The advantageous of such an approach are two-fold; the demand for the rapid and frequent action of the control rods is reduced resulting in high reliability and the cost associated with the control system is reduced due the simplifications resulting from the control system design.

Under normal operating conditions, the basic function of the control system is to keep the plant in balance, that is to match the power produced in the core to the power demanded from the electricity grid. Under abnormal operating conditions, the control system should be able to bring the reactor to a safe condition, which in the extreme case is neutronic shutdown with proper decay heat removal. The op-

erating conditions experienced during such a transient should be within acceptable limits; they should not result in significant damage to the components of the plant.

The available control modes can be inferred from Eq. (4.2), repeated here with an additional term representing the reactivity introduced by the control rods;

$$0 = \alpha_{T_{in}} \delta T_{in} + \alpha_{pf} \delta \left(\frac{p}{w} \right) + \alpha_p \delta p + \rho_{cont} \tag{5.1}$$

The purpose is to adjust the variations in the core inlet temperature and flow rate so that a desired power level is obtained while introducing the minimum amount of control rod reactivity ($\rho_{cont} \approx 0$). The two options available are controlling the reactor by keeping the flow rate constant and controlling the reactor by adjusting the flow rate so that the desired power level is reached. In the first case, inlet temperature control, the reactor inlet temperature is allowed to change freely in response to the changes in the heat removed from the IHXs by the secondary sodium while keeping the reactor flow rate constant. In the second case, flow rate control, the controlled variable is the pump speed.

The load following characteristics of the TR for inlet temperature control can be inferred from the results of the unprotected LOHS and OCL accident presented in Chapter 4. In the LOHS case the heat removed from the reactor through the IHXs was almost zero and the internal feedback effects of the reactor caused the fission power generated in the reactor to vanish. In the OCL case the decrease in the secondary sodium inlet temperature resulting in an increase of the heat removed from the IHXs caused the reactor power to increase in order to match the increased demand. In both cases the primary pump speeds were kept constant. This mode of control is possible in the TR due the relative reactivity coefficient of the inlet temperature and the power reactivity decrement. Since a degree change in the

inlet temperature causes a percent change in the power produced, by allowing the secondary inlet temperature to decrease as a result of increased heat removal from the steam generators and consequently from the IHXs will cause the reactor power to match the heat removed from the steam generators. The existence of a secondary loop will cause a certain time delay between the time at which the steam demand increases and the time at which the reduction in the secondary sodium temperature occurs. Apart from this delay, the elimination of a large heat capacity associated with the core inlet temperature causes a fast response of the primary system. The results of various step load changes in the secondary side are shown in Figure 5.1. The reactor operates with basically constant hot end temperatures, these being the core exit and the IHX exit temperature on the secondary side, while the change in the cold end temperatures cause the reactor to produce the required power level.

In order to cause a reactor shutdown, the control system has to simply cause a LOHS accident. The results of the LOHS accident showed that no significant damage occured as a result of this accident. The secondary sodium flow rate can be controlled to obtain a more smooth increase in the core inlet temperature. This will increase the time at which fission power decays, but a very reliable shutdown mechanism which is controlled from outside the primary system is obtained.

The second option is to use the primary flow rate as the controlled variable to achieve the required power level. The control is achieved by controlling the pump speed. The pump inertia and the maximum torque that can be supplied by the pump are important factors that need to be considered. A large pump inertia implies a long coastdown time for the primary pumps and an increase in the torque that must supplied. The maximum speed at which the pump can work also limits

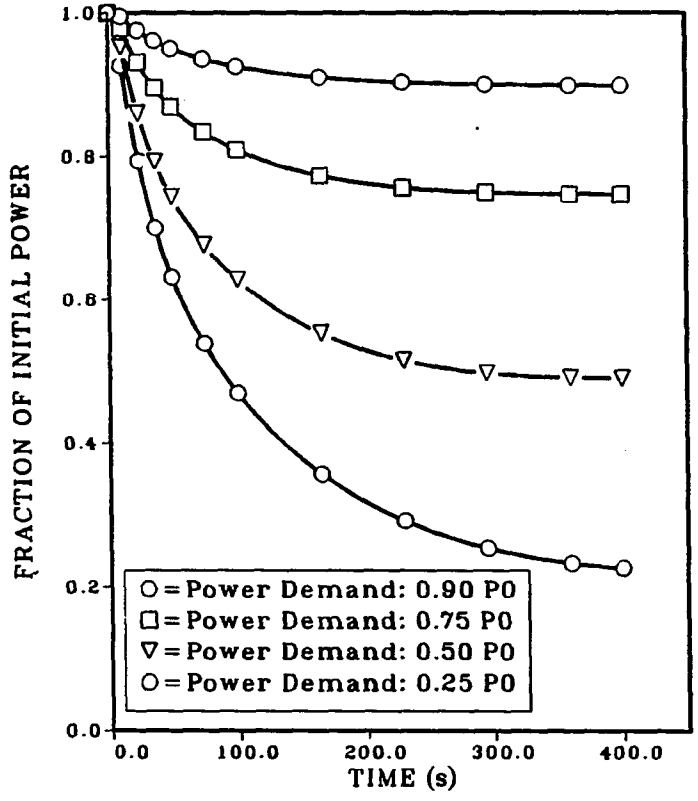

a. Normalized power (Initial power P0=800MW)

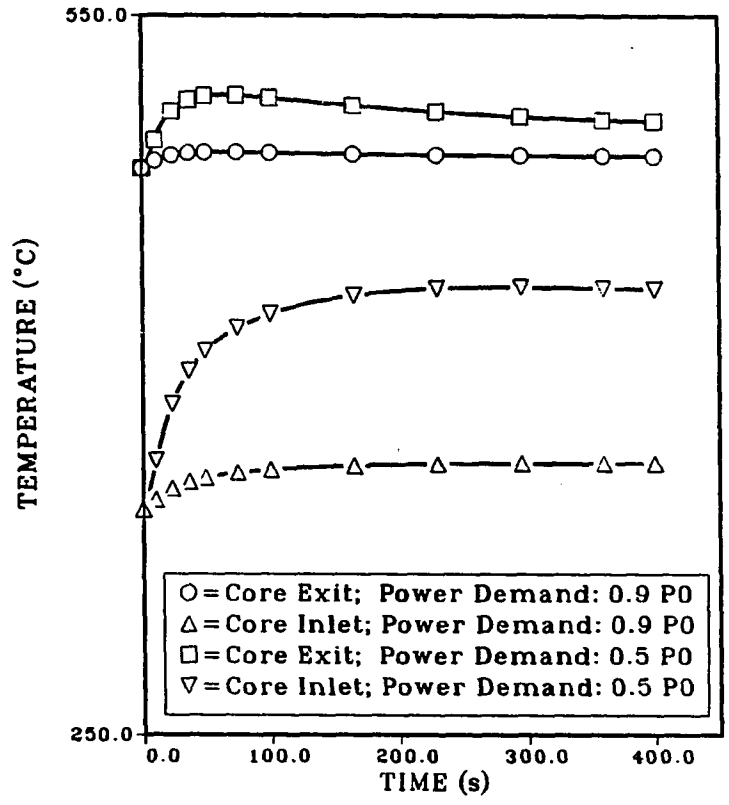

b. Core inlet and core exit temperature variation

Figure 5.1: Results of constant flow rate control

the upper limit of the control achievable with control mode.

In order to simulate flow rate control, a proportional-integral (PI) controller was assumed. The pump torque was calculated by

$$\frac{dT_{pm}}{dt} = K(W_d - W) \tag{5.2}$$

where T_{pm} is the torque supplied by the pump, W is the core flow rate and the W_d is the flow rate required or the set point for the controller. K is the controller gain. The reason for choosing a PI controller was to eliminate the steady state error through the integral action.

In this case, one has to decide on a the set point for the flow. Several options are available. The first one is to adjust the flow so that flow rate is changed according to

$$W_d = W(0)\frac{P_d}{P(0)} \tag{5.3}$$

which will result in changing the core flow rate so that the final power to flow ratio is unity. In the above equation P_d is the power demand. The results of this control mode for a 10% reduction in the load are shown in Figure 5.2. The controller adjusts the core flow rate in proportion to the load and as steady state is reached the power to flow ratio approaches to unity. The increase in the primary system temperature is about 15^oC for this case. The results indicate that the gain of the controller should be load dependent; that is, the gain of the controller should decrease as the magnitude of the reduction in the load increase. This is required in order to avoid a large overshoot in the core exit temperature for large changes in the load. Since the power approaches the demand, no control rods are required for this case.

Other options can be achieved by controlling the primary flow rate so that the

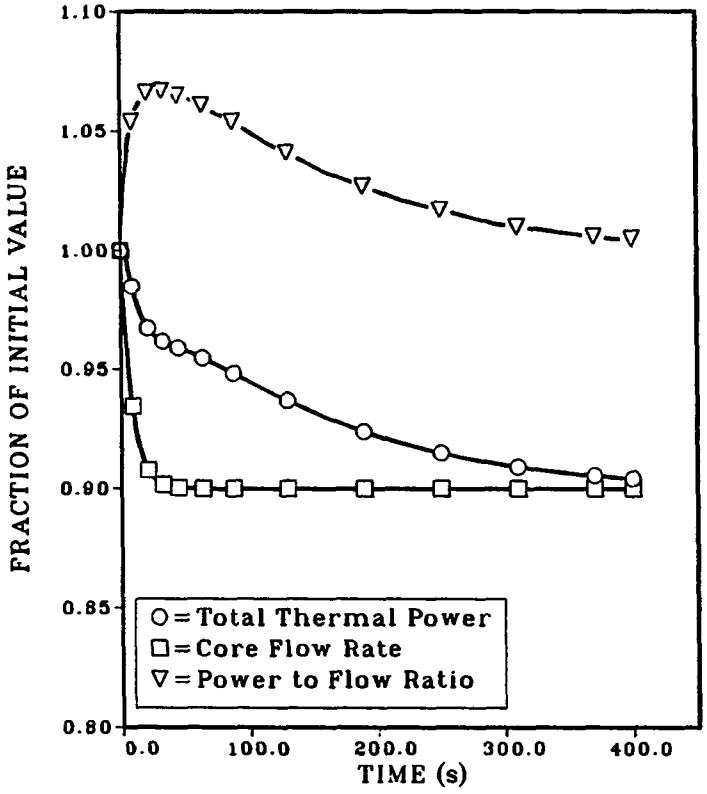

a. Normalized power and power to flow ratio (Initial power P0 = 800MW initial flow rate W0 = 4400kg/s, power demand PD = 0.9)

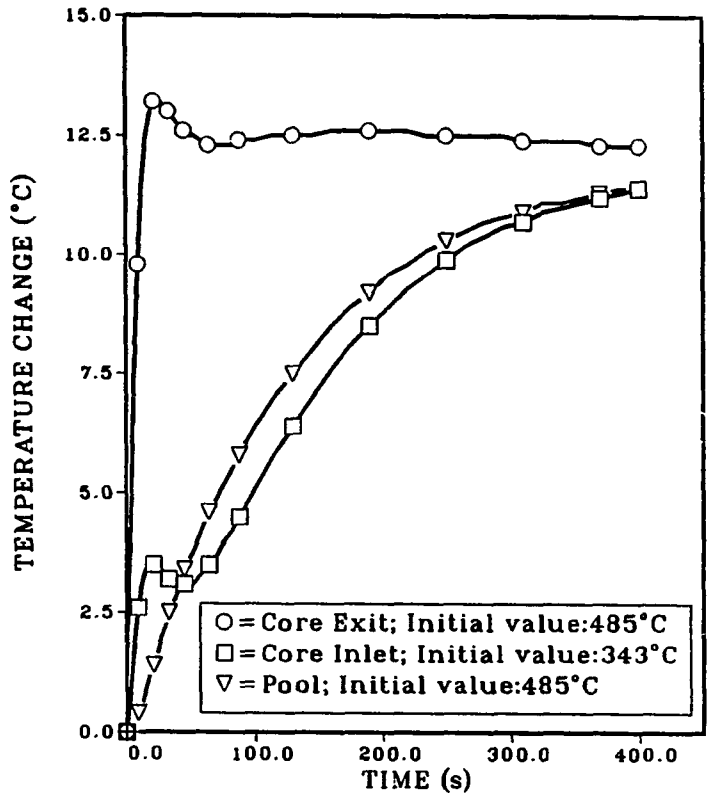

b. Core inlet, core exit and pool temperature change

Figure 5.2: Results of flow rate control mode

change in either the hot or cold end of the reactor or the temperature rise across the core is limited. If the core flow rate is controlled so that the core inlet temperature is fixed at its steady state value, load following is obtained by changing the primary flow rate. Since a change in core inlet temperature affects the power, this mode of control may be used to obtain the desired change in power by a small variation in the core temperatures. From Eq. (5.1) it can be shown that at steady state the normalized flow will be given by

$$w = \frac{\alpha_{pf} p}{\alpha_{pp} - (\alpha_p + \alpha_{pf})} \tag{5.4}$$

and during the transient the set point for the controller will be

$$W_d = \frac{P(t)}{C_p(T_{cx} - T_{in}(0))} \tag{5.5}$$

where T_{cx} and T_{in} are the core inlet and core exit temperatures and C_p is the specific heat. The results of this case are shown in Figure 5.3. In this case the controller eventually satisfies the constant core inlet temperature setting. The magnitudes of the overshoot and undershoot in the change in the core inlet temperature indicate that the gain setting used in the calculations is too high for this case. Regardless, this mode of control is clearly not desirable, because of the fluctuating response of temperatures, power and flow. Even if by using a smaller gain setting these fluctuations can be avoided, the necessity to control the core inlet temperature precisely makes this mode of control disadvantageous. A better method of achieving a constant core inlet temperature may be obtained by controlling the secondary flow rate.

The core exit temperature can be controlled by setting the controller so that

$$W_d = \frac{P(t)}{C_p(T_{cx}(0) - T_{in})} \tag{5.6}$$

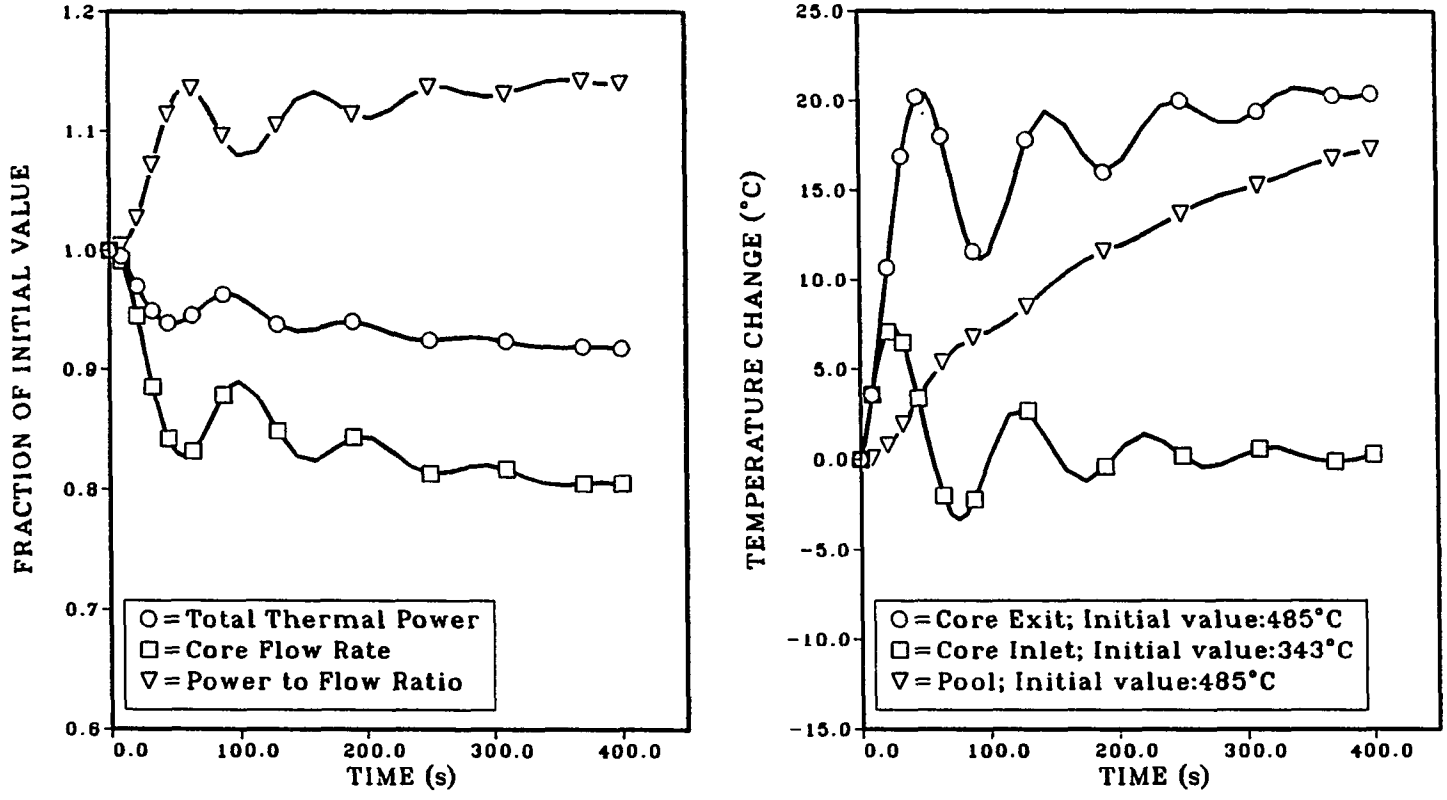

a. Normalized power and power to flow ratio (Initial power P0 = 800MW, initial flow rate W0 = 4400kg/s, power demand PD = 0.9)

b. Core inlet, core exit and pool temperature change

Figure 5.3: Results of constant core inlet temperature control mode

is satisfied. The results of this case for a 10% decrease in load are shown in Figure 5.4. At the end of the simulation the normalized value of the power is 0.89 and the maximum increase in the core exit temperature is about 2.5^{o}C. There is no need for control rods to adjust the power to match the load. The reduction in the power is caused by the increase in the core inlet temperature and flow rate. This mode of control seems to be superior to other modes of control by limiting the core exit temperature not only in the load following mode but in transient overpower accidents. Since the maximum amount of flow that can be supplied by the pump is limited in case of an overpower transient, if this mode of control is operational the controller will increase the flow until its maximum value is reached. The maximum flow rates that can be achieved from the pumps are typically about 15% higher than their design point. This will help to reduce the increase in the core exit temperature at the initial stages of such a transient.

One other option is to control the flow rate so that the power to flow ratio is kept at unity during the transient. In this case the required core flow rate will be given by

$$W_d = W(0)\frac{P(t)}{P(0)} \tag{5.7}$$

By keeping power to flow ratio at unity the temperature rise across the core is kept constant during the transient. The results of this case for a 10% decrease in the heat removed from the secondary loop are shown in Figure 5.5. Again the reactor power decreases to match the load and there is no need for control rod action. Both the core exit and inlet temperature rise by approximately 10^{o}C, and the control system objective of keeping the power to flow ratio at unity and the core temperature increase at its initial value are satisfied during most of the transient.

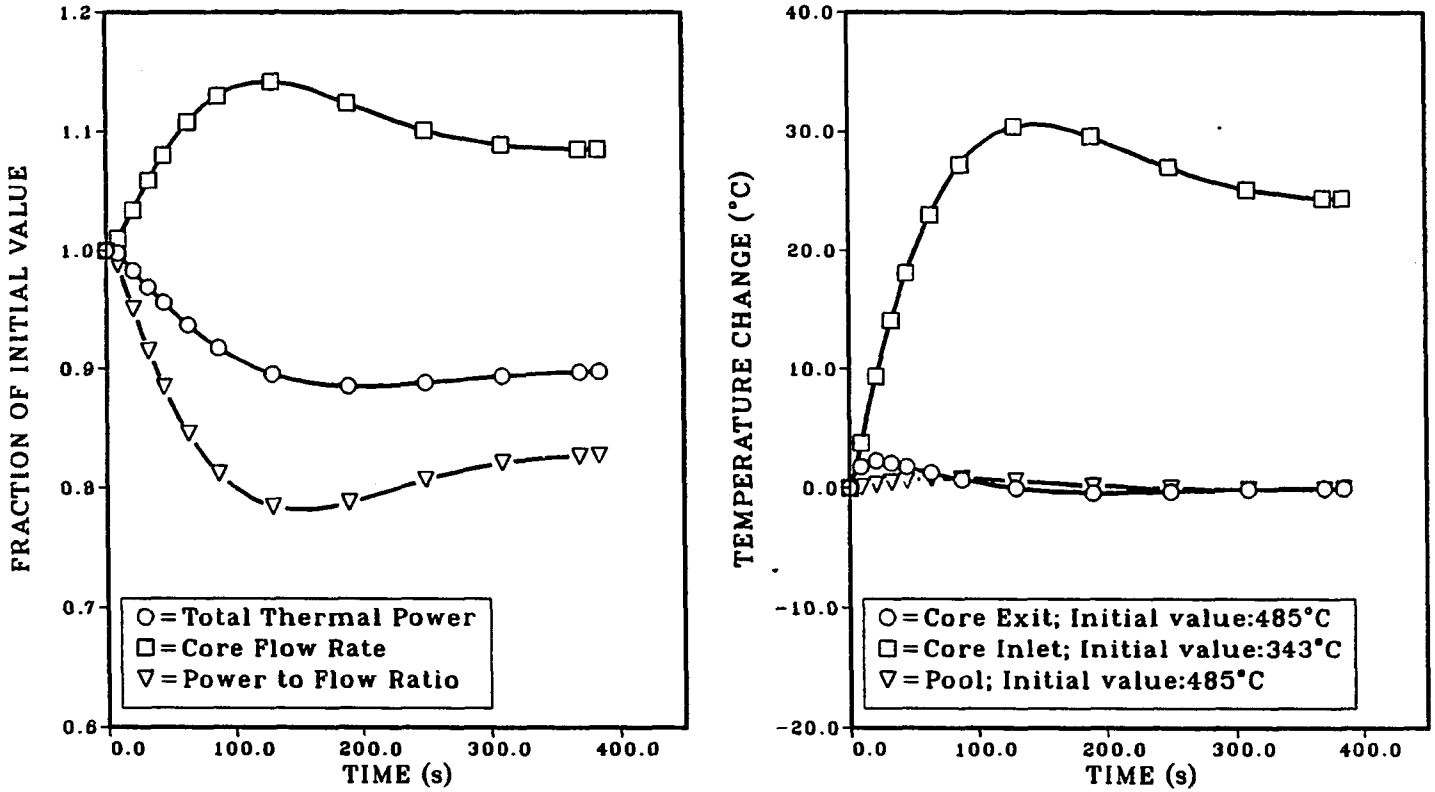

a. Normalized power and power to flow ratio (Initial power P0 = 800MW initial flow rate W0 = 4400kg/s, power demand PD = 0.9)

b. Core inlet, core exit and pool temperature change

Figure 5.4: Results of constant core exit temperature control mode

This mode of control is suggested by reference [37]. The major deficiency of this control mode will be in transients approaching a LOHS accident during which the core inlet temperature increases considerably. Since this mode will try restore the core temperature increase to its initial value, the core exit temperature increase will be greater than it would be during a LOHS with a flow rate control mode operational.

Note that except for the control mode given by Eq. (5.3), the power demand is not used in the controller setting, but the final power level is expected to follow the load as a result of Eq. (5.1) and this is achieved in all the cases considered. This confirms the load following character of the TR reactor regardless of the control mode used. The time delay between the change in the load and the matching of the reactor power to the load is approximately 7 minutes with the controller gain setting used. There will be an additional delay in the secondary sodium loop of the order of a few minutes. Depending on the magnitude of the change in the load, these time delays will change. If this time delay can be tolerated, there is no need to use the control rods for load following purposes in the short term. However, use of control rods may be required to return the reactor to operation at the design temperature.

5.2 Plant Protection System Concepts

Besides the control system, the plant protection system, an independent system that will assure the safety of the reactor in case the control system system fails or malfunctions is required. The main purpose of this system is to shut down the reactor in a major accident situation in adverse conditions. It is desirable to have

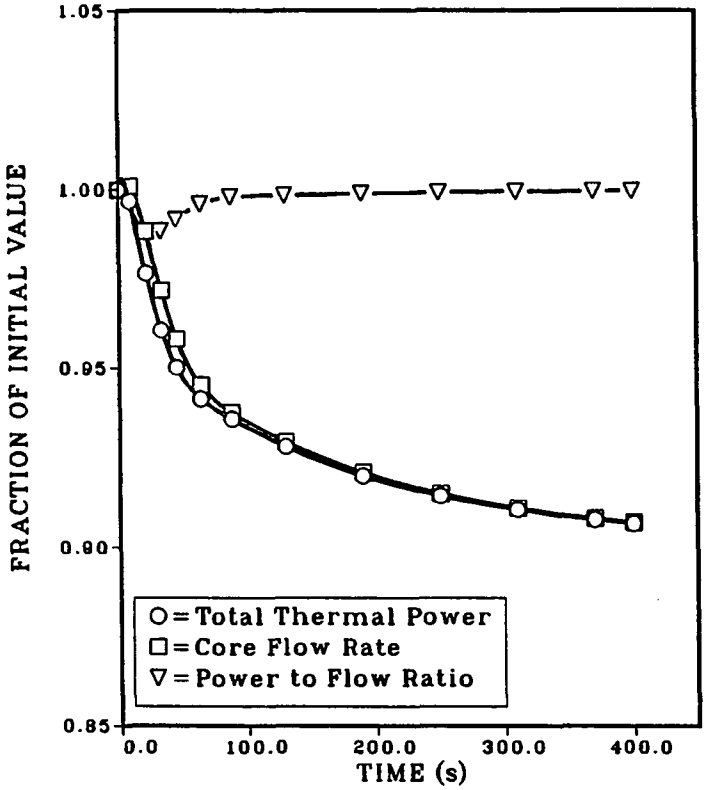

a. Normalized power and power to flow ratio (Initial power P0 = 800MW initial flow rate W0 = 4400kg/s, power demand PD = 0.9)

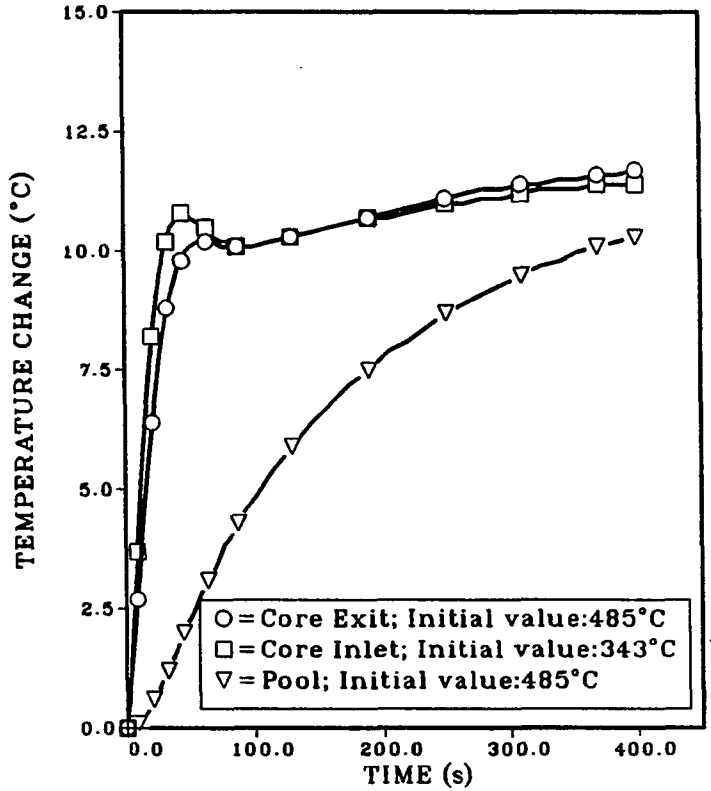

b. Core inlet, core exit and pool temperature change

Figure 5.5: Results of constant power to flow ratio control mode

such a system acting without the need for an external system or operator action. In the TR, such a system is required in the positive reactivity insertion accidents acting alone or coupled with other accidents and coupled LOF-OCL accidents. In both types of accidents, particularly in TOP accident, the temperatures predicted to occur during the transient were high enough to challenge the reactor core and the vessel integrity.

A self-actuated shutdown system (SASS) has been developed by Westinghouse [72] and is being used in the current U.S. LMR concepts. This systems contains an electromagnet holding the neutron absorbers and is oriented vertically. The magnetic force holding the neutron absorbers is obtained by using a coil and a metallic alloy composed of a Ni-Fe alloy. A small fraction of the sodium that exits the reactor core is guided around the absorber assembly. When the core exit temperature increases, the temperature of the Ni-Fe alloy also increases. The composition of the Ni-Fe alloy may be selected such that the temperature at which the material loses its magnetic properties, or curie point temperature, is close to the safety limits. At such a temperature the magnetic force that holds the absorbers will be lost and the absorbers will be released. This system does not require any external drives or operator action. Since its principle is based only on the material properties it can to a certain extent can be considered an inherent protection system.

Such a system can be applied to the TR as a final level of defense. In the original application of SASS the Ni-Fe composition was selected such that the curie point was near 600^{o}C. This temperature is to low for TR in view of the results obtained from Chapter 4. A higher temperature is desirable in order to reduce the number of shutdowns.

In order to see the effects of a shutdown system on the worst transient a coupled LOF-TOP was selected. A step reactivity insertion of 50 cents and a pump time constant of 10 seconds was assumed. The secondary flow rate was assumed to be at its initial value of 1800kg/s. The total amount of reactivity contained in the absorbers was assumed to one dollar. The temperature at which the absorbers were released was set to 675^{o}C. The results are shown in Figure 5.6, Figure 5.7 and Figure 5.8. The initial peak in the core exit temperatures cause the absorbers to be released. This results in a rapid reduction in the power and the core exit temperatures. Since the natural circulation flow has not established the flow is still decreasing. This results in a smaller peak after the release of the absorbers. The heat removed by the secondary system through the IHXs forces the core inlet temperature to drop. Since the power is also decreasing due to the negative reactivity inserted by the absorbers the core exit temperature decreases and becomes less than the pool temperature.

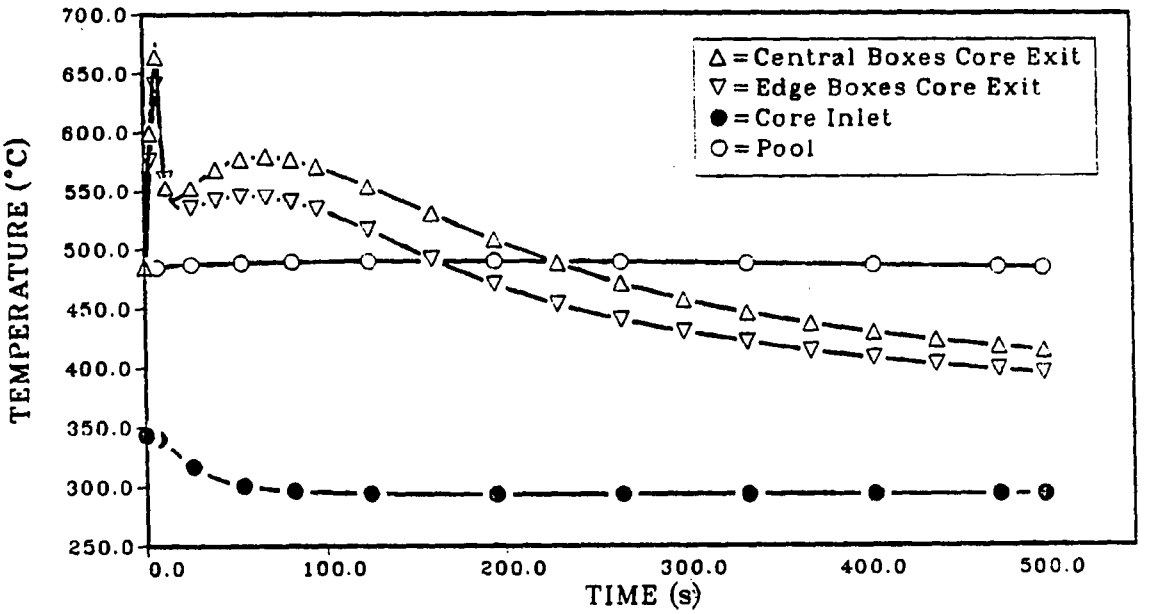

Figure 5.6: Variation of primary sodium temperatures during a coupled LOF-TOP accident with shutdown

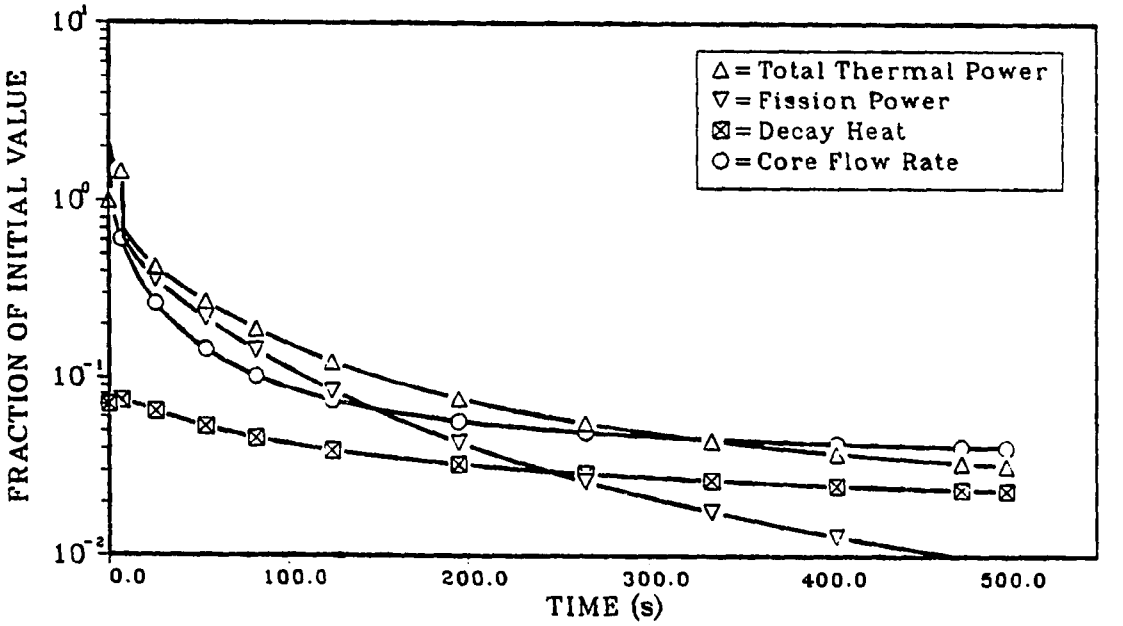

Figure 5.7: Variation of reactor power and flow during a coupled LOF-TOP accident with shutdown

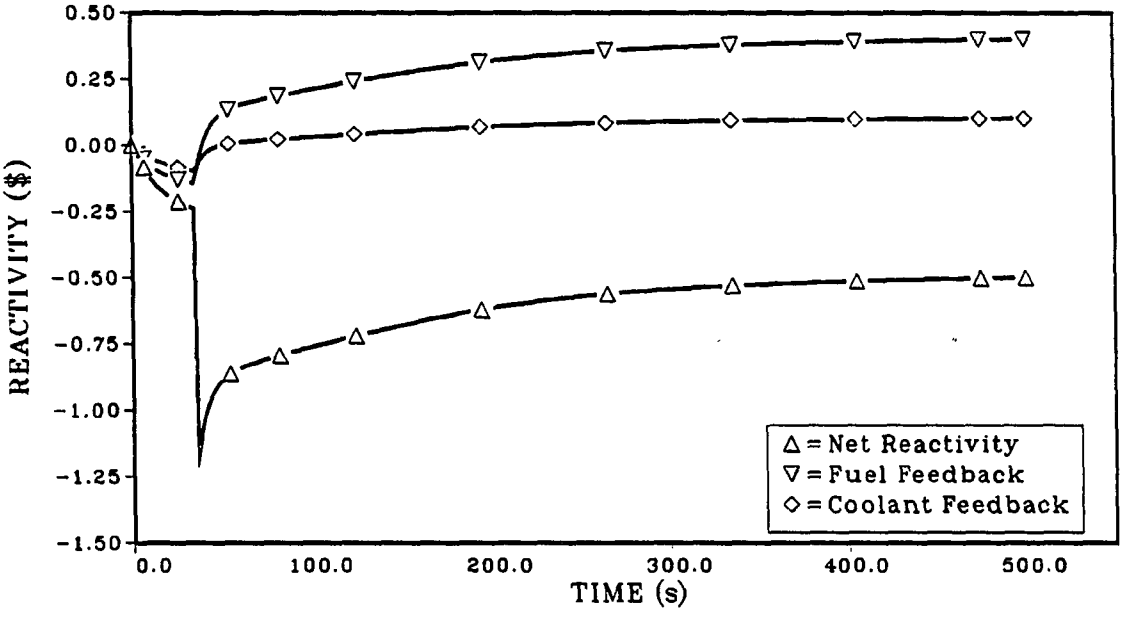

Figure 5.8: Variation of reactivity during a coupled LOF-TOP accident with shutdown

6 CONCLUSIONS

The description of the thermal-hydraulic and transient behavior of the TR concept presented in the previous chapters shows that the objective of achieving a simple and inherently safe nuclear power reactor is met by the present configuration. The main features of the TR that contribute to the simplicity and to the inherent safety of the plant are the small thermal power, the use of metal fuel and the configuration of the primary system.

TR has the advantages of a small power plant. The current technology can be applied to build the main components of the reactor system. The operating conditions do not impose strict requirements on the components due to the large safety margins. The failure mechanisms of the metal fuel are such that the time to failure is long. The favorable feedback characteristics of the metal fuel and the core provide operational ease and safety. The large sodium pool protects the reactor from rapid increases in temperature. These characteristics, which are common to most of the current LMFR concepts in the U.S. are obtained in TR concept in a unique configuration.

One of the major design changes introduced in TR is the reduction in the heat capacity effects associated with the cold end of the primary system. Several advantages of this change were observed.

First, it is possible to eliminate the problems associated with having a hot pool and a cold pool in the same vessel. Among the problems eliminated, one can mention, for example, assuring proper physical and thermal separation of pools and having some parts of the shell of the IHX in the hot pool and some in the cold pool which causes thermal stress problems. The result is a simplification in the primary system layout.

Secondly, the response of the TR reactor to a wide range of accidents is improved, resulting in a safer reactor. This improvement is a result of the elimination of the time delay introduced by the cold pool. The effects of changes in the core inlet temperature are felt early in a transient. This allows the reactor power to adjust to the changes in the heat removed from the primary system through the IHXs.

With the elimination of the time delay from the cold part of the primary system it is possible to improve the load following characteristics of the TR without resorting to rapid control rod maneuvers.

Finally, this change introduces a reliable and rapid reactor power control system based on core inlet temperature. By causing the core inlet temperature to increase, for example by reducing the secondary loop sodium flow rate to small values, it is possible to control the reactor power or even to cause a neutronic shutdown as was observed from the results of the simulated LOHS accidents.

However, there are some disadvantages to this approach. Under normal operating conditions, the primary pumps are subject to higher operating temperatures than the pool type LMFRs which employ the two pool concept. This penalty is not expected to be a major handicap, because previous experience with sodium pumps

has shown that the current pump designs are capable of functioning properly at the temperature levels employed in the TR.

The second disadvantage associated with this approach is observed during transients caused by loss of only the primary pumping power. During such accidents the core inlet temperature decreases and introduces positive reactivity resulting in a slower decay of fission power. The estimated peak temperatures indicate eutectic penetration into the cladding, but cladding failure is not predicted. The damage accumulated by the cladding during such a transient is small enough to permit continuation of normal reactor operation after such an accident. This disadvantage can be avoided in a simple and reliable manner by assuring that the secondary pumps are turned off whenever the primary pumps are turned off. Such a solution implies that the secondary pumps are also related to the safety of the primary system if permanent damage to cladding is to be avoided under any circumstance. Therefore, the goal of limiting the safety related components to the primary system is not quite achieved with such a solution.

In general, the *"no cold pool"* concept is favorable for a wide range of operating conditions. The requirement that no eutectic penetration should occur seems to be too conservative, since the time span for eutectic penetration is short and longer periods are needed to cause a considerable reduction in the cladding lifetime. Further work on this matter seems to be necessary, however.

The second major design change introduced in the layout of the primary system is the pumping concept. The concept employed in TR reactor retains the advantages of both loop and pool type concepts. The elimination of the cold pool and the location of pumps in the upper part of the sodium pool eliminate the need for

long pump shafts. This concept also makes the maintenance of the primary pumps easier.

Another major design change introduced in the TR is the overall shape of the primary vessel and the core. The trench like shape of the reactor vessel has a larger surface area than, for example a cylinder, providing an adequate removal of heat removal from the primary vessel. The heat removal from the vessel was seen to be high enough to remove the decay heat and avoid a large increase in the pool temperature following an accident that might impair all forced cooling. The height of the vessel is sufficient to provide the necessary separation between the thermal centers of the IHXs and the core so that natural circulation cooling of the core is possible when the primary pumping is lost.

The shape of the core and the substitution of core boxes containing a large number of fuel pins for a large number of subassemblies containing a small number of fuel pins have several advantages. The elimination of the subassemblies enhances mixing to give a uniform temperature and results in a simpler core layout. Reactor control is possible without having control rods in the reactor core. The fuel pin diameters used in TR are large in diameter and should be easier to manufacture. The tight packing of fuel pins results in sufficiently strong feedback coefficients to give an inherently safe behavior. The only disadvantage of this arrangement is the relatively higher pressure drop.

The simulations performed on unprotected accidents show that the most threatening accident sequence is an unterminated TOP accident. TR can survive a 25 cent step reactivity insertion, however, a 50 cent reactivity insertion, if not terminated quickly can damage the vessel. During such an accident, the heat removal

from the IHXs and through the VCS cooling system is insufficient to remove the heat generated in the core, with the excess heat being deposited in the pool. The increasing pool temperature after such an accident could lead to vessel damage. However, the failure of the vessel due to increasing temperature is delayed for long time long enough to allow recovery from the accident.

The TOP accident when accompanied with LOHS or LOF accidents is not threatening to the vessel integrity but it challenges the sodium boiling limit. The worst accident simulated was a coupled TOP-LOF accident, results of which indicated that sodium boiling may occur as a consequence of such an accident. TOP and LOHS accidents occurring at the same time do not violate the safety criteria. However, the probability that TOP-LOF accidents will simultaneously occur is very small, and the reactor is also protected by the control and safety blade systems.

The LOHS and OCL accidents are mild accidents with no major consequences. The LOF accident when coupled with LOHS accident with pump time constants greater than 10 seconds does not violate any of the safety criteria. The LOF accident with the secondary pumps on causes eutectic formation for the hottest fuel pin. However, the magnitude of the predicted eutectic formation was not large enough to cause cladding failure.

The large amount of sodium in the form of a large hot pool, the large initial margins to any of the failure limits and the favorable feedback characteristics of the metal fuel played a major role in the accidents simulated.

The load following characteristic of the TR indicate that there is no need for rapid control action in order to adjust the power. The desired change in the reactor power can brought about by letting the core inlet temperature respond to

the changes in the heat removal rate from the IHXs. The primary pumps can be controlled to limit the changes in the primary system temperatures. The control of primary pumps to obtain a constant core flow rate, a constant core exit temperature and a constant power to flow ratio does not interfere with the load following characteristics while achieving the control goal. Limiting the use of control rods to slow motions for longer term control will reduce the probability of an accidental reactivity insertion.

The application of a defense in depth approach in nuclear power reactor safety to the TR concept offers a different interpretation of the various levels of defense. The first level of defense, avoiding accidents from happening, is achieved in the TR by the relaxed requirements on the behavior of the components, large safety margins to failure and simple configuration of the plant. The second level of defense, preventing accidents from causing large scale failure, is supplied by the properties of the materials used and the passive mechanisms. For a wide range of accident initiators, the TR does not require active safety systems to limit the consequences of accidents. The passive safety mechanisms are strong enough to mitigate the consequences of such accidents. Furthermore, the risk from the potentially most dangerous accident, an overpower accident caused by reactivity insertion, is reduced to negligible levels when the ability of the metal fuel to respond to the changes in the coolant temperature and the power level is taken into account. The role of active safety systems is in the third level of defense, preventing complete plant loss and avoiding radioactive release.

7 SUGGESTIONS FOR FURTHER STUDY

There are several areas on which further research may be beneficial. These can be grouped into two main categories, one involving modifications to the TR concept and the other involving modeling considerations.

7.1 Modifications to the TR Concept

The estimates of damage to the cladding during unprotected accidents showed that this damage is generally small. The major damage acquired by the cladding was caused by eutectic formation, not by the stresses caused by the fission gas pressure. This indicates that the length of the fission gas plenum may be reduced from its current dimension. Such a reduction in the length of the fission gas plenum will help to reduce the core pressure drop and separate the thermal centers of the IHX and the core resulting in an increase in the core flow rate during natural circulation conditions. Furthermore, this will also result in smaller primary pump diameters.

In the TR, the heat capacity of the primary system is approximately 2 full power seconds per degree centigrade and almost all of this heat capacity is contained in the hot pool. The response of TR to loss of primary pumping power with the secondary pumps at their initial speeds has been the only accident sequence during which the reduction of the heat capacity effects associated with the core inlet temperature

resulted in temperatures that are higher than temperatures obtained with larger cold plenum volumes. In other transients considered the "no cold plenum" design has been favorable. The EBR-II contains a cold sodium pool whereas TR contains a hot pool and there are several designs containing both a hot and a cold pool. The response of EBR-II to the unprotected accidents has similar characteristics as in TR. The answer to "what is the optimum division of cold and hot plenum volumes given a specified amount of sodium ?" may result in another modification. The main difficulty in answering the above question is defining the optimum division. A larger cold plenum will delay the response of the TR in transients during which the core inlet temperature rise causes the reactor power to decrease. It will also slow down the load following characteristics of the TR. However, by decoupling the primary system from the secondary system to a greater extent or by introducing more time delay between the secondary system and the primary system, with a larger cold plenum, it may be possible to avoid eutectic formation for a wider range of accident scenarios. Therefore, in defining the optimum division of cold and hot sodium volumes in the pool, the relative merits of each division under different circumstances need to be compared to each other. Such criteria can be best obtained through probabilistic methods which in turn needs a detailed engineering design.

The fuel management strategy adopted for the TR does not result in large power variations along the core. However, the power produced in blankets will increase due to production of new fissile material towards the end of the fuel cycle. The current practice in breeder reactors is to use a multiple orificing for blanket and fuel assemblies to be able to compensate for the changes in power produced in the blankets and the fuel elements through the lifetime of the reactor. In the

core design of the TR, the blanket elements and the fuel elements are not contained in different subassemblies, but are next to each other. An orificing scheme which takes the large power skew, hence enhanced mixing, between the fuel and blanket elements may result in simplifications in the core inlet design.

7.2 Modeling

The large number of physical processes occurring makes any list of improvements to the modeling of the TR incomplete. However, some aspects that were not considered in this study will be mentioned below.

A quasi-continuum or porous medium approach to the modelling of the core thermal-hydraulics under steady state and natural convection conditions seems to be more appropriate than the subchannel approach employed in this study. Such a method, I believe, will show the advantages of the innovative core design of the TR. However, a porous medium approach requires a three dimensional treatment of the reactor core. By making use of the rather uniform power distribution in the core it is possible to reduce the computational costs.

The possible stratification that may occur in the pool also needs to be considered. Though detailed studies of this subject on several LMFRs indicate that such effects are small due to the high thermal conductivity of the sodium, the layout of the pool of the TR may cause certain stagnant regions on the opposite side of the IHXs resulting in an increased IHX inlet temperature. Such an increase, if the large margins to failure are considered, will not adversely affect the safety of the reactor during transients which result in an increase in the core inlet temperature but will be beneficial for those transients during which the core inlet temperature decreases.

As a starting point, a two dimensional treatment that neglects the changes in the short dimension may suffice. However, a three dimensional treatment is necessary to establish the temperature distribution in the reactor vessel and other components contained in the pool.

The modeling of the fuel element behavior under transient operating conditions, in particular during rapid increases in power resulting from a positive reactivity insertion, and a quantitative assessment of the transient swelling of the metal fuel may introduce an important negative feedback mechanism. The relative thermal expansion of the core and the control rods is another important feedback mechanism that needs to be considered.

The inclusion of the secondary circuit in the transient simulation program is expected to result in more realistic and less severe accident sequences. Therefore, it is not expected to change the conclusions with respect to the safety of the reactor. However, such a modification is necessary if an optimal control strategy is to be investigated. A simulation program including the components of the secondary system, in particular the steam generators, does not seem very practical due to the long computation time, at least with the version of DSNP that has been used in this study.

A final suggestion may seem contrary to the above suggestions. Development of simple models that can adequately describe the overall behavior of the reactor plant would be useful. The pool type LMFRs with metal fuel offer a potential with respect to being amenable to such analysis. The small time constant of the metal fuel, the small transport delay of sodium across the core, almost linear sodium temperature distribution along the core and the large time constant of the pool make

simple models sufficiently accurate to predict the overall tendencies. A prompt jump approximation for the fission power or semi-analytical methods, such as the one used in DSNP's NEUTS1 module, can circumvent the numerical problems associated with the point kinetics equations. The quasistatic feedback reactivity equation Eq. (4.2) can be used to model the feedback mechanisms. Such models can be used in initial scoping calculations to investigate the effects of major design changes and help to increase understanding of the interdependencies of major reactor parameters.

8 BIBLIOGRAPHY

[1] Unattributed article. "World List of Nuclear Power Plants". Nucl. News p. 20, February 1989.

[2] R. R. Schmidt. "Core Physics of an Unconventional Liquid Metal Cooled Fast Power Reactor Concept". M. S. Thesis. Department of Nuclear Engineering, Iowa State University, Ames, Iowa, 1988.

[3] L. C. Lin. "Economic Analysis of the Trench Liquid Metal Fast Reactor". M. S. Thesis. Department of Nuclear Engineering, Iowa State University, Ames, Iowa, 1988.

[4] J. T. Sankoorikal, A. F. Rohach, B. I. Spinrad, R. Schmidt and L. C. Lin. "Fuel Managament of the Trench Fast Power Reactor". Trans. ANS 109:200, 1988.

[5] J. Lofshult. *Progress Report.* Unpublished. Department of Nuclear Engineering, Iowa State University, Ames, Iowa, May 1988.

[6] C. Goetzmann. "Low Specific Capital Cost: The Design Problem of Small Reactors". Nucl. Engrg. Des. 109:11-18, 1988.

[7] R. W. Hardie and S. V. Jackson. "US Market Potential for Small and Medium-Sized Nuclear Reactors". Nucl. Engrg. Des. 109:365-371, 1988.

[8] A. M. Weinberg, I. Spiewak, J. N. Barkenbus, R. S. Livingston and D. L. Phung. *The Second Nuclear Era.* Praeger Publishers, New York, New York, 1985.

[9] F. Wald. "Small and Medium Power Reactors in Developing Countries Present Status". Nucl. Engrg. Des. 109:343-347, 1988.

[10] J. G. Collier, L. M. Davies and S. Levy. "The Accident at Three Mile Island". In *Nuclear Reactor Safety Heat Transfer*, pp. 929-946. Edited by O. C. Jones. Hemisphere Publishing Company, Washington D. C., 1981.

[11] Unattributed Report. *Chernobyl and the Safety of Nuclear Reactors in OECD Countries.* OECD, Paris, France, 1987.

[12] G. H. Golden, H. P. Planchon, J. L. Sackett and R. M. Singer. "Evolution of Thermal-Hydraulics Testing in EBR-II". Nucl. Engrg. Des. 101:3-12, 1987.

[13] R. D. Smith. "Fast Reactor Progress-Slow But Sure". Prog. Nucl. Energy 20:71-88, 1987.

[14] Unattributed report. *Fast Breeders.* INFCE Working Group 5. IAEA, Vienna, Austria, 1980.

[15] J. I. Sackett, G. H. Golden, R. R. Smith and H. K. Fauske. "Transient Response of Liquid Metal Fast Breeder Reactors". In *Nuclear Reactor Safety Heat Transfer*, pp. 161-184. Edited by O. C. Jones. Hemisphere Publishing Company, Washington D.C., 1981.

[16] F. X. Gavigan. "Impact of Safety and Licensing Considerations on MONJU". *Proc. Int. Topl. Mtg. Fast Reactor Safety*, Knoxville, Tennesse, April 21-24, 1985. CONF-850410. Oak Ridge National Laboratory, Oak Ridge, Tennessee, July 1985.

[17] E. L. Gluekler, N. W. Brown, C. L. Cowan, A. Hunsbedt and R. A. Meyer. "Safety Characteristics of a Small Modular Reactor". *Proc. Int. Topl. Mtg. Fast Reactor Safety*, Knoxville, Tennessee, April 21-24, 1985. CONF-850410. Oak Ridge National Laboratory, Oak Ridge, Tennessee, July 1985.

[18] R. T. Lancet and J. F. Marchaterre. "Inherent Safety of the SAFR Plant". *Proc. Int. Topl. Mtg. Fast Reactor Safety*, Knoxville, Tennessee, April 21-24, 1985. CONF-850410. Oak Ridge National Laboratory, Oak Ridge, Tennessee, July 1985.

[19] B. R. Seidel and L. C. Walters. *Status of Performance and Fabrication of Metallic U-Pu-Zr Fuel for the Integral Fast Reactor.* ANL-IFR-1. Argonne National Laboratory, Chicago, Illinois, November 1984.

[20] L. C. Walters, B. R. Seidel and J. H. Kittel. "Performance of Metallic Fuels and Blankets in Liquid-Metal Fast Breeder Reactors". Nucl. Tech. 65:179-231, 1984.

[21] C. M. Walter, G. H. Golden and N. J. Olson. *U-Pu-Zr Metal Alloy: A Potential Fuel for LMFBR's.* ANL-76-28. Argonne National Laboratory, Chicago, Illinois, November 1975.

[22] E. E. Gruber and J. M. Kramer. *Analysis of Fission-Gas Behavior with the Stars Code: Steady-State Irradiation of U-Pu-Zr Fuel Pins.* ANL-IFR-90. Argonne National Laboratory, Chicago, Illinois, July 1988.

[23] R. H. Sevy and J. E. Cahalan. *An Assessment of Fission-Gas-Induced Transient Swelling in Metallic Fuel.* ANL-IFR-6. Argonne National Laboratory, Chicago, Illinois, March 1985.

[24] E. E. Gruber. *The Stars Model for Fission Gas Behavior: I. Steady State Behavior.* ANL-IFR-58. Argonne National Laboratory, Chicago, Illinois, December 1986.

[25] J. M. Kramer, T. H. Hughes and E. E. Gruber. *Validation of Models for the Analysis of the Transient Behavior of Metallic Fast Reactor Fuel.* ANL-IFR-66. Argonne National Laboratory, Chicago, Illinois, April 1987.

[26] R. E. Einziger and B. R. Seidel. "Irradiation Performance of Metallic Driver Fuel in Experimental Breeder Reactor II to High Burnup". Nucl. Tech. 50:25-39, 1980.

[27] G. L. Hofman. "Irradiation Behavior of Experimental Mark-II Experimental Breeder Reactor II Driver Fuel". Nucl. Tech. 47:7-22, 1980.

[28] R. G. Pahl, W. N. Beck, G. L. Hofman and R. Villarreal. *Postirradiation Examinations of U-Pu-Zr Fuel Elements from Subassemblies X419 and X419A.* ANL-IFR-55. Argonne National Laboratory, Chicago, Illinois, October 1986.

[29] R.G. Pahl, W. N. Beck and J. E. Sanecki. *Postirradiation Examination of the HT9 Clad Fuel Test at 2.9% Burnup.* ANL-IFR-81. Argonne National Laboratory, Chicago, Illinois, November 1987.

[30] Y. Y. Liu and M. C. Billone. *Thermoelastic Stresses in U-Pu-Zr Alloy Fuels-an Analytical Interpretation of Results in the IFR Lead Irradiation Experiments.* ANL-IFR-49. Argonne National Laboratory, Chicago, Illinois, August 1986.

[31] G. L. Hofman, L. Leibowitz, J. M. Kramer, M. C. Billone and J. F. Koenig. *Metallic Fuels Handbook.* ANL-IFR-29. Argonne National Laboratory, Chicago, Illinois, November 1985.

[32] W. L. Bell, T. Lauritzen and S. Vaidyanathan. "Ferritics for Breeder Reactor in Core Applications: A Survey of Alloys, Properties and Microstructures".

In *Proceedings of Topical Conference on Ferritic Alloys for Use in Nuclear Energy Technologies*, pp. 113-124. Edited by J. W. Davis and D. J. Michel. AIME, New York, New York, 1983.

[33] D. S. Gelles and L. E. Thomas. "Effects of Neutron Irradiation on Microstructure in Experimental and Commercial Ferritic Alloys". In *Proceedings of Topical Conference on Ferritic Alloys for Use in Nuclear Energy Technologies*, pp. 559-568. Edited by J. W. Davis and D. J. Michel. AIME, New York, New York, 1983.

[34] G. D. Hudman, D. D. Keiser and D. L. Porter. *Ex-Reactor Testing for Carbon Loss from HT9 Cladding in the Presence of Metal Fuels.* ANL-IFR-70. Argonne National Laboratory, Chicago, Illinois, June 1987.

[35] C. E. Lahm, J. F. Koenig, P. R. Betten, J. H. Bottcher, W. K. Lehto and B. R. Seidel. "EBR-II Driver Fuel Qualification for Loss-of-Flow and Loss-of-Heat-Sink Tests without Scram". Nucl. Engrg. Des. 101:25-34, 1987.

[36] C. E. Till, Y. I. Chang and J. H. Kittel. *Fast Breeder Reactor Studies.* ANL-80-40. Argonne National Laboratory, Chicago, Illinois, July 1980.

[37] T. Y. C. Wei. *Inherency Control Strategies.* ANL-IFR-88. Argonne National Laboratory, Chicago, Illinois, July 1988.

[38] A. G. Hins. *Compatibility of U-Pu-Zr Fuels with Advanced Clad Alloys: Onset-of-Melting Results.* ANL-IFR-36. Argonne National Laboratory, Chicago, Illinois, February 1986.

[39] H. Tsai, L. A. Neimark, M. C. Billone, R. M. Fryer, J. F. Koenig, W. K. Lehto and D. J. Malloy. *Test Design Description (TDD), Volume 1a, Design Description and Safety Analysis for IFR-1 Metal Fuels Irradiation Test in FFTF.* ANL-IFR-33. Argonne National Laboratory, Chicago, Illinois, January 1986.

[40] J. M. Kramer, J. D. Demaree and E. E. Gruber. *The Dynamics of Axial Extrusion of Metallic Fuel During Overheating Transients.* ANL-IFR-30. Argonne National Laboratory, Chicago, Illinois, December 1985.

[41] E. E. Gruber and J. M. Kramer. *Gas-Bubble Growth Mechanisms in the Analysis of Metal Fuel Swelling.* ANL-IFR-27. Argonne National Laboratory, Chicago, Illinois, October 1985.

[42] R. L. Eichelberger and W. F. Brehm. "Effect of Sodium Environment on Breeder Reactor Components". In *Materials Considerations in Liquid Metal Systems in Power Generation*, pp. 1-13. Edited by G. A. Whitlow and N. J. Hoffman. NACE, Houston, Texas, 1978.

[43] P. F. Tortorelli and J. H. Devan. "Liquid Metal Corrosion Considerations in Alloy Development". In *Optimizing Materials for Nuclear Applications*, pp. 3-15. Edited by F. A. Garner, D. S. Gelles and F. W. Witten. AMS, Warrendale, Pennsylvania, 1985.

[44] M. M. El-Wakil. *Nuclear Energy Conversion.* ANS, La Grange Park, Illinois, 1982.

[45] H. F. Fenech. "General Considerations on Thermal Design and Performance Requirements of Nuclear Reactors". In *Heat Transfer and Fluid Flow in Nuclear Systems*, pp. 1-41. Edited by H. Fenech. Pergamon Press, New York, New York, 1981.

[46] H. K. Fauske. "Core Disruptive Accidents". In *Nuclear Reactor Safety Heat Transfer*, pp. 481-491. Edited by O. C. Jones. Hemisphere Publishing Company, Washington D.C., 1981.

[47] F. X. Gavigan. "Impact of Safety and Licensing Considerations on Fast Reactor Design". *Proc. Int. Topl. Mtg. Fast Reactor Safety*, Knoxville, Tennesse, April 21-24, 1985, CONF-850410, Oak Ridge National Laboratory, July 1985.

[48] M. V. Quick, R. S. Hall, M. S. Grieve and N. E. Buttery. "Fast Reactor Safety: The Convergence of Principles and Practice". Nucl. Safety 28:181-190, 1987.

[49] R. A. Dancals, J. E. Schmidt, R. A. Markley, J. E. Kalinowski, R. D. Coffield, J. A. Lake and R. K. Sievers. "The Westinghouse Approach to an Inherently Safe Liquid Metal Reactor Design". *Proc. Int. Topl. Mtg. Fast Reactor Safety*, Knoxville, Tennessee, April 21-24, 1985. CONF-850410. Oak Ridge National Laboratory, Oak Ridge, Tennessee, July 1985.

[50] J. T. Sankoorikal. Personal Communication. Department of Nuclear Engineering, Iowa State University, Ames, Iowa, June 1988.

[51] M. D. Carelli and A. J. Friedland. "Hot Channel Factors for Rod Temperature Calculations in LMFBR Assemblies". Nucl. Engrg. Des. 62:155-180, 1980.

[52] M. P. Carelli. "A Comprehensive Approach to Uncertainty Analysis in LMFBR Core Thermal-Hydraulic Design". In *Proceedings of the ANS/ASME/NRC International Topical Meeting on Nuclear Reactor Thermal-Hydraulics.* Volume 3, pp:1698-1723. ANS, Saratoga Springs, New York, 1980.

[53] D. D. DeFur. "An IHX design for Pool Type LMFBR System Application". J. Eng. Power. 102:563-567, 1980.

[54] L. N. Salerno, R. C. Berglund, G. L. Gyorey, F. E. Tippets and P. M. Tschamper. "PRISM Concept. Modular LMR Reactors". Nucl. Engrg. Des. 109:79-86, 1988.

[55] R. A. Johnson, S. Golan and E. Guenther. "SAFR, An Economic, Inherently Safe Liquid Metal Reactor". Nucl. Engrg. Des. 109:87-95, 1988.

[56] J. T. Cochran, G. G. Glenn, W. J. Purcell, R. W. Smith and E. A. Wright. "CRBRP Main Pump Sodium Test Experience". In *Liquid Metal Engineering and Technology.* Volume 2, pp:1-6. BNES, London, England, 1984.

[57] A. H. Spring and D. D. DeFur. "A High Reliability Straight Tube LMFBR Steam Generator Design". J. Eng. Power. 102:568-572, 1980.

[58] C. C. Stone, J. A. Ford, F. E. Tippets, J. S. Mcdonald, G. Grant and J. L. Epstein. "Experience with Liquid-Metal Fast Breeder Reactor Steam Generators U.S. Design". Nucl. Tech. 55:60-87, 1981.

[59] M. G. Robin. "Intermediate Heat Exchangers and Steam Generators for Sodium Cooled Systems". In *Heat Transfer and Fluid Flow in Nuclear Systems*, pp. 497-540. Edited by H. Fenech. Pergamon Press, New York, New York, 1981.

[60] J. C. Whipple and C. N. Spalaris. "Design of the Clinch River Breeder Reactor Plant Steam Generators". Nucl. Tech. 28:305-313, 1976.

[61] L. Duchatelle, L. de Nucheze and M. G. Robin. "Theoretical and Experimental Study of Phenix Steam Generator Prototype Modules". Nucl. Tech. 24:123-136, 1974.

[62] C. J. Mueller. *Uncertainties in Inherent Shutdown of Generic Unprotected Loss-of-Flow and Transient Overpower Events in Innovative Designs.* ANL-IFR-80. Argonne National Laboratory, Chicago, Illinois, October 1987.

[63] D. L. Hetrick. *Dynamics of Nuclear Reactors.* University of Chicago Press, Chicago, Illinois, 1971.

[64] K. O. Ott. "Inherent Shutdown Capabilities of Metal-Fueled Liquid-Metal-Cooled Reactors During Unscrammed Loss-of-Flow and Loss-of-Heat-Sink Accidents". Nucl. Sci. Eng. 99:13-27, 1988.

[65] H. P. Planchon, J. I. Sackett and G. H. Golden And R. H. Sevy. "Implications of the EBR-II Inherent Safety Demonstration Test". Nucl. Engrg. Des. 101:75-90, 1987.

[66] D. C. Wade and Y. I. Chang. "The Integral Fast Reactor Concept: Physics of Operation and Safety". Nucl. Sci. Eng. 100:507-524, 1988.

[67] D. Saphier. *The DSNP User's Manual; Dynamic Simulator for Nuclear Power Plants.* ANL-CT-77-22. Georgia Institute of Technology, Atlanta Georgia, October 1985.

[68] I. K. Madni, E. G. Cazolli and A. K. Agrawal. "Single Phase Sodium Pump Model for LMFBR Thermal-Hydraulic Analysis". In *Proceedings of the International Meeting on Fast Reactor Safety.* Volume 3, pp.1273-1285. ANS, Seattle, Washington, 1979.

[69] T. Ramin, *Emergency Natural Convection Cooling of the Trench Reactor.*, Unpublished, Department of Nuclear Engineering, Iowa State University, Ames, Iowa, May 1988.

[70] N. C. Messick, P. R. Betten, W. F. Booty, L. J. Christensen, R. M. Fryer, D. Mohr, H. P. Planchon and W. H. Radtke. "Modification of EBR-II Plant to Conduct Loss-of-Flow-Without-Scram Tests". Nucl. Engrg. Des. 101:13-23, 1987.

[71] E. E. Lewis. *Nuclear Power Reactor Safety.* John Wiley & Sons, New York, New York, 1977.

[72] R. B. Tupper, M. H. Cooper and R. K. Sievers. "A Self Actuated Shutdown System For Liquid Metal Cooled Reactors". *Proc. Int. Topl. Mtg. Fast Reactor Safety*, Knoxville, Tennessee, April 21-24, 1985, CONF-850410, Oak Ridge National Laboratory, Oak Ridge, Tennessee, July 1985.

[73] B. I. Spinrad. Personal communication. Department of Nuclear Engineering, Iowa State University, Ames, Iowa, July 1988.

9 APPENDIX

9.1 Transient Model for Unprotected Accidents

The transient simulations were performed by using DSNP which is a modular, general purpose simulation program. The input to DSNP consists of statements to define which component will be simulated by which module, necessary statements for establishing the relations of the components, an iteration loop to compute the steady state conditions and the integration loop. The precompiler of the DSNP reads the input statements, translates the input statements and writes a FORTRAN program. Most of the modules in the DSNP are contained in libraries in generic form. The modules can be simple FORTRAN programs or a set of instructions to generate a FORTRAN program, called macros. An example of a macro is given in the end of the DSNP input listed in Section 9.2. More information on DSNP can be found in reference [67].

In order to model the TR reactor certain modifications were necessary. The following discussion will describe the model used in the simulations. The modifications or additions made to the original DSNP libraries will also be described. Section 9.2 lists the input to the precompiler and along with some explanatory remarks.

9.1.1 Active Core Model

This is a lumped parameter core model. It can represent up to 5 boxes or subassemblies. Each box contains a fuel, cladding, coolant, and a structure node. The equations for average fuel (T_f), average cladding (T_l), coolant core exit (T_{cx}) and average structure temperature (T_s) for a particular box are

$$M_f C_f \frac{dT_f}{dt} = P_i - (UA)_1(T_f - T_l) \tag{9.1}$$

$$M_l C_l \frac{dT_l}{dt} = (UA)_1(T_f - T_l) - (UA)_2\left(T_l - \frac{T_{cx} + T_{ci}}{2}\right) \tag{9.2}$$

$$(\rho VC)_{Na}\frac{dT_{cx}}{dt} = (WC)_{Na}(T_{ci} - T_{cx}) + (UA)_2\left(T_l - \frac{T_{cx} + T_{ci}}{2}\right) - (UA)_3\left(\frac{T_{cx} + T_{ci}}{2} - T_s\right) \tag{9.3}$$

$$M_s C_s \frac{dT_s}{dt} = (UA)_3\left(\frac{T_{cx} + T_{ci}}{2} - T_s\right) - (UA)_4(T_s - T_p) \tag{9.4}$$

where the subscript indicating the particular box in consideration has been retained only in the fuel equation for the power term. In the above equations UA_i are the overall heat transfer coefficients in units of W/^{o}C, T_{ci} is the coolant inlet temperature and T_p is the pool temperature.

For each box modeled, this set of four equations is solved. The various heat transfer coefficients are evaluated in a different subroutine (subroutine CORTH0) for each time step. This routine also contains the various material property functions used. Apart from the values of the variables at a previous time step, this module requires the flow rate (W), coolant inlet temperature (T_{ci}), pool temperature (T_p), and power generated (P_i) to be known at the current integration step.

Reactor averaged temperatures are obtained by mass weighting for fuel, cladding

and structure nodes, and by flow rate weighting for coolant temperatures.

The macros to define and generate the subroutine are included in the level zero library. This module requires the use of another level 0 library module for the computation of reactivity feedbacks.

In order to obtain a uniform core exit temperature at steady state from all the boxes modeled another subroutine is used in order to determine the orificing required for each core box. This subroutine first adjusts the flow rates for each box so that the core exit temperatures are uniform, then by using the hydraulic pipe definitions for the active and the inactive core segments adjusts the loss coefficients in order to obtain a uniform pressure drop.

9.1.2 Pool Model

The pool model contains a fluid node only. The thermal interaction between the pool and the vessel has been neglected. It is assumed that the pool is at a uniform temperature. The equation for the fluid temperature in the pool is

$$\rho V C_p \frac{dT_p}{dt} = \sum W_{in} C_p T_{in} - \sum W_{ex} C_p T_p - Q_R + Q_H \qquad (9.5)$$

where 'in' and 'ex' refers to inlet from the pool and exit from the pool. Q_R is the heat removed per unit time due to the vessel cooling by natural convection. It was assumed to be a linear function of the pool temperature. Q_H is the heat generated in the pool per unit time. This term was included in order to account for the heat generated due the pumps and the heat transfer between the structural components of the core and pool.

9.1.3 Inlet Plenum Model

This model is the mixing plenum model of DSNP. It contains a fluid and a structure node. The governing equations are

$$\rho V C_p \frac{dT_c}{dt} = \sum W_{in} C_p T_{in} - \sum W_{ex} C_p T_p - UA(T_c - T_s) \quad (9.6)$$

$$M_s C_s \frac{dT_s}{dt} = UA(T_c - T_s) \quad (9.7)$$

where 'in' and 'ex' refer to the inlet and exit conditions to and from the plenum. T_c denotes the average sodium temperature in the inlet plenum and T_s refers to the average temperature of the structural materials in the plenum. The heat transfer coefficient UA was computed by assuming natural convection and was kept constant throughout the simulations.

9.1.4 Pipe Thermodynamics

The pipes to and from the intermediate heat exchangeres and the inactive core was modeled as fluid flowing in insulated pipes. The energy equation for the liquid flowing in the pipe and for the pipe wall can be expressed as

$$\rho C_p \frac{\partial T}{\partial t} + \rho C_p u \frac{\partial T}{\partial x} = \frac{\partial q}{\partial y} \quad (9.8)$$

$$M C_w \frac{\partial T_w}{\partial t} = \frac{\partial q}{\partial y} \quad (9.9)$$

where x is parallel to the direction of the flow and y is normal to the direction of the flow. These equations are cast into finite difference form by dividing the length of the pipe into n segments and integrating over the pipe cross sectional area. A backward difference for the convective term is used. For a node j, this gives

$$\rho_j V_j C_{pj} \frac{dT_j}{dt} = W C_{pj}(T_{j-1} - T_j) + Q_j \quad (9.10)$$

$$MC_{wj}\frac{dT_{w,j}}{dt} = Q_j = (UA)_j\left(\frac{T_{j-1}+T_j}{2} - T_{w,j}\right) \tag{9.11}$$

where W is the mass flow rate of the coolant and the $(UA)_j$ is the heat transfer coefficient for the segment. This results in 2n differential equations. Typically 5 nodes were used. If the pipe cross sectional area is not circular the equivalent diameter concept is used. This module was named THPSN and added to DSNP's library 3 and the macro definition for this module was added to the level 1 library. It is considerably faster than DSNP's level 1 thermal pipe module.

9.1.5 Intermediate Heat Exchanger Model

The IHX conditions were computed by using DSNP's GIHX module. This module is based on the assumption that the heat flux distribution along the length of the IHX during a transient will remain the same as the steady state heat flux distribution. This approximation is referred as the Addington approximation.

9.1.6 Neutronics Modules

The modules consist of subroutines to compute the fission power, power generated due to decay of fission fragments, total reactor power, feedback and external reactivity.

Fission Power: The power from fission is computed by using point kinetics equations with six group delayed neutron groups. The equations solved are

$$\frac{dP_f}{dt} = \frac{\rho-\beta}{\ell}P_f + \sum_{i=1}^{6} C_i\lambda_i \tag{9.12}$$

$$\frac{dC_i}{dt} = \frac{\beta_i}{\ell}P_f - \lambda_i C_i \quad i = 1,\ldots,6 \tag{9.13}$$

where β_i's are the delayed neutron fractions, β is the total delayed neutron fraction, C_i's are the delayed neutron precursor concentrations with decay constants λ_i, ℓ is the prompt neutron lifetime, ρ is the net reactivity. These equations were solved by DSNP's NEUTR1 module. This module is based on a pre-integrated form of the point-kinetics equations and is considerably faster than other numerical methods. For accidents during which the fission power decreases to very small values for example below 0.0001 of its initial value, this modules must either bypassed or the error criteria for the integration needs to be reduced in magnitude. Otherwise, either a large reduction in time step occurs increasing the computation time considerably or oscillatory results for fission power are obtained.

Reactivity: The net reactivity is the sum of the feedback reactivity and the externally input reactivity. The external reactivity has to be specified. External reactivity can be specified through the CNTRL1 module. It is also possible to specify the external reactivity in the DERIV1 module.

The feedback reactivity mechanisms considered are Doppler, fuel expansion, sodium expansion, and structure (grid plate and clad) expansion. The feedback reactivity for a particular box is computed by

$$\textit{Doppler} : \quad \rho_{dp} = \alpha_{dp} ln\left(\frac{T_f + 273.15}{T_f(0) + 273.15}\right) \tag{9.14}$$

$$\textit{Fuel Expansion} : \quad \rho_{fe} = \alpha_{fe}(T_f - T_f(0)) \tag{9.15}$$

$$\textit{Structure Expansion} : \quad \rho_{st} = \alpha_{st}(T_{ca} - T_{ca}(0)) \tag{9.16}$$

$$\textit{Coolant Expansion} : \quad \rho_{Na} = \alpha_{Na}(T_{ca} - T_{ca}(0)) \tag{9.17}$$

and net feedback reactivity for this box is given by

$$\rho_i = \rho_{dp} + \rho_{fe} + \rho_{st} + \rho_{Na} \tag{9.18}$$

In the above equations, the temperatures are the average temperatures in that box and a zero in parenthesis indicates the temperature at the steady state conditions.

In order to obtain the net feedback reactivity for the whole reactor core the following equation is used [73];

$$\rho_{fd} = \frac{\sum_{i=1}^{NBOX} \left(\frac{f_i^2}{V_i}\right) \rho_i}{\sum_{i=1}^{NBOX} \left(\frac{f_i^2}{V_i}\right)} \tag{9.19}$$

where f_i and the V_i represent the fraction of the power and the fraction of the volume contained in the region in consideration.

Finally, the net reactivity is computed by adding the net feedback and if there is any, the externally introduced reactivity. The final value computed is used in the calculation of the fission power in the point kinetics equation.

Dceay Power: The decay heat is computed by using DSNP's GAMAR1 module. This module solves

$$\frac{dP_{d,i}}{dt} = (\beta_{d,i} P_{NJ} - P_{d,i})\lambda_{d,i} \quad i = 1, \ldots, 4 \tag{9.20}$$

where $P_{d,i}$ is the fraction of the decay heat produced by the i'th group, $\beta_{d,i}$ is fraction of the fission products produced by the i'th group, and $\lambda_{d,i}$ are the disintegration constants, P_{NJ} is the normalized fission power. The total decay heat is computed by using

$$P_{DH} = P_{DH0} \sum_{i=1}^{4} P_{d,i} \tag{9.21}$$

where P_{DH0} is the initial power produced due to decay heat.

9.1.7 Fluid Flow Modeling

The flow rates through various components were modeled within the framework of several DSNP modules with certain modifications. In general the rate of change of mass flow rate in units of (kg/s) is given by;

$$\frac{dW}{dt} = \frac{P_{in} - P_{out} + \Delta P}{I} \tag{9.22}$$

where P_{in} and P_{out} are the inlet and outlet pressures at the end points of the flow path, ΔP is the pressure drop along the flow path, and I is the inertia of the fluid contained in the flow path. The pressure unit is Pascals and the inertia is in units of inverse meters.

The pressure drop along the flow path is computed by DSNP's DELPF function which uses

$$\Delta P = \sum_{i=1}^{N} \left\{ (Z_{in} - Z_{out})\rho_{av} g - \left(\frac{fL}{D_e} + K \right) \left(\frac{W}{A_f} \right) \frac{1}{2\rho_{av}} \right\}_i + \Delta P_p \tag{9.23}$$

where Z_{in} and $Z - out$ are the inlet and outlet elevations, ρ_{av} is the average density in the flow segment, g is the acceleration of gravity, l is the length of the segment, a_f is the flow area, f is the friction factor, K is the loss coefficient including acceleration,losses, W is the flow rate, and ΔP_p is the pressure change across the pump. The first term is the driving force for the natural circulation flow. This term needs to be computed as an integral along the flow path in order to account for the shift in the thermal centers when a loss of flow accident occurs; however such a modification required extensive changes in the flow modules of DSNP

and was not attempted. Using the density obtained from the average temperature underestimates the driving force for the natural convection, particularly in the IHX during LOF accidents.

The pump head was computed by using the pump model of reference [68]. Detailed description of the model and the flow chart of the subroutine written can be found in the same reference. The subroutine written was added to the level 1 library under the name of HOMPU1. In most of the simulations performed, instead of solving the angular speed of the pump the angular speed of the pump was specified as a function of time.

Figure 4.2 gives a schematic of the flow chart for the hydraulic part of the simulation. Only one of the loops is simulated and the other loop conditions are assumed to be the same as the simulated loop conditions.

The core was modeled as parallel channels. The loss of coefficients of each individual channel was computed by assuming that the flow rates were such that the core exit temperatures and the pressure drop across each of the channels are uniform. This computation was performed by CORIF module and is in the level 0 library, that is it needs to be included in the DSNP input program.

The pool was modeled as an open cavity subject to an atmospheric cover pressure at the top surface. DSNP's HCVT1 module was used for this purpose.

The core inlet plenum conditions were computed as a hydraulic junction. DSNP's hydraulic junction module can not handle multiple exit junctions; therefore it was

not used. The junction pressure was computed by

$$P_L = I_L \left(\sum_{i=1}^{NBOX} \frac{P_U - \Delta P_{W_{c,i}}}{I_{W_{c,i}}} + 2\frac{P_I + \Delta P_{W_{IHX}}}{I_{IHX}} \right) \tag{9.24}$$

where

$$\begin{aligned}
I_L &= \left(\sum_{i=1}^{NBOX} \frac{1}{I_{Wc,i}} + \frac{2}{I_{IHX}} \right)^{-1} \\
I_{W_{c,i}} &= \textit{inertia of fluid in i th core channel} \\
I_{W_{IHX}} &= \textit{inertia of fluid in the IHX loop} \\
P_{W_{c,i}} &= \textit{pressure drop across the i th channel} \\
P_{W_{IHX}} &= \textit{pressure drop in the IHX loop} \\
P_U &= \textit{hydrostatic pressure in the pool at the core exit} \\
P_i &= \textit{hydrostatic pressure in the pool at the pump inlet}
\end{aligned} \tag{9.25}$$

The pool pressures are assumed to be hydrostatic and are given by

$$\begin{aligned}
P_I &= (2m) \times \left(9.81 \frac{m}{s^2}\right) \rho(T_{pool}) + P_{atmos} \\
P_U &= (13m) \times \left(9.81 \frac{m}{s^2}\right) \rho(T_{pool}) + P_{atmos}
\end{aligned}$$

Note that this model does not force the IHX flow rate to be equal to half of the core flow rate since both flows are separated by the pool which is simulated as an open tank. This was done in order to be able to simulate pipe break accidents or asymmetric accidents during which the two loops behave differently.

The initial condition computations require a convergence on the flow rates so that the right hand side of Eq. (9.22) is less than a specified error criterion. The iteration scheme of DSNP was very slow, so a different iteration scheme based on

quadratic interpolation for the last three iterations was programmed and added to level 3 library under the name of GUESS3 to be used with the flow modules.

9.2 Input Listing for DSNP

```
C-----------------------------------------------------------------------
C  COMMON BLOCKS
C  MAINF5 : FUEL CONDUCTIVITY PARAMETERS
C  MAING5 : CORE BOX AND FUEL PIN GEOMETRIC PARAMETERS
C  CORIF5 : LOSS COEFFICIENTS FOR HYDRAULIC PIPE SEGMENTS
C           VALVK(I) ARE COMPUTED IN SUBROUTINE CORORO
C  MAINP5 : SOME DATA TO BE USED IN DERIV1 AND OTHER ROUTINES
C  POMPA5 : PRIMARY PUMP PARAMETERS; COMPUTED IN THE INITIAL SEGMENTS
C-----------------------------------------------------------------------
.COMON /MAINF5/A(10),B(10),C(10),P(10),BECNS(10);
.COMON /MAING5/DEQ(10),AFLOW(10),XL,RCO,RCI,RF,POD,NPIN(10);
.COMON /NIYAZ5/PAR(10);
.COMON /CORIF5/VALVK(10),VALVL,VALVU,VALV5,VALV6,VALV7,TPIPO2;
.COMON /MAINP5/TECXU1,TECXU2,PRESL,PRESU,ZINCOR,ZINIHX,ZINLPE,ZPLOWP;
.COMON /POMPA5/ZHRPU(1),ZFLOR(1),ZTORPR(1),ZREVR(1),ZREV(1),ZHEAD(1),
.              PUMPTC;
C-----------------------------------------------------------------------
C  FOLLOWING SEGMENT INCLUDES THE PUMP SUBROUTINE
C     THIS SHOULD BE USED FOR CALCULATIONS WITH THE
C     PUMP SPEED SPECIFIED
C-----------------------------------------------------------------------
.INCLUDE HOMPU1;
C-----------------------------------------------------------------------
C=======================================================================
C      T H E R M O D Y N A M I C S
C=======================================================================
C--- THERMAL PIPE SEGMENTS--------------------------------------------
C   MACRO DEFTHPSN3 IS LISTED AT THE END OF THE LISTING OF THE INPUT
C     DEFINITON OF THE PARAMETERS ARE GIVEN THERE
C   N : UPPER PLENUM PIPE
C   S : LOWER PLENUM PIPE
C   A,B : TIME DELAY PIPES
C-----------------------------------------------------------------------
.DEFTHPSN3(5,SO,SS,0.4DO,0.05DO,6.0DO,ZTPFU,TEAPI,FPAI);
.DEFTHPSS3(5,SO,SS,0.4DO,0.05DO,19.0DOO,TEAPX,TPIPO2,FPAI);
.DEFTHPSA3(5,SO,SS,0.4DO,0.05DO,6.0DO,ZTPFU,TEAPI,FPAI);
.DEFTHPSB3(5,SO,SS,0.4DO,0.05DO,19.0DOO,TEAPX,TPIPO2,FPAI);
.DESTROY;
C-----------------------------------------------------------------------
C  DEFINITION OF THE IHX
C    SEE DSNP USERS MANUAL FOR USAGE
C-----------------------------------------------------------------------
.DFGIHXMA1(10,3500,1.4,SO,SO,SS,6.0DOO,7.5DOO,1.17D-02,1.27D-02,
.          0.0DO,1.0D-01,1.0D-03,15,15,1,1,1.11DO,1.0DO,0.0DO,0.0DO);
.DESTROY;
C-----------------------------------------------------------------------
C  POOL MODEL
C   AFTER THE FORTRAN PROGRAM IS OBTAINED THE FOLLOWING CHANGES
C     SHOULD BE MADE :
C    1. THE ARGUMENTS OF THE 'CALL' STATEMENTS TO SS SPECIFIC
C       HEAT, DENSITY AND THE THERMAL CONDUCTIVITY INCLUDE
C       PRESSURE AS A PARAMETER. THIS SHOULD BE REMOVED, SINCE
C       IN THE LIBRARIES THIS SUBRUTINES DO NOT HAVE PRESSURE
C       AS AN ARGUMENT.
C    2. INCLUDE THE HEAT REMOVED BY THE VESSEL COOLING SYSTEM
C       IN THE FORM
C          QVCS = AVCS * ZTPFU - BVCS
C       ALSO INCLUDE OTHER HEAT SOURCE OR SINKS IN A SIMILAR
C       MANNER TO THE DIFFRENTIAL EQUATION CORRESPONDING TO
C       ZTPFU (POOL TEMPERATURE).
```

```
C     3. SET THE RIGHT HAND SIDE OF THE DIFFERENTIAL EQUATION FOR
C        FOR THE TEMPERATURE OF THE METAL NODE TO ZERO
C        SO THAT THE METAL NODE TEMPERATURE IS NOT COMPUTED
C!!!!! NOTE THAT THE IN THE USERS MANUAL ONE OF THE ARGUMENTS OF THIS
C       DEFINITION MACRO IS NOT INCLUDED.
C       THE CORRECT FORM SHOULD AS BE BELOW; SEE ALSO THE LISTING OF
C       LIBRARY 1 FOR YHIS MACRO.
C-----------------------------------------------------------------------
.DFMXPLENU(SO,SS,1.2417D03,7.9D05,518.036D03,
.          INFLO(WCOREN(1),TECXN(1),WCOREN(2),TECXN(2)),
.          EXFLO(FPAI,ZTPFU,FPAI,ZTPFU),PRESU,
.          CORCN5,IHXMA5,MAINP5);
C-----------------------------------------------------------------------
C  INLET PLENUM MODEL
C  MODIFICATION 1 OF THE POOL MODEL SHOULD ALSO BE DONE HERE
C-----------------------------------------------------------------------
.DFMXPLENL(SO,SS,2.0475,877.5D0,1.335D03,
.          INFLO(FPAI,TPIPO2,FPAI,TPIPO2),
.          EXFLO(WCOREN(1),TECIN(1),WCOREN(2),TECIN(2)),
.          PRESL,CORCN5,IHXMA5,MAINP5);
.DESTROY;
C-----------------------------------------------------------------------
C  THE FOLLOWING TWO MACROS ARE LIBRARY ZERO MACROS; THAT IS
C    ARE NOT IN THE ORIGINAL DSNP LIBRARIES BUT SHOULD BE
C    INCLUDED WITH THE INPUT.
C    IT DEFINES THE CORE MODEL USED FOR MODELLING THE TRENCH REACTOR
C      SEE THE LISTING IN THE LIBRARY ZERO SEGMENT
C  DFCORBO(N) : DEFINES THAT TWO CORE BOXES ARE GOING TO USED
C  DFFDBKO(N) : DEFINES THE APPROIATE FEEDBACK REACTIVITY CALCULATION
C-----------------------------------------------------------------------
.DFCORBO(2);
.DFFDBKO(2);
.DESTROY;
C-----------------------------------------------------------------
C=================================================================
C       H Y D R O D Y N A M I C S
C     PIPE AND FLOW PATH DEFINITIONS
C=================================================================
C-----------------------------------------------------------------
C DEFHPIPii(ZW    ,TIN   ,TEX   ,
C           ZXHI          ,ZXHX         ,ZXLP         ,ZXLE         ,
C           ZXDE          ,ZAFL         ,SO ,PRESRE,COMBLK,-1.0,VALV1);
C-----------------------------------------------------------------
C  PIPE      LOCATION
C       1    ACTIVE CORE CENTERAL 3 BOXES
C       2    ACTIVE CORE SIDE 2 BOXES
C       3    INACTIVE CORE CENTER BOXES
C       4    INACTIVE CORE SIDE BOXES
C       5    POOL PIPE FROM PUMP TO IHX
C       6    IHX TUBE SIDE
C       7    PIPE FROM IHX TO LOWER PLENUM
C-----------------------------------------------------------------
C!!!!!!! NOTE THAT THE ORDERING OF THE PIPE SEGMENTS REPRESENTING
C        THE CORE ARE IN THE ORDER REQUESTED BY THE ORIFICING ROUTINE
C        SUBROUTINE CORORO
C-----------------------------------------------------------------
. DEFHPIPO1(WCOREN(1),TECIN(1) ,TECXN(1) ,
.           1.5D00        ,3.2D00       ,1.7D0        ,1.7D0        ,
.           3.12D-03      ,0.45D00 ,SO ,PAVR1 ,CORCN5,-1.0,VALVK(1));
. DEFHPIPO2(WCOREN(2),TECIN(2) ,TECXN(2) ,
```

```
.           1.5D00        ,3.2D00       ,1.7D00       ,1.7D0        ,
.           3.12OD-03     ,0.3ODO ,SO ,PAVR1 ,CORIF5,-1.0,VALVK(2));
. DEFHPIPO3(WCOREN(1),TECXN(1) ,TECXN(1),
.           3.2DO         ,6.0DO        ,2.8DO        ,2.8DO        ,
.           3.12D-03      ,0.45D00 ,SO ,PAVR1 ,MAINP5,-1.0,VALVU);
. DEFHPIPO4(WCOREN(2),TECXN(2) ,TECXN(2),
.           3.2DO         ,6.0DO        ,2.8DO        ,2.8DO        ,
.           3.12D-03      ,0.30     ,SO ,PAVR1  ,*    ,-1.0,VALVU);
C-------------------------------------------------------------------
. DEFHPIPO5(FPAI   ,ZTPFU ,TEAPI ,
.           1.5DO1        ,1.5DO1       ,6.0DO        ,7.0DO        ,
.           0.8DO         ,0.5026DO     ,SO ,PAVR1 ,MXPLU5,-1.0,VALV5);
. DEFHPIPO6(FPAI   ,TEAPI ,TEAPX ,
.           1.5DO1        ,7.5D00       ,7.5D00       ,8.0DO        ,
.           2.34D-02      ,1.161D00     ,SO ,PAVR1 ,IHXMA5,-1.0,VALV6);
. DEFHPIPO7(FPAI   ,TEAPX ,TPIPO2,
.           7.5DO         ,1.5DO        ,19.0DO       ,22.0DO       ,
.           0.8DO         ,0.5026DO     ,SO ,PAVR1 ,THPSS5,-1.0,VALV7);
C-------------------------------------------------------------
C  THE FOLLOWING DEFINITION MACRO SHOULD BE INCLUDED
C      IF THE DYNAMIC EQUATION FOR THE PUMP IS TO BE SOLVED
C      RATHER THAN SPECIFYING THE PUMP SPEED AS A FUNCTION OF TIME.
C      IF THE FOLLOWING MACRO IS INCLUDED DELETE THE LINE ON THE
C      BEGINING OF THIS FILE THAT SAYS " .INCLUDE HOMPU1".
C   SEE DSNP MANUAL FOR DETAILS OF THIS MACRO.
C   IT IS RECOMMENDED THAT THE PUMP DEFINITION PARAMETERS BE INCLUDED
C      IN THE ITERATION LOOPS IN THE INITIAL SEGMENTS.
C-------------------------------------------------------------------
C DFPUMPO1(ZHRPU  ,ZHRZF  ,ZREVR  ,ZPPIN  ,ZTORPR  ,ZFLO  ,ZFLOR,
C          ZIPUMP,ZPU1,ZPU2,ZREV,ZTEPIN,ZPUMAT,KITMX,COMBLCK)
C-------------------------------------------------------------------
C   FLOW DEFINITION
C     IF THE PUMP DYNAMICS IS SOLVED CHANGE THE "PUMP(*)" PART OF THE
C        THIRD DEFINTION TO "PUMP(X)" WHERE X IS THE NAME OF THE PUMP
C-------------------------------------------------------------------
.DFLOWO1(WCOREN(1))=(2860.0DO,PL,PU,2O,PIPES(O1,O3),PUMPS(*));
.DFLOWO2(WCOREN(2))=(1590.0DO,PL,PU,2O,PIPES(O2,O4),PUMPS(*));
.DFLOWO3(FPAI)=(2200.0DO,PIA,PL,2O,PIPES(O5,O6,O7),PUMPS(*));
C-------------------------------------------------------------------
C  HYDRAULIC CAVITY MODEL: NO CHANGES
C  COMPUTED PARAMETRS ARE THE PRESSURES
C    PU=PUU; PIA=PIB=PI
C    101.3D3 IS THE ATMOSPHERIC PRESSURE IN PASCALS
C-------------------------------------------------------------------
.DFCAVTO1(17.0DO,101.3D3,ZTPFU,73.0DO,INFLO(O1,6.0DO,PU,O2,6.0DO,PUU),
.         EXFLO(O3,15.0DO,PIA,O3,15.0DO,PIB),
.         PIPES(O1,O2,O3,O4,O5,O6,O7),1.496DO3,SO);
.DESTROY;
C-------------------------------------------------------------------
C THE FOLLOWING MEANS; PI=PIB
C-------------------------------------------------------------------
.CNCTUU(PI,PIB);
C-------------------------------------------------------------------
C===================================================================
C   I N I T I A L   C O N D I T I O N   C A L C U L A T I O N
C   MODULE   PURPOSE
C   CNTRL1 : EXTERNALLY INSETED REACTIVITY
C   FEDBKO : COMPUTES THE FEEDBACK REACTIVITY
C   NEUTS1 : POINT KINETICS EQAUTIONS AND FISSION POWER
C   GAMAR1 : DECAY HEAT EQUATIONS
```

```
C   TPOWR1 : REACTOR TOTAL THERMAL POWER
C   CORORO : ORIFICING ROUTINE
C   CAVTO1 : POOL HYDRAULICS
C   FLOWO1 : CENTRAL BOXES FLOW (WCOREN(1))
C   FLOWO2 : EDGE BOXES FLOW (WCOREN(2))
C   FLOWO3 : IHX FLOW (FPAI)
C   CTISUO : CORE
C
C=======================================================================
BEGIN AT 0.0DO
         PUMPTC=10.0DO
         ZPTRIP=1.0DO
         ZTPFU=485.0
         ZLATSA=420.0
         TEAPX=343.0DO
    1    CONTINUE
.CNTRL1; FEDBKO; NEUTS1; GAMAR1; TPOWR1;
       TECXRF = ZTPFU
       CALL CORORO(LOOP,TECXRF,TAMB,QAMB,VALVL,VALVK,VALVU)
       FPAI = (WCOREN(1)+WCOREN(2))/2.0DO
.CAVTO1; CNCTUU;
C---------------------------------------------
C    ESTIMATE THE CORE PRESSURE DROP
C---------------------------------------------
      K     = 1
      CORDLP= DPHPI1( K        ,WCOREN(K),TECAN(K),PAVR1,X,VALVK(K))+
     C        DPHPI1((K+NOCNS),WCOREN(K),TECXN(K),PAVR1,X,VALVU)
C---------------------------------------------
C    PRESSURE IN PIPES 5,6,7
C---------------------------------------------
      DLPLOP= DPHPI1( 5   ,FPAI,ZTPFU ,PAVR1,X,VALV5)+
     C        DPHPI1( 6   ,FPAI,ZLATSA,PAVR1,X,VALV6)+
     C        DPHPI1( 7   ,FPAI,TEAPX ,PAVR1,X,VALV7)
C-------------------------------------------------------------
C    LOWER PLENUM PRESSURE PU-CORDLP=PL
C    PUMP  HEAD (PA)       PL=PI + DLPLOP + PUMP
C                          PUMP = PL - PI - DLPLOP
C                               = PU - CORDLP - PI - DLPLOP
C-------------------------------------------------------------
      PL = PU - CORDLP
      PUM= PL - PI - DLPLOP
C-------------------------------------------------------------
C    PUMP CHARACTERISTICS
C-------------------------------------------------------------
      CALL SODEN1(ZTPFU,ROPU,PRAV1)
      HEAD = PUM/ROPU/ZZZ981
      PQPM = FPAI/ROPU
      PPNS = DSQRT(PQPM)/(DSQRT(DSQRT(HEAD)))**3
      PPNR = 35.0/PPNS
      ZHRPU(1)  = HEAD
      ZREVR(1)  = PPNR * ZZZ314/30.0DO
      ZFLOR(1)  = FPAI
      ZTORPR(1) = PQPM * PUM / ZREVR(1)
      ZREV(1)   = ZREVR(1)
.FLOWO1; FLOWO2; FLOWO3;
C-------------------------------------------------------------
C   LOWER PLENUM CONDITIONS TO BE USED LATER
C-------------------------------------------------------------
      ZINCOR =1.0DO/(1.0DO/ZINERF(1)+1.0DO/ZINERF(2))
      ZINIHX =1.0DO/(1.0DO/ZINERF(3))
```

```
      ZINLPE= 1.0D0/( 1.0D0/ZINERF(1) + 1.0D0/ZINERF(2) +
     C                1.0D0/ZINERF(3) + 1.0D0/ZINERF(3) )
      ZPLOWP =ZINLPE*( (PU-ZDPFL(1))/ZINERF(1) +
     C                 (PU-ZDPFL(2))/ZINERF(2) +
     C                 (PI+ZDPFL(3))/ZINERF(3) +
     C                 (PI+ZDPFL(3))/ZINERF(3) )
      PRESL = ZPLOWP
      PRESU = PU
C-----------------------------------------------------------------
      ERROR = ( WCOREN(1)+WCOREN(2) - 2.0*FPAI ) / FPAI
      ERROR = DABS(ERROR)
      IF(ERROR.GT.1.0D-3) GO TO1
C---------- FLOW ITERATION END HERE ----------------------------
.CTISUO; MXPLENU; ;THPSN3; IHXGA1; THPSS3; MXPLENL;
.CONVERGR(TEAPX,1.0D-3,1,20,P);
.CONVERGR(ZTPFU,1.0D-3,1,20,P);
C------------- TEMPERATURE ITERATION ENDS HERE ------------------
C              INITIAL CONDITIONS END HERE
C=================================================================
C      S I M U L A T I O N  S T A R T S  H E R E
C=================================================================
C   THERE ARE FOUR LOOPS
C   THE FORMAT IS: SIMULATE LOOP# METHOD
C   NOINT MEANS DO NOT CALL AN INTEGRATOR;
C       NEUTS1 HAS ITS OWN INTEGRATOR.
C-----------------------------------------------------------------
SIMULATE LOOPO1 NOINT1
.CNTRL1; FEDBKO; NEUTS1;
SIMULATE LOOPO2 STIFF1
.GAMAR1;
.TPOWR1;
.MXPLENL;
       DO 333 ICORE=1,NOCNS
         CALL CORTHO(DEQ(ICORE),AFLOW(ICORE),NPIN(ICORE),XL,RCO,
     C          RCI,RF,POD,ICORE)
 333   CONTINUE
.CTISUO;
.MXPLENU;
SIMULATE LOOPO3 SIMPS1;
. THPSN3;
. IHXGA1;
. THPSS3;
SIMULATE LOOPO4 ADAMS1
. CAVTO1;
. CNCTUU;
      ZPLOWP =ZINLPE*( (PU-ZDPFL(1))/ZINERF(1) +
     C                 (PU-ZDPFL(2))/ZINERF(2) +
     C                 (PI+ZDPFL(3))/ZINERF(3) +
     C                 (PI+ZDPFL(3))/ZINERF(3) )
      PL = ZPLOWP
C-----------------------------------------------------------------
C   THIS IS AN EXAMPLE OF HOW TO INCLUDE THE TRANSIENTS
C     ANY LEGAL FORTRAN STATEMENT WILL WORK
C     THE EASIEST APPROACH IS TO CHANGE THE FOLLOWING STATEMENTS
C         ACCORDING TO THE TRANSIENT BEING SIMULATED
C         RATHER THAN GENERATE A DIFFERENT DSNP PROGRAM FOR
C         EACH CASE.
C      THIS WORKS AS LONG AS THE NUMBER OF DIFFERENTIAL EQUATIONS ARE
C         NOT CHANGED.
C    THE FOLLOWING STATEMENT STARTS A LOSS OF HEAT SINK ACCIDENT
```

```
C     FOR A LOSS OF FLOW: HAVE ZREV(1) = ZREVR(1)/(1+TIME/PUMTC)
C    THESE STATEMENTS WILL APPEAR IN SUBROUTINE DERIV1
C-----------------------------------------------------------------------
         IF(TIME.GT.ZZZ1) THEN
               FHAI     = 0.18
         ENDIF
. FLOWO1;
. FLOWO2;
. FLOWO3;
C=======================================================================
C  END OF SIMULATION
C=======================================================================
TERMINATE AT 1000.0
C-----------------------------------------------------------------
C PRINTING
C-----------------------------------------------------------------
P 'LOSS OF HEAT SINK DEC-10 '
P ZWTHMW,PWJ,WGT,
P REAK,RKD,RKS,RKCE,RKFE,
P RKFBN(1-2),RKDN(1-2),RKSN(1-2),RKCEN(1-2),RKFEN(1-2),
P WCOREN(1),WCOREN(2),FPAI,FHAI,ZDPFL(1-3),ZREV(1),ZHEAD(1),
P ZDPH(1-7),
P ZEGXC,ZEGXCN(1-2),
P TECI,TECX,TECA,TELA,TEFA,
P TECXN(1-2),TEFAN(1-2),TELAN(1-2),TECAN(1-2),
P TECXU1,TECXU2,
P ZTPFU,ZTPMU,TEAPI,TEAPX,ZLATHA,TEAHI,TEAHX,ZLATSA,
P ZROPXA,ZROHXA,ZEGIIA,ZEGIXA,
P TEAH(1-10),TEAW(1-10),TEAP(1-10),
P ZTPFL,ZTPML,ZTMLA
P BY 0.25 TO 1.0 BY 0.5 TO 10.0 BY 2.5 TO 100.0 BY 5.0 TO 800.0
C-----------------------------------------------------------------
C-------------------------------------------------
C   TEST FOR CORE ORIFICING AND HEAT TRANSFER MODULES
C-------------------------------------------------
C=========================================================
C    DATA STATEMENTS
C=====================================
. DATA(CORIF) = VALVL/1.0D0/,VALVU/0.5D0/,
.               VALV5/1.0D0/,VALV6/1.5/,VALV7/2.5/;
. DATA(FDBEK) = RKDC/-4.089D-03/,
.               RKFEC/-3.6D-06/,
.               RKSC/6.40D-06/,
.               RKVC/0.0D0/,
.               RKCEC/-10.4D-06/;
. DATA(GAMAR) = BGM/2.7D-01,2.1D-01,1.6D-01,3.6D-01,0.0D0/,
.               GAM/1.0D-05,3.0D-03,1.0D-02,4.0D-02,0.0D0/,
.               IGAM/4/,
.               GA/5.0D-01/,
.               WGTO/56.0D06/;
. DATA(TIMER) = LETM/2/, DTMAX/0.05D0/, DTMIN/1.0D-07/, DELT/5.0D-03/,
.               TICPU/43.20D03/;
. DATA(TPOWR) = PWO/744.0D06/ ;
. DATA(NEUTR) = BETA/0.128600D-4,0.947580D-4,0.730990D-4,0.111002D-3,
.                    0.348574D-4,0.118448D-4/,
.               PNO/1.0D0/ ,
.               EPSN1/1.0D-04/,EPSN2/1.0D-03/,
.               EL/0.1004002D-6/,
.               ELAMDA/ 0.0129,0.0311,0.1340,0.3310,1.2600,3.2100/;
. DATA(CORTP) = CF/144.8/, CL/502.4/,QMF/45.0D03/,QML/7.885D03/,
```

```
.                VC/2.50519D0/, ULA/32.6619D09/,UCA/98.1434D06/,
.                TECA0/343.3/, TECA/343.3/ZPCORA/1.5D06/,
.                ZFLCOR/4400.0D0/ ;
. DATA(CORCN) = TECIN/2*343.3D0/,
.                CFN/2*144.8/,
.                QMFN/27.397D03,18.2648D03/,
.                CLN/564.32,564.32/,
.                QMLN/3.8098D03,2.54D03/,
.                QMWLN/7.3328D03,1.2221D03/,
.                CWN/564.32,564.32/,
.                UCWN/5*0.0D0/,
.                UWPN/5*0.0D0/,
.                VCN/0.765,0.510/,
.                ULAN/5*7.5D06/,
.                UCAN/5*20.0D06/,
.                FPWR/0.715,0.285/,
.                VPWR/0.6D0,0.4D0/,
.                WCOREN/3.1460D03,1.2540D03/,
.                NOCNS/2/;
. DATA(NIYAZ)=  PAR(1)/6.0D-03/,
.                PAR(2)/0.5D-01/,
.                PAR(3)/13.0D-06/,
.                PAR(4)/0.0D0/,
.                PAR(5)/0.0D0/,
.                PAR(6)/0.0D0/,
.                PAR(7)/0.0D0/,
.                PAR(8)/0.0/;
. DATA(MAINF)=  A/2*7.1957D-00/,
.                B/2*14.711D-03/,
.                C/2*6.8854D-03/,
.                P/2*0.0D0/,
.                BECNS/2*0.25D0/;
. DATA(MAING)=  DEQ/2*3.12D-3/,
.                AFLOW/0.45,0.30/,
.                XL/1.7D0/,
.                RCO/6.0D-3/,
.                RCI/5.43D-3/,
.                RF/4.84D-3/,
.                POD/1.083D0/,
.                NPIN/13860,9240/;
. DATA(IHXMA)=  TEAHI/293.0D0/,FHAI/1800.0D0/,TEAHX/463.5/,
.                TEAPI/485.0D0/,FPAI/2200.0D0/,ZLATHA/420.0D0/;
. DATA(MXPLU)=  ZTPFU/485.0D0/;
. DATA(MXPLL)=  ZTPFL/343.0D0/;
C===================
C   END
C===================
FORTRAN
      SUBROUTINE CORORO(LOOP,TECXRF,TAMB,QAMB,VALVL,VALVN,VALVU)
      IMPLICIT REAL*8(A-H,O-Z)
      DIMENSION GW(3,10),FW(3,10),PDROPS(10),IOKEY(10),INEW(10),
     C          GV(10),FV(10),VALVN(10)
.     COMIN CORTP5,CORCN5,MAINF5,HPIPE5,MAING5;
C---------
C  FIND CORE FLOW RATES SO THAT TECX ARE SAME
C  ASSUMES THAT CORE CHANNELS ARE REPRESENTED BY
C  K AND K+NOCNS 'TH HYDRAULIC PIPES,AND K STARTS
C  FROM 1
C  MAINF5 CONTAINS FUEL CONDUCTIVITY EQAUTION PARS
C  MAING5 CONTAINS CHANNEL GEOMETRY PARS
```

```
C    CORTHO(DEQ,AFLOW,NPIN,XL,RCO,RCI,RF,POD,N)
C   /MAING5/DEQ(K),AFLOW(K),XL,RCO,RCI,RCF,POD,NPIN(K)
C-----------
      MAXIT=100
      DO 100 I=1,NOCNS
         IOKEY(I)=0
         WCOREN(I)=ZFLCOR/NOCNS
 100  CONTINUE
      DO 110 I=1,NOCNS
         GW(1,I)=0.8*WCOREN(I)
         GW(2,I)=1.0*WCOREN(I)
         GW(3,I)=1.2*WCOREN(I)
 110  CONTINUE
      DO 140 I=1,3
         DO 120 K=1,NOCNS
            WCOREN(K)=GW(I,K)
            CALL CORTHO(DEQ(K),AFLOW(K),NPIN(K),XL,RCO,RCI,RF,POD,K)
 120     CONTINUE
      CALL CORFBO(LOOP,TAMB,QAMB)
         DO 130 K=1,NOCNS
            FW(I,K)=TECXRF-TECXN(K)
 130     CONTINUE
 140  CONTINUE
      DO 180 ITER=1,MAXIT
         DO 150 K=1,NOCNS
            IF(IOKEY(K).EQ.1) GO TO 150
            CALL CORTHO(DEQ(K),AFLOW(K),NPIN(K),XL,RCO,RCI,RF,POD,K)
            CALL GUESS3(FW(1,K),GW(1,K),GNEW,INEW(K),DERR,DERA)
            IF(DERR.LT.1.0D-5) THEN
               WCOREN(K)=GNEW
               IOKEY(K)=1
            ELSE
               GW(INEW(K),K)=GNEW
               WCOREN(K)=GNEW
               IOKEY(K)=0
            ENDIF
 150     CONTINUE
         CALL CORFBO(LOOP,TAMB,QAMB)
         DO 160 K=1,NOCNS
            FW(INEW(K),K)=TECXRF-TECXN(K)
 160     CONTINUE
         MIN=1
         DO 170 K=1,NOCNS
            MIN=IOKEY(K)*MIN
 170     CONTINUE
         IF(MIN.EQ.1) GO TO 200
 180  CONTINUE
 200  CONTINUE
      PMAX=0.0D0
      DO 210 K=1,NOCNS
         PDROPS(K)=DPHPI1( K        ,WCOREN(K),TECAN(K),PAVR1,X,VALVL)+
     C             DPHPI1((K+NOCNS),WCOREN(K),TECXN(K),PAVR1,X,VALVU)
         IF(DABS(PDROPS(K)).GT.PMAX) THEN
            PMAX=DABS(PDROPS(K))
            IMPD=K
         ENDIF
 210  CONTINUE
      VALVN(IMPD)=VALVL
      DO 250 K=1,NOCNS
         IF(K.EQ.IMPD) GO TO 250
```

```
         GV(1)=0.8*VALVL
         GV(2)=1.0*VALVL
         GV(3)=1.2*VALVL
         DO 220 I=1,3
            FV(I)=PMAX-
     C       DABS(DPHPI1( K        ,WCOREN(K),TECAN(K),PAVR1,X,GV(I)))-
     C       DABS(DPHPI1((K+NOCNS),WCOREN(K),TECXN(K),PAVR1,X,VALVU))
 220     CONTINUE
         DO 230 ITER=1,MAXIT
            CALL GUESS3(FV,GV,GNEW,IV,DERR,DERA)
            IF(DERR.LT.1.0D-5) GO TO 240
            GV(IV)=GNEW
            FV(IV)=PMAX -
     C       DABS(DPHPI1( K        ,WCOREN(K),TECAN(K),PAVR1,X,GV(IV)))-
     C       DABS(DPHPI1((K+NOCNS),WCOREN(K),TECXN(K),PAVR1,X,VALVU ))
 230     CONTINUE
        WRITE(*,*) ' DID NOT CONVERGE IN VALV COMP '
 240     CONTINUE
         VALVN(K)=GNEW
 250     CONTINUE
         RETURN
         END
      SUBROUTINE CORTHO(DEQ,AFLOW,NPIN,XL,RCO,RCI,RF,POD,N)
      IMPLICIT REAL*8(A-H,O-Z)
.COMIN CORCN5,MAINF5;
C-------------------------------------------------------------
C   STATEMENT FUNCTIONS FOR SODIUM PROPS
C-------------------------------------------------------------
      SODEN(T)=950.076+T*(-0.2297+T*(-1.46049D-5+T*5.637788D-9))
      SOCON(T)=92.948+T*(-5.809D-2+T*1.1727D-5)
      SOVIS(T)=0.001*10.0D0**(0.5108+220.65/T-0.4925*DLOG10(T))
      SOCPH(T)=1436.05+T*(-0.5802+T*4.62506D-4)
      FUELK(A,B,C,P,BETA,T)=A+T*(B+C*T)*(1.0D0-P)/(1.0D0+BETA*P)
      CDCON(T)=11.5+0.013*T
      W   =WCOREN(N)
      TNA=TECAN(N)
      TCL=TELAN(N)
      TFL=TEFAN(N)
      TDT=TCBWN(N)
      R11=1.0/FUELK(A(N),B(N),C(N),P(N),BECNS(N),(TFL+273.15))
      R12=DLOG(RCI/RF)/SOCON( (TFL+TCL)/2.0D0 )
      R13=DLOG( (RCO+RCI)/(2.0D0*RCI) )/CDCON(TCL)
      R1 = R11+R12+R13
      VIS=SOVIS(TNA+273.15)
      REY= (W/AFLOW)*DEQ/VIS
      PRN= VIS*SOCPH(TNA)/SOCON(TNA)
      PEC= REY*PRN
      IF(POD.LE.1.15) GO TO 1
      XNU=4.0+0.33*POD**3.8+(PEC/100.0D0)**0.88+0.16*POD**5
      GO TO 2
    1 XNU=(-16.15+24.96*POD-8.55*POD*POD)
      IF(PEC.LE.150.0D0) GO TO 3
      XNU=XNU*PEC**0.3
      GO TO 2
    2 XNU=XNU*4.496
    3 CONTINUE
      H=XNU*SOCON(TNA) /DEQ
      R2=DLOG(2.0D0*RCO/(RCO+RCI))/CDCON(TCL) + 1.0D0/H/RCO
      UFTOC=6.28318530800 * XL /R1 * NPIN
      UCTOC=6.28318530800 * XL /R2 * NPIN
```

```
      ULAN(N)=UCTOC
      UCAN(N)=UFTOC
      RETURN
      END
C======= MACROS ==================
M <DFCORBO(#)>=<%D CORFBO>;
M <DFFDBKO(#)>=<%D FDBEKO>;
C======= LIBRARY ZERO =============
L
*CORFBO
M <DFCORBO(#)>=<%Z21 %XO %M<CTISUO>=<%%B CALL CORFBO(LOOP,TAMB,QAMB)>%E
      SUBROUTINE CORFBO(LOOP,TAMB,QAMB);
. TICIL; CHRTR;  COMIN TIMER5,DERIV5,TPOWR5,CORTP5,GAMAR5,CORCN5;
. COMON /CORTP5/ TECA, TECAO, TECI, TECX, TEFA, TEFAO, TELA, TELAO, CF,
. CL, QMF, QML, VC, ULA, UCA, ROCA, ZFLCOR,ZROCX,ZPCORA,ZEGXC,
. ZTECBL,ZVOLFC,ZHCX,ZFLCRO;
. COMON /CORCN5/ TECAN(#01), TECAON(#01), TECIN(#01),TECXN(#01),
. TEFAN(#01),TEFAON(#01), TELAN(#01), TELAON(#01), CFN(#01),CWN(#01),
. CLN(#01), QMFN(#01), QMLN(#01), VCN(#01), ULAN(#01), UCAN(#01),
. ROCAN(#01),FPWR(#01),WCOREN(#01),ZROCXN(#01),ZEGXCN(#01),VPWR(#01)
. ,TCBWN(#01),TCBWNO(#01),QMWLN(#01),UCWN(#01),UWPN(#01),NOCNS;
. DIMENSION_TECA1(10),TECX1(10),DTEFAN(10),DTELAN(10),DTECXN(10),
. CCN(10),DTWALL(10);
. LOGICAL_LT,LFIRST;  DATA_ TECA1,TECX1/20*0.D0/;
. DATA_LFIRST/.FALSE./;
.  TASNA('CORFBO'); NOCNS=#01;
.      IF(LFIRST)_ GO_ TO_ 1;
.      LFIRST=.TRUE. ;
.      DO_56_ICNS=1,NOCNS;
.  56 IF(TECXN(ICNS).LT.TECIN(ICNS))_ TECXN(ICNS)=TECIN(ICNS)+150.D0;
.    1 CONTINUE;
.      DO_ 5656_ ICNS=1,NOCNS;
.      TECAN(ICNS)=(TECIN(ICNS)+TECXN(ICNS))/ZZZ2;
.      LT=DABS(TECAN(ICNS)-TECA1(ICNS)).LT.ZZZ1;
.    2 IF(LT)_ GOTO_ 3;
.      TECA1(ICNS)=TECAN(ICNS);
.      CALL SODCP1(TECAN(ICNS),CCN(ICNS),ZPCORA);
.      CALL SODEN1(TECAN(ICNS),ROCAN(ICNS),ZPCORA);
.    3 IF(JTIM.GT.0) GOTO 10;
.      TECXN(ICNS)=TECIN(ICNS)+
.       FPWR(ICNS)*(PWJ+WGT)/(WCOREN(ICNS)*CCN(ICNS));
.      TECAN(ICNS)=(TECIN(ICNS)+TECXN(ICNS))/ZZZ2;
.      TECAON(ICNS)=TECAN(ICNS);
.  TELAN(ICNS)=TECAN(ICNS)+FPWR(ICNS)*(PWJ+WGT*(ZZZ1-GA))/ULAN(ICNS);
.  TELAON(ICNS)=TELAN(ICNS);
.  TEFAN(ICNS)=TELAN(ICNS)+FPWR(ICNS)*(PWJ+WGT*(ZZZ1-GA))/UCAN(ICNS);
.  TEFAON(ICNS)=TEFAN(ICNS);
.  TCBWNO(ICNS)=TECAN(ICNS);
.      ZEGXCN(ICNS)=WCOREN(ICNS)*CCN(ICNS)*(TECXN(ICNS)-TECIN(ICNS));
.  GO_TO_ 80;
.   10 CFMN=CFN(ICNS)*QMFN(ICNS);
.      CLMN=CLN(ICNS)*QMLN(ICNS);
.      CVRN=CCN(ICNS)*VCN(ICNS)*ROCAN(ICNS);
.      CCBN=CWN(ICNS)*QMWLN(ICNS);
.      ZEGXCN(ICNS)=WCOREN(ICNS)*CCN(ICNS)*(TECXN(ICNS)-TECIN(ICNS));
.      QAMB=  UWPN(ICNS) * ( TCBWN(ICNS)-TAMB );
.      QWAL=  UCWN(ICNS) * ( TECAN(ICNS)-TCBWN(ICNS) );
.      QCLA=  ULAN(ICNS) * ( TELAN(ICNS)-TECAN(ICNS) );
.      QFCL=  UCAN(ICNS) * ( TEFAN(ICNS)-TELAN(ICNS) );
.      DTECXN(ICNS)=( WGT*GA*FPWR(ICNS)-ZEGXCN(ICNS)+QCLA-QWAL)/CVRN;
```

```
.       DTELAN(ICNS)=( QFCL -QCLA )/CLMN;
.       DTEFAN(ICNS)=( FPWR(ICNS)* (PWJ+WGT*(ZZZ1-GA))-QFCL)/CFMN;
.       DTWALL(ICNS)=( QWAL - QAMB )/CCBN;
.    80 IF(DABS(TECX1(ICNS)-TECXN(ICNS)).LT.ZZZ1)__GO__TO__5656;
.       CALL SODEN1(TECXN(ICNS),ZROCXN(ICNS),ZPCORA);
.       TECX1(ICNS)=TECXN(ICNS);
. 5656 CONTINUE;
.       IF(JTIM.GT.0)_ GO_ TO_ 5629;
.       TEFAO=ZZZ0;
.       TELAO=ZZZ0;
.       TECAO=ZZZ0;
.       ZFLCRO=ZZZ0;
.       DO_ 5628_ ICNS=1,NOCNS;
.          TEFAO=TEFAO+FPWR(ICNS)*TEFAON(ICNS);
.          TELAO=TELAO+FPWR(ICNS)*TELAON(ICNS);
.          TECAO=TECAO+FPWR(ICNS)*TECAON(ICNS);
.          ZFLCRO=ZFLCRO+WCOREN(ICNS) ;
. 5628 CONTINUE;
.       ZFLCOR=ZFLCRO;
.       GO_ TO_ 999 ;
. 5629 CONTINUE;
. VNTGRL(TEFAN(I))=(TEFAN(I),DTEFAN(I),#01,I=1,#01);
. VNTGRL(TELAN(I))=(TELAN(I),DTELAN(I),#01,I=1,#01);
. VNTGRL(TECXN(I))=(TECXN(I),DTECXN(I),#01,I=1,#01);
. VNTGRL(TCBWN(I))=(TCBWN(I),DTWALL(I),#01,I=1,#01);
. 999     TEFA=ZZZ0;
.       TELA=ZZZ0;
.       TECA=ZZZ0;
.       TECX=ZZZ0;
.       TECI=ZZZ0;
.       ZEGXC=ZZZ0;
.       ZFLCOR=ZZZ0;
.       CPNA=ZZZ0;
.       DO_ 5630_ ICNS=1,NOCNS;
.          TEFA=TEFA+FPWR(ICNS)*TEFAN(ICNS);
.          TELA=TELA+FPWR(ICNS)*TELAN(ICNS);
.          TECA=TECA+FPWR(ICNS)*TECAN(ICNS);
.          TECX=TECX+WCOREN(ICNS)*TECXN(ICNS)*CCN(ICNS);
.          TECI=TECI+WCOREN(ICNS)*TECIN(ICNS)*CCN(ICNS);
.          ZEGXC=ZEGXC+ZEGXCN(ICNS);
.          ZFLCOR=ZFLCOR+WCOREN(ICNS);
.          CPNA=CPNA+CCN(ICNS);
. 5630 CONTINUE;
.       TECX=TECX/ZFLCOR/CPNA*NOCNS;
.       TECI=TECI/ZFLCOR/CPNA*NOCNS;
. 99 KSUBST=KSUBST-1; RETURN;
.     END; % 100 >
.     END

*FDBEKO
M <DFFDBKO(#)>=<%Z21 %X0 %M<FEDBKO>=<%%B CALL FDBEKO>%E
      SUBROUTINE FDBEKO;
. TICIL;  CHRTR;
. COMON /FDBEK5/ RKFB,RKS,RKSC,RKD,RKDC,RKFE,RKFEC,RKV,RKVC,RKCE,RKCEC,
. RKSTE,RKSTC;
. COMON /FDBE05/ RKFBN(#01),RKSN(#01),RKDN(#01),RKFEN(#01),RKVN(#01),
. RKCEN(#01),RKSTEN(#01);
. COMIN,NEUTR5,TIMER5,FDBEK5,FDBE05,CORTP5,CORCN5; TASNA('FDBEKO');
.       IF(JTIM.GT.0)_ GO_TO_ 10;
.       DO_ 5656_ I=1,NOCNS;
```

```
. 5656 RKFBN(I)=ZZZO;
.   10 CONTINUE;
.      DO_ 2929_ I=1,NOCNS;
.      RKSN(I)=RKSC*(TECAN(I)-TECAON(I));
.      RKDN(I)=RKDC*DLOG((TEFAN(I)+ZZZ273)/(TEFAON(I)+ZZZ273));
.      RKFEN(I)=RKFEC*(TEFAN(I)-TEFAON(I));
.      RKCEN(I)=RKCEC*(TELAN(I)-TELAON(I));
.      RKSTEN(I)=RKSTC*(TCBWN(I)-TCBWNO(I));
.      RKV=RKVC*ZVOLFC;
.      RKFBN(I)=RKSN(I)+RKDN(I)+RKFEN(I)+RKV+RKCEN(I)+RKSTEN(I);
. 2929 CONTINUE;
.      RKFB=ZZZO;
.      RKS=ZZZO;
.      RKD=ZZZO;
.      RKFE=ZZZO;
.      RKCE=ZZZO;
.      RKSTE=ZZZO;
.      WEIG=ZZZO;
.      DO_ 5629_ I=1,NOCNS;
.      FACTOR = FPWR(I)**2/VPWR(I);
.      RKS  = RKS  + FACTOR * RKSN(I);
.      RKD  = RKD  + FACTOR * RKDN(I);
.      RKFE = RKFE + FACTOR * RKFEN(I);
.      RKCE = RKCE + FACTOR * RKCEN(I);
.      RKSTE= RKSTE+ FACTOR * RKSTEN(I);
.      WEIG= WEIG + FACTOR;
. 5629 CONTINUE;
.      RKS=RKS/WEIG; RKD=RKD/WEIG; RKFE=RKFE/WEIG; RKCE=RKCE/WEIG;
.      RKSTE=RKSTE/WEIG;
.      RKFB = (RKS + RKD + RKFE + RKCE);
. 99 KSUBST=KSUBST-1; RETURN;
.      END; % IOO >
.      END
```